Acta Universitatis Agriculturae Sueciae

SLU

Doctoral Thesis No. 2023:49
Faculty of Forest Sciences

Production and characterisation of pine wood powders from a multi-blade shaft mill

Atanu Kumar Das

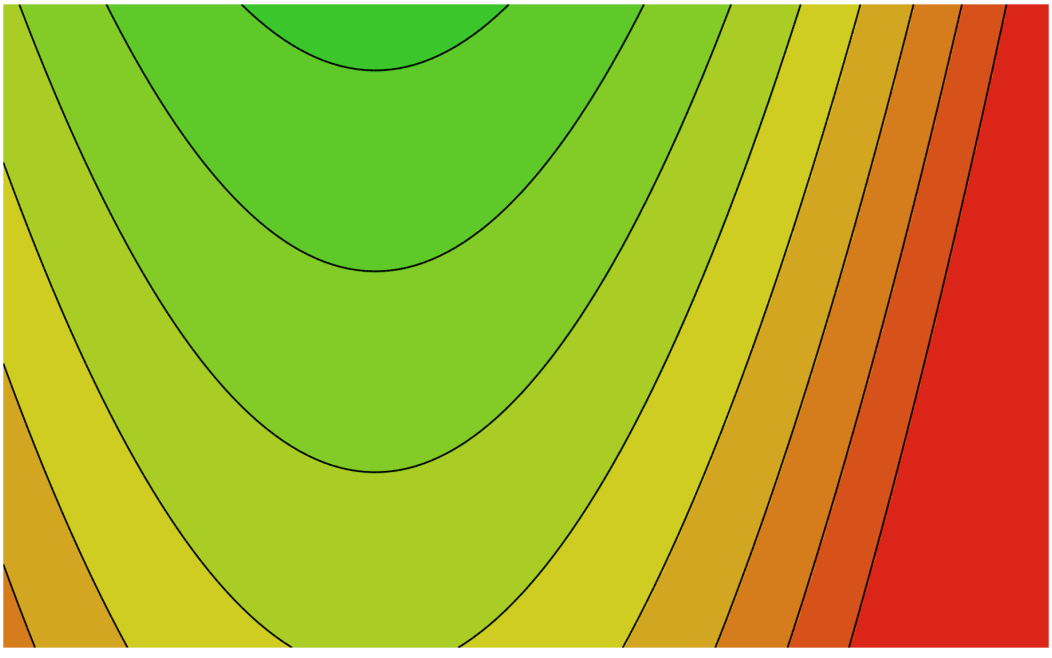

Production and characterisation of pine wood powders from a multi-blade shaft mill

Atanu Kumar Das
Faculty of Forest Sciences
Department of Forest Biomaterials and Technology
Umeå

SLU
SWEDISH UNIVERSITY OF AGRICULTURAL SCIENCES

DOCTORAL THESIS
Umeå 2023

Acta Universitatis Agriculturae Sueciae
2023:49

Cover image: Contour plot of modelled particle size distribution

ISSN 1652-6880
ISBN (print version) 978-91-8046-150-4
ISBN (electronic version) 978-91-8046-151-1
https://doi.org/10.54612/a.7jcf9n9bte

Swedish University of Agricultural Sciences, Department of Forest Biomaterials and Technology, Umeå, Sweden

Print: NRA Repro AB, Umeå 2023

Production and characterisation of pine wood powders from a multi-blade shaft mill

Abstract

Wood is an important raw material for the manufacture of consumer products and in achieving societal goals for greater sustainability. Wood powders are feedstock for many biorefining and conversion techniques, including chemical, enzymatic and thermochemical processes and for composite manufacture, 3D printing and wood pellet production. Size reduction, therefore, is a key operation in wood utilisation and powder characteristics, such as shape, particle size distribution and micromorphology play a role in powder quality and end-use application. While in a green state, the native chemical composition and structure of wood are preserved. Powders are commonly produced from wood chips using impact mills, which require pre-sized, pre-screened and pre-dried chips. These steps necessitate repeated handling, intermediate storage and contribute to dry matter losses, operation-based emissions and the degradation of the wood chemistry.

This thesis investigated a new size reduction technology, known as the multi-blade shaft mill (MBSM). The MBSM performance was studied through the milling of Scots pine (*Pinus sylvestris* L.) wood using a designed series of experiments and through modelling with multi-linear regression (MLR) analyses. Light microscopy combined with histochemical techniques were used to investigate particle micromorphology and distribution of native extractives in powders. The aim was to evaluate the technical performance of the MBSM with relation to operational parameters, to characterise the produced powders and to evaluate the technology through comparison with impact milling.

The results showed that the MBSM could effectively mill both green and dry wood. Produced powders showed distinct differences compared to those obtained using a hammer mill (HM). The specific milling energy of the MBSM was lowest for green wood and within the range of other established size reduction technologies. However, much narrower particle size distributions were observed in MBSM powders and they had significantly greater amounts of finer particles. Particles with high aspect ratio and sphericity were a characteristic of MBSM powders and this

was true for wood milled above and below its fibre saturation point. MBSM powders from green wood showed evidence of higher specific surface area, larger pore volume and greater micropore diameter than those from HM powder. Preliminary microscopic examination suggested that cell walls in MBSM powders showed evidence of retaining their original native wood structure. Consequently, their extractive content appeared intact. This was in contrast to HM powder and it may reflect the differences between the two size reduction mechanisms. According to the produced MLR models, the results suggest that MBSM milling is more akin to a sawing process and opposite to that of impact-based mills.

Keywords: wood milling, powder technology, multi-blade shaft mill, size reduction, powder characterisation, experimental design, wood microscopy, particle size distribution

For my mother, wife and son who always encouraged me to aim for PhD.

Contents

List of publications

This thesis is based on the work contained in the following papers, referred to by Roman numerals in the text:

I. **Atanu Kumar Das**, David A. Agar, Sylvia H. Larsson, Tobias Holdo, Dinesh Fernando, Magnus Rudolfsson (2021). Multi-blade milling from log to powder in one step – Experimental design and results. Powder Technology, 378, 593–601.

II. **Atanu Kumar Das**, David A. Agar, Sylvia H. Larsson, Magnus Rudolfsson (2021). Investigating the influence of work piece geometry on the specific energy use in size reduction with a multi-blade shaft mill. Biosystems Engineering, 209, 210-215.

III. **Atanu Kumar Das**, David A. Agar, Mikael Thyrel, Magnus Rudolfsson (2022). Wood powder characteristics of green milling with the multi-blade shaft mill. Powder Technology, 407, 117664.

IV. **Atanu Kumar Das**, David A. Agar, Magnus Rudolfsson, Dinesh Fernando (2023). Investigation of micromorphology and native extractive behaviour of wood powder during milling for possible applications in biorefinery. (Manuscript).

V. **Atanu Kumar Das**, Magnus Rudolfsson, David A. Agar (2023). Production of wood powders, their characteristics and applications – A review. (Manuscript).

Papers I-III are published in open access journals.

Additional publications that are not included in the thesis:

I. **Atanu Kumar Das**, David A. Agar, Magnus Rudolfsson and Sylvia H. Larsson (2021). A review on wood powders in 3D printing: processes, properties and potential applications. Journal of Materials Research and Technology, 15, 241-255.

II. **Atanu Kumar Das**, David A. Agar, Mikael Thyrel, Sylvia H. Larsson, Magnus Rudolfsson (2021). Green milling of biomass and implications for conversion processes, 2021 PEERS Conference (21PEE04).

The contribution of Atanu Kumar Das to the papers included in this thesis was as follows:

I. Atanu Kumar Das was the main author of the paper. He actively participated in the experimental design and material acquisition, carried out the milling experiments, sampled and characterised the wood powders, analysed the data and developed the multi-linear regression (MLR) models.

II. Atanu Kumar Das was the main author of the paper. He participated in conducting the experiments, analysed the data and developed the MLR model.

III. Atanu Kumar Das was the main author of the paper. He participated in the planning, conducted the camsizer experiments, synthesised data, analysed the data, interpreted the results and participated in orthogonal projections to latent structures (OPLS) model development.

IV. Atanu Kumar Das was the main author of the paper. He prepared the powder samples, conducted the staining and light microscopy work, carried out visual analysis of the images and participated in the interpretation of the results.

V. Atanu Kumar Das was the main author of the paper. He conducted the literature review, organised the relevant studies and evaluated the subject matter.

List of tables

List of figures

Nomenclature

AL	Aged of log
ANN	Artificial neural network
AoR	Angle of repose
BD	Bulk density
BET	Brunauer-Emmett-Teller
BS	Blade speed
BTC	Biomass technology centre
DES	Deep eutectic solvent
DM	Dry mass
DMP	MBSM powder from dry wood
DOE	Design of experiment
DS	Wood basic density
FDM	Fused deposition modelling
FMP	MBSM powder from wood at fibre saturation point
FS	Feeding speed
FSP	Fibre saturation point
GMP	MBSM powder from green wood
HGI	Hardgrove grindability index
HM	Hammer mill

HMP	Hammer mill powder
HR	Hausner ratio
HTL	Hydrothermal liquefaction
MBSM	Multi-blade shaft mill
MC	Moisture content
MLR	Multi-linear regression
NK	Number of knots
OPLS	Orthogonal projections to latent structures
OPLS-DA	Orthogonal projections to latent structures discriminant analysis
PCA	Principal component analysis
PF	Phenol formaldehyde
PHA	Polyhydroxyalkanoate
PLS	Partial least squares
PSD	Particle size distribution
SD	Standard deviation
SLA	Stereolithography
UF	Urea formaldehyde
VIP	Variable importance of the projections
WPC	Wood plastic composites
wb	Wet basis
D_{ml}	Dry mass of log (kg)
D_{mp}	Dry mass of powder (kg)
e_M	Specific milling energy (kWh t^{-1})
h_p	Height of the pile of powder (mm)
m_h	Mass of the hammer-milled powder (kg)
m_M	Mass of milled log (kg)

P_c	Chipping power (kW)
P_f	Log feeding power (kW)
P_h	Hammer-milling power (kW)
P_m	Log milling power (kW)
Q^2	Coefficient of multiple determination
R^2	Coefficient of determination
$RMSE_{CV}$	Root mean square error
r_p	Radius of the pile of powder (mm)
t_c	Chipping time (s)
t_h	Hammer-milling time (s)
t_M	Log milling time (s)
Yp	Yield of powder (%)
Y_{BD}	Modelled bulk density (kg m^{-3})
Y_E	Modelled specific milling energy (kWh t^{-1})
Y_{PSD}	Modelled particle size distribution (mass %)

1. Introduction

Wood is an important biomaterial to enable the shift to a sustainable development and the eventual phase-out of fossil-based resources [1]. Many pathways to wood utilisation in the bioeconomy rely on size reduction to powders (i.e. wood particulates having a diameter less than approximately 1 mm). For example, applications for wood powder may include feedstock for biorefining processes (such as biochemicals) [2], making bio-based composites (such as particleboard or wood plastic composites (WPC)) [3, 4], 3D printing [5], water treatment [6, 7], paperboard manufacturing [8], paper making [9] and the manufacture of wood fuel pellets [10].

Wood, the product of living trees, retains its natural chemical composition, when it is still green. The utilisation of wood in this state is especially desirable for biorefining where native chemicals and cell wall structure are conserved in the material as long as the wood maintains its moisture content (MC), whether used immediately after felling or temporarily stored in water [11].

Common size reduction technologies require several steps to reduce wood to a powder [12] (Figure 1). Technologies presently used in industries are impact mills (i.e., hammer mills), attrition mills (i.e., disc mills) and knife mills [12]. Pre-sized, pre-screened, and pre-dried sizes are necessary for these mills in order to facilitate handling and prevent clogging.

For instance, hammer mills can produce 0.2 to 2.0 mm powders from wood chips that range in size from 10 to 70 mm [13-15]. This two-step pathway to powder requires chipping, screening, intermediate storage, handling and drying. These operations increase the risk of material loss and the deterioration of the wood. They also have associated emissions which may include decomposition losses in the wood [16]. Moreover, each of the

operations with these technologies [13] take up time, demand extra financial resources and the potential for undesirable environmental pollution [17].

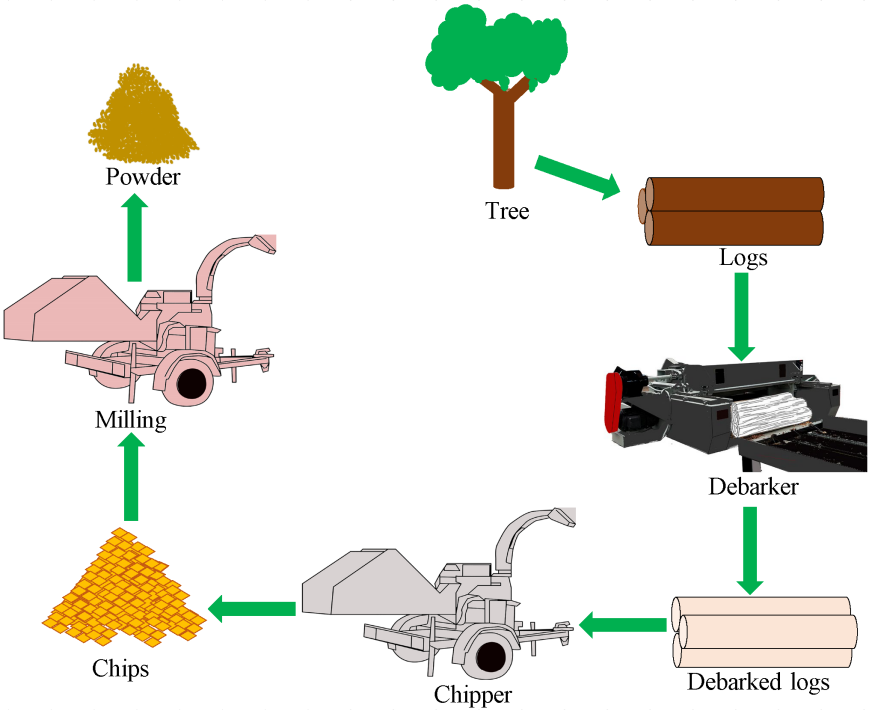

Figure 1. A common pathway to reduce wood to a powder.

The properties of wood powders can vary widely. Powder characteristics, including particle shape, particle size distribution (PSD) and micromorphology are key factors that may strongly affect their success in utilisation. The physical characteristics of wood powders are dependent on the size reduction technology used to produce them [18]. Chipping and drying [19] changes the cell structure of wood. Size reduction then has an impact on the particle micromorphology, surface characteristics, porosity and surface properties as well as particle aspect ratio and sphericity. The bulk behaviour of the powder is influenced by the above properties. Well-known examples include how wood powder combustion is a function of particle shape and PSD [20] and how the feeding behaviour of powder depends on its bulk density [21].

Size reduction technologies also affect the chemical characteristics of wood powders and influence their uses. For instance, wood drying and chipping in the pulp and paper industry influence the turpentine and tall oil yields in the kraft pulping process [11]. Fracture mechanisms in wood are influenced by to what extent water is present in the material; green and dry wood break differently. When wood is milled, a high moisture content lead to greater exposure of carbohydrates on the particulates and a low moisture content tends to expose more lignin [22]. Observable differences in enzymatic digestibility are brought about by these morphological features [18].

Wood powder production requires energy input due to the fracturing of wood cells through applying forces, i.e., shear, compression, impact, and cutting [12]. The hydrogen bonds between cells play a vital role preventing its fracture. Therefore, the water in wood regulates the bonds that produce strength characteristics. As MC increases, the bonding weakens until it reaches the fibre saturation point (FSP) and beyond [23, 24]. If the MC falls below the FSP, the bonding is enhanced. As a result, the strength of wood with a high MC is compromised [25], making it simpler to break and turn into wood particles. Conversely, to transform wood into a powder, a MC at or above the FSP requires less energy than with dry wood. Although the excess water in cell cavities has no effect on the strength of wood [25], it has a significant role in size reduction [26] and sawing by working as lubricant [27]. The above behaviour of wood and the influence of MC on energy requirements in milling is similar to that in sawing processes.

The energy input and degree of size reduction are proportionally associated; the finer the powder generated, the greater the required energy input [12, 14, 28]. This well-known relationship has been postulated for biomass from existing inorganic materials [29]. For both wood sawing and impact milling, the effects of wood species, wood density, grain orientation and temperature on energy consumption have been investigated [30].

1.1 Size reduction technologies

Technologies for the size reduction of wood are various in kind with the end purpose of utilisation in mind. Based on the principles employed, the characteristics of the product can be very different. The downstream operations determine the desired size. For instance, the chemical and

mechanical pulp industries, which make pulp, consider the chip length, breadth, and thickness. As a result, they employ wood chips and chipping equipment that can produce chips of the appropriate grade. The chipper is unable to create finer particles so that chips must subject to fine grinding. However, green wood chips cannot normally be used in fine grinding so drying step is necessary. This and the mill type used affects the final properties of the powder. Powder production technologies have been divided into five major classes and these are impact mills, ball media mills, air jet mills, roller mills and other types such as the shearing attrition mill [31].

1.1.1 Impact mills

Impact mills are widespread and can be subdivided into different types based on their mechanical actuators such as hammers, high speed rotating discs, annular and axial flows [31]. The mechanical stresses created are shear and impact [32].

Hammer mills are almost exclusively used for milling wood [13, 33]. In these designs, hammers are set on the rotor to move freely or fixed, and ground products are discharged through the slot or screen [31]. Schell and Harwood [34] have described a similar type in which suction fan is used to draw feed material and air flow is applied to collect the pulverized products, which are separated by a cyclone. The particle size is possible to control by maintaining rotational speed and number of the hammers, and air flow, which controls the residence time of the particle inside the mill [34]. The opening size of the screen or sieve can control the particle size [14]. Several authors have observed the smaller size of powders, the smaller screen size and the high rotational speed has provided more homogenize size of powders. Gil *et al.* [35] milled poplar (*Populus sp.*) wood by hammer mill with two different sieve sizes namely 5 mm and 2 mm. The obtained size of the particles was <0.1 mm to 5 mm for the 5mm sieve and <0.1 mm to 2 mm for the 2 mm sieve [35]. The geometric mean of the particle size was 0.63 mm when the used sieve size was 5 mm and 2 mm resulting in a geometric mean particle size of 0.30 mm [35]. The size reduction is dependent on the comminution ratio (ratio of initial and final particle size) during milling [36]. The same authors obtained a hardwood powder of 1.60 to 6.35 mm with comminution ratio of 3.5 to 14 using a 11 kW hammer mill.

1.1.2 Ball media mills

Ball media mills use either balls or beads to pulverize the input materials. These are categorised into two types, i.e., a vessel and agitator drive, based on the driving mechanism of the balls or beads. Vessel drive ball media mills can be further divided into three varieties, i.e., tumbling, vibrating, and planetary/oscillatory ball mill, depending on the method agitation [31]. The ball type has an impact on milling performance [33]. The double impact technique is used by oscillatory ball mill [37]. Attrition and compression are mechanical stresses for vibration ball mill; these stresses are maintained by vibration of the tank [38]. In terms of energy consumption, the vibration mill with multiple tube is more efficient in comparison to vibration ball mill with single tube [39]. All kinds of materials can be ground to superfine powders by a vibrated and planetary ball mill [40]. For example, Karinkanta *et al.* [41] and Karinkanta *et al.* [42] have produced 0.02 to 0.10 mm and 0.02 to 0.25 mm Norway spruce (*Picea abies*) wood powders, respectively by oscillatory ball mill.

1.1.3 Air jet mills

In air jet mills, the jet is used to generate high impact energy to produce fine powders. These mills disperse the powders to avoid re-aggregation. The jet mills are further categorised into three typical types such as fluidised-bed, target collision and attrition types. In the case of fluidised-bed, the feed particles are inserted into the fluidised material and the grinding mechanism is due to collisions among particles. For the target collision type, the feed particles are agitated using an air jet stream to produce collisions. The attrition type has two types of structures, a tubular ring and a pan shaped structure. The grinding takes place by the collision of feed particles with tube wall and among particles [31]. Karinkanta *et al.* [43] have used fluidised-bed opposed jet mill to produce 0.19 to 0.21 mm Norway spruce (*P. abies*) wood powder.

1.1.4 Roller mills

There are generally two types of roller mill; one of them is the roller-type and another one is roll-type mill. Roller-type mills are that type where rollers are rolled in a vessel or on a table, but in roll-type mills, particles are fed and

pulverised between two cylindrical rolls. The main principle of this concept is the cracking of feed particles through high pressure followed by disintegrating to fine particles [31]. Researchers have used roll-type mills to make powders from wood shavings prior to enzymatic hydrolysis [44-46]. Tamura et al. [33] used vertical roller mill (roller-type) to mill 10 mm waste wood chips to obtain particle size ≤ 1.0 mm.

1.1.5 Attrition mills

Disc mills are the main type of attrition mill. These are used in the pulp and paper industry [34] and disc milling is the chief method for mechanical pulping [18]. Disc mills are classified as single and double disc having straight profiled blades [15]. A double disc mill consists of either a stationary or a rotating plate or both of them as counter rotating plate. The particle size depends on machine speed, plate spacing and type of plate and refiner [34]. Disc mills have also been applied in wood milling. Fougere *et al.* [18] have produced 0.05 to 0.11 mm aspen (*Populus sp.*) wood powder using a single disc mill.

1.1.6 Other mills

Vibration mill

A vibration mill works like ball mills with the difference being the media used for pulverisation. In this mill, ball and rods are used as pulverisation media. It consists of a vessel and vibration meter. Mechanical shock and shear forces are utilised to pulverise the wood in this mill [47]. Kobayashi *et al.* [48] has used a vibration mill to obtain 0.02 to 0.50 mm pine (*Pinus sp.*) wood powder.

Centrifugal mill

Centrifugal mill employs impact and shear forces to pulverise materials. It has a rotor and a ring sieve and pulverisation takes place between them [49]. Repellin *et al.* [30] have produced 0.50 mm spruce (*Picea sp.*) and beech (*Fagus sp.*) powders using a centrifugal mill.

Air classifier mill

This mill is comprised of a feeding screw, milling section, and air classifier [42]. There is an impact beater and a fixed triangular-ribbed grinding track around the milling chamber [50]. A study on an air classifier mill has shown that it can produce 0.02 to 0.25 mm wood powders [42].

1.2 Factors affecting wood milling

Factors affecting the size reduction of wood include mill type [31, 51], size, grinding equipment, speed and air flow [51] and material quality, which comprises density [31, 51], toughness, hardness [31], young's modulus [51], and strength [31, 51].

Milling technology has an influence on the powder properties, i.e., mechanical and surface properties [52]. Mill type [32], the rotation speed (angular speed) of the mill and opening size of the screen [14] can control the particle size. The size dispersion of the particles becomes lower when higher rpm is used. The smaller opening of the screen generates finer particles compare to the bigger opening of the screen.

The properties of wood also contribute to the milling performance. For example, toughness inhibits the breakage of the wood. The toughness of wood is correlated with its density [23]. Researchers have observed that the higher density of pine (*Pinus sylvestris* L.) (258 kg m^{-3}) is more difficult to mill than the lower density of poplar (*Populus sp.*) (149 kg m^{-3}) [13].

Prediction of the mill ability of wood can indicate the energy requirement, performance and capacity of the desired mill. Researchers have adapted the Hardgrove grindability index (HGI) to know the grindability of the particular wood species and it indicates that the appropriate methods need to be considered prior to mill [53]. HGI was originally developed for coal types [54]. Bridgeman *et al.* [53] have checked the milling ability of <10 mm and >20 mm short rotation coppice willow (*Salix sp.*) chip (MC 8.9 %) by ball mill following the method of Agus and Waters [55] and Joshi [56].

1.3 Energy consumption in size reduction

The elasticity of lignocellulosic fibres in wood makes size reduction an energy-intensive operation. With energy expenditure comes cost and achieving fine powders from wood can be challenging [13].

The energy consumption depends on the MC of material and the target size of particles [26, 57]. Miao et al. have confirmed the relationship between high consumption and small particle size [58]. Temmerman *et al.* [57] have adapted milling theories from inorganic materials to wood with some success.

Moisture content plays a key role in the strength of wood and there is a strong relationship between wood MC and the extent of hydrogen bonding between organic polymers in its cell walls. Bonding decreases as moisture increases for the MC range between oven dry wood and its fibre saturation point [23, 24]. Moisture then causes a reduction in the strength properties of wood [25] and it enhances the breakage of wood during milling within this range, leading to lower energy consumption.

The specific energy consumption in relation to particle size has been relatively well studied. Holtzapple *et al.* [59] evaluated energy consumption from milling poplar (*Populus sp.*) wood chips (initial size 25.4 × 6.4 mm) in a two-stage double disc attrition mill, an attrition mill and hammer mill. They observed an electrical energy demands of: 656 kWh t^{-1} (2.36 MJ kg^{-1}) to obtain a 0.106 mm powder with the two-stage double disk attrition mill; 261 kWh t^{-1} (0.94 MJ kg^{-1}) to obtain a 0.850 mm powder with the attrition mill and 50 kWh t^{-1} (0.18 MJ kg^{-1}) to obtain a 2 mm powder by two-stage hammer mill. Similar relationships between energy and particle size were seen by Gil *et al.* [26] and Temmerman *et al.* [57]. These results demonstrate the elevated energy use required to obtain especially fine powders from wood.

The wood species also has an influence on energy consumption. A study on poplar (*Populus sp.*) and pine (*P. sylvestris* L.) milling showed that the required energy for producing 1000 µm mesh pass as 95 % weight product was 120 and 150 kWh t^{-1} DM, respectively, using a two-stage hammer mill. (11 kW and 15 kW with rotation speed 3000 rpm). The sizes, initial MC and bulk densities (based on arithmetic means) were 9.52 mm, 11.9 % and 149 kg m^{-3} and 12.1 mm, 14.3 % and 258 kg m^{-3} from poplar and pine chips, respectively [13]. The higher bulk density of pine chips (in part due to pine's higher density) was the attributed cause of the higher energy consumption compared to poplar. Repellin *et al.* [30] also compared the milling of two

wood species, spruce and beech, milled 2 to 4 mm chips using a knife mill followed by a centrifugal mill to obtain a 0.5 mm powder. Milling the spruce consumed 750 kWh t^{-1} while the beech consumed 850 kWh t^{-1} to achieve the target powder size. Although the authors did not consider the influence of the basic density, nor the bulk densities of the chips, on the energy used, they are likely important factors in explaining the observed differences. For example, the basic density of spruce (*P. abies*) (430 kg m^{-3}) [60] and beech (*Fagus sylvatica* L.) (752 kg m^{-3}) [61] wood differ appreciably.

Besides wood species, wood MC and selection of screen size also contribute to energy consumption during milling. Gil *et al.* [26] used a hammer mill with different screen sizes to reduce poplar chips to powders. The size and MC of the chips were in the range of 8.64 to 18.42 mm and 5.11 to 31.80 %, respectively. The energy consumption was 27.5 to 219 kWh t^{-1} to obtain particle sizes of 0.28 to 0.93 mm. In another study, Temmerman *et al.* [57] performed hammer milling of pine (*Pinus sp.*), spruce (*P. abies*), oak (*Quercus sp.*) and beach (*F. sylvatica* L.) wood chips with moisture contents of 1.1 to 22.4 % and maximum sizes of 4.93 to 7.38 mm using different screen sizes. They obtained minimum product sizes were 0.40 to 0.46 mm using 4.9 to 307 kWh t^{-1} of milling energy. Both of the above studies have reported the high-energy consumption associated with milling wet wood chips and the increase of energy consumption with the decrease in screen size. Although this can be predicted based on milling theory, the relationship between MC and the effective energy used on the feedstock is not clear. As wet materials cause clogging issues with the screens of hammer mills, the high energy use is a result of long duration milling (due to clogging) and not necessarily due to production of fine particles. This dilemma stems from the fact that hammer mills are not designed to mill wet wood.

It follows that milling technologies themselves influence the energy required to produce wood powders. Hammer mills required from 8 to 130 kWh t^{-1} to produce particle sizes of 1.6 to 9.5 mm from 19 mm hardwood chips having MC of 6 %, while energy consumption for disc mills ranged from 200 to 400 kWh t^{-1} for 1.6 mm powders [15]. This indicates that disc mill require more energy than hammer mills to achieve similar particle sizes. Karinkanta *et al.* [41] observed oscillatory ball mills required 100 to 380 kWh t^{-1} for 0.020 to 0.10 mm powders from 1 to 2 mm Norway spruce (*P. abies*) saw dust. Yet a classifier mill uses 1 664 to 38 160 kWh t^{-1} to obtain a 0.023 to 0.25 mm powder [42]. Jet mills require energy inputs of 12 981 to

29 703 kWh t^{-1} (47 to 107 kJ g^{-1}) to get 0.0199 to 0.0692 mm powders from pre-grinding Norway spruce saw dust of 0.193 to 0.205 mm [62]. Kobayashi *et al.* [47] milled 22 mm Norway spruce wood chips to a size of 0.15 mm using a vibration mill having an energy consumption of 800 kWh t^{-1} (0.8 kWh kg^{-1}). This shows that the oscillatory ball mill needs lower energy input compared to air classifier, jet and vibration mills.

1.4 Wood powder properties

Wood powder properties are important for end-use applications. Physical properties can be described by particle density, shape, size distribution, mean size, flow ability and moisture content for thermochemical conversion and pelletisation [63]. These physical properties are interdependent and may affect processing, transportation and storage operations in terms of cost and the feasibility [64-70].

1.4.1 Moisture content

Wood powder MC is an important parameter which affects quality itself, such as handling characteristics and flow ability [63] and processes in different ways [65]. High MC in wood powders lowers their heating value and influence the gasification and combustion of fuels in the boiler [65]. It also affects the filling or feeding in fluidised beds, feed hoppers as well as other equipment [67, 71].

Milling itself can alter the MC of the material. The MC reduction of the poplar (*Populus sp.*) wood powder (8.1 %) was 30 % during two stage hammer milling of poplar chips (11.8 %) [13]. Gil et al. [26] have observed a MC reduction in the range of 12.3 to 38.9 % during hammer milling of poplar wood. The authors have used different level of moisture content of chips (5.11 to 31.8 %). The MC reduction was 10.2 % for hammer milling of douglas fir (*P. menziesii* or *P. douglasii*) wood chips with moisture content of 12.8 % [63].

The reduction of MC depends on the type of mill, initial MC and target size of wood powder. Researchers have observed that hammer mills can contribute to reducing moisture content more than a knife mill [69]. Higher MC reduction occurs for smaller particles and higher initial MC of wood chips. In hammer mills, obtaining smaller particles takes longer retention times. Consequently, the MC reduction is higher for smaller particles. The

drying mechanisms are attributed to diffusion and capillary processes. The process starts when free moisture is evaporated from the surface by diffusion when warm air passes over the particle and then moisture in the material is transported to the surface. Evaporation takes place from the internal solid surface during the last stage of drying [72]. Wood particles break many times during the milling process and this increases surface area rapidly. The greater surface area enhances contact with conveying air, working as a drying agent in the chamber of mill and this creates better opportunity to evaporate moisture from the particle [35]. The other factors affecting drying are residential time of particles inside the milling chamber and the frequency of impacts [73, 74]. Heat is released for a single impact during milling [73, 74] and this heat is used within the mill chamber to evaporate moisture.

1.4.2 Particle size distribution

The particle size distribution (PSD) of a powder depends on the mill type used to produce it. For example, the two-stage hammer mill can produce <1 mm wood particle while knife mill produces <1.5 mm wood particle. Particle size is normally defined as the nominal diameter of the particle [63]. PSD is an important characteristic of a powder and has implication for downstream processes. For example, the burn-out time of fuel particles is dependent on size of that particle [63]. During the utilisation of fines as ignition primers, size distribution is an essential parameter to control the flame and flow criteria in fluidised beds [67, 70].

1.4.3 Shape

Particle shape factor is defined by two or three dimensions of the particle [63]. In general, two dimensions are inadequate for representing the shapes of irregular particles [69, 75]. Mohsenin [76] has used thirteen standard charted shapes to define the particles using a photograph or cross section of that particle. Schell and Harwood [34] observed different shapes of hybrid poplar wood particles from hammer and disk mills. Particle shapes tended to be needle-like and elongated for hammer mills, while disk mills produced shorter and broader particles. Paulrud *et al.* [69] found that hammer mills produced elongated, narrow, rectangular and regular shape wood powders from a mixture of pine and spruce wood. On the other hand, a knife mill produced short, broad and quadratic-shaped particles. Gil *et al.* [35] have observed rectangular, fibrous and hook-shaped poplar wood particles in

hammer milling. Kobayashi *et al.* [47] reports rounded particle shape from Norway spruce milled in a vibration mill. Tannous *et al.* [63] found that larger particles had a needle-like shape whereas smaller particles were close to spherical when milling Douglas fir (*Pseudotsuga menziesii* L.) in a hammer mill. Therefore, the milling technology, species, and screen size affect the resulting shapes of the wood powder. The shape of wood particles is also dependent on the particle size.

Shape is obtain described by shape factors such as aspect ratio and sphericity (Paper III). The aspect ratio can be defined as the ratio of particle length and particle diameter [68, 77] or alternately, the ratio particle width to length (Paper III).

Kobayashi *et al.* [47] have reported aspect ratios of <0.5 for Norway spruce wood powders produced by vibration mill. Karinkanta *et al.* [41] and Karinkanta *et al.* [42] have found the aspect ratio ranges of 0.56 to 0.69 and 0.29 to 0.43, respectively for Norway spruce wood powder obtained from oscillatory ball mill. The high aspect ratio was for the smallest particles. Norway spruce powder produced with a jet mill showed and aspect ratio range of 0.34 to 0.42 [62]. Vibration milled pine wood powder [48] and hammer milled Douglas fir wood powder [63] showed aspect ratios of 0.20 to 0.33 and 0.31 to 0.55, respectively.

1.4.4 Specific surface area

Researchers have also studied the specific surface area of wood powders. The specific surface area of willow wood powder milled by hammer mill [58], Norway spruce powder milled by oscillatory ball mill [42] and pine wood powder milled by vibration mill [48] was 0.01 to 0.10, 1.6 – 3.4, and 1.79 – 2.92 $m^2 g^{-1}$, respectively. The specific surface area is dependent on the size and shape of the particle. For a given mass of a powder, the specific surface area grows exponentially as the particle size decrease.

1.4.5 Bulk density

Bulk density is a measure of how much particulate mass is contained in a volume of space. It is often measured and defined in two ways; there is the loose (or poured) density and the tapped density [63, 69, 77]. Density determination depends on different factors include cylindrical vessel diameter [78], volume and mass of material, frequency of tapping, particle orientation [77, 79, 80], particle distribution [81, 82], particle length [83, 84],

particle density [81, 82] and moisture content of particles [77, 81, 82]. Bulk density has an influence on the flow ability, compressibility [85, 86], storage and transportation operations [87, 88].

The bulk density of hammer milled poplar and pine wood powder was 226 and 329 kg m^{-3} dry mass (DM) respectively [13]. Gil *et al.* [26] have observed the poplar wood powder milled by hammer mill in the range of 174 to 265 kg m^{-3}. Willow wood powder produced by hammer mill [58] and pine wood powder produced by knife mill [89] showed a bulk density range of 158 to 280 and 381 kg m^{-3}, respectively.

Tapped density values have also been reported in literature. Gil *et al.* [35] milled poplar wood by hammer mill with two different sieve sizes namely 5 mm and 2 mm. The poured and tapped bulk density of the particle for the 5 mm sieve was 166 to 172 kg m^{-3} and 176 to 204 kg m^{-3} and for the 2 mm sieve it was 197 to 211 kg m^{-3} and 214 to 262 kg m^{-3}, respectively. The increased tapped bulk density was 5.12 and 20 % for the 5 mm sieve, and 3.98 to 24 % for the 2 mm sieve. In another study, Tannous *et al.* [63] have found the loose and tapped bulk density of Douglas fir wood powder of 95 to 181 and 157 to 239 kg m^{-3}, respectively.

The milled wood powder has higher bulk density compared to initial raw material. The increment of bulk density was 11 to 97 % compared to the feed material for hammer milled poplar wood [26]. The increment of density was >50 % for poplar and 27 % for pine wood powder produced by hammer mill [13]. The reasons behind the increasing of milled product density are moisture content of input material, homogenized particle shape, resilient downsized particle and production of wide as well as well graded PSD by the hammer mill which have distinctive criteria of size distribution [26].

Bulk densities depend on particle density, particle shape, moisture content, inter-particle friction, applied pressure and the porosity of bulk powder [35]. Hook shaped particles have an interlocking tendency [90] and this type of shape is typical of larger particles, which worsen the rearrangement of the particles and decrease the bulk density [35].

1.4.6 Hausner Ratio

Hausner Ratio (HR) is the ratio of loose or poured bulk density and tapped density [91]. Tannous *et al.* [63] have measured the HR for hammer milled Douglas fir wood powder to be in the range of 1.31 to 1.85.

1.4.7 Angle of Repose

The angle of repose (AoR) is one key criteria of powders and refers to the angle between the inclination of free surface and the horizontal bulk solid pile. It is an indication of the interparticle friction [92]. It characterises the flow behaviour of powders [92] and granular materials [93]. It is correlated with many crucial criteria, which include stratification [94, 95], avalanching [96-98] and segregation [99-101]. For instance, the angle of repose was 45.27 to 52.05 º, 37.46 to 46.41 º, 45.61 to 51.65 º and 38.76 to 51.18 º for four different types of poplar wood powders [26]. The powders were produced with differing parameters using a hammer mill rpm and initial size of poplar wood chip. The controlling variables for AoR are moisture content [26], particle size [26, 100, 102], particle shape [103, 104], particle density [104] and bulk density [35].

1.5 Wood powder properties vs applications

The physical properties of wood powders, for example shape and PSD, are influenced by the mechanical milling process and are important criteria for using powders in different kinds of applications [4, 105-115].

1.5.1 Raw materials for composites

Wood powder is mainly used for composites called particleboards [116], and they are one of the most important wood-based products in Europe [117]. The first commercial wood powder composite was made in 1916 [118]. Global particleboard production is at 93 Mm^3 and comprises 2.2 % of total global wood production [119]. There are important criteria for these feedstock, for example, low density, strength properties, flexibility and cost effectiveness are the main criteria for using wood powder in composite products [120]. The binding agents of wood powder composites are adhesive i.e., UF (urea formaldehyde) [117, 121-125], epoxy-resin [126], PF (phenol formaldehyde) [127, 128]; thermoplastic i.e., polyethylene, polypropylene, polystyrene, polyvinyl chloride, polyethylene-terephthalate [108, 113, 118, 120, 129-141]; natural adhesive [142, 143] and Portland cement [144-151]. There is no need for binding agents in particleboards from wood powder [152]. Recently, wood plastic composites have become more popular. The range of wood powder for wood powder plastic composites is 0.18 to 0.45 mm [118].

Wood powder morphology, i.e., size and shape, has a great impact on the quality of wood-based composites [128, 146, 152]. The size of the particles affects the physical and mechanical properties of the board [121, 124, 150, 153, 154]. The finishing of composites made from smaller particles is smooth and uniform in appearance [118]. Larger particle increases the strength properties significantly [108, 123, 124, 130, 132-134, 141, 145, 155]. On the other hand, Jaya *et al.* [135], Rasat et al. [139], Leu *et al.* [156], Khalil *et al.* [136], Takatani *et al.* [113] and Maiti and Singh [138] have investigated that smaller fractions of wood powders enhance the strength properties of the composite in comparison to composite fabricated from larger size wood powder. The internal bonding [124, 153, 154] and water absorption [113, 124] were higher for smaller particle compared to larger particle but water absorption is higher for larger particles in other studies [134, 136, 137, 155]. Rimdusit *et al.* [140] have reported that the suitable size of wood powder for better mechanical properties is 0.20 to 0.30 mm but the wood powder size <0.125 mm is the best for the composite quality investigated by other researchers [156]. Shape of the wood particles also affects the quality of board [146]. There is also a positive correlation between aspect ratio of the particles in the powder and the strength properties of the composite [108, 132, 137].

1.5.2 Power generation

Wood is often combusted as a powder or a pellet at power plants [20]. The size of wood powder for combustion is dependent on the type of boiler, for example, fluidised bed or fixed bed and feeding position, such as, in-bed, under-bed or over-bed [157]. The size of wood powder influences the residence time [158-160] and its thermodynamic conversion in the burner [14]. The volatile yields decrease with the increasing of particle size [109] and both particle size and shape have an influence on the devolatilisation time [161]. Particles smaller than 0.1 mm play an important role on flame stability in wood powder burners [14]. Typical size of woody biomass particles are 6 mm for combustion process [162] but the co-firing of wood powders with coal generally require particle size <1.0 mm [13, 163]. Wood particles larger than 3 mm in co-firing applications significantly increase the probability of incomplete combustion [160, 164]. According to Adams *et al.* [105], wood powders, <0.1 mm, are also crucial for ignition time.

1.5.3 Wood pellet production

Wood powders are used as a feedstock in the production of wood pellets [20]. The motivation for pelleting include the heterogeneous structure [165] and the low bulk density (154 to 165 kg m^{-3}) of woody biomass [166] which causes poor handling [165] and storing [167]. These can be overcome though densification [163, 168]. The densification process can be categorised into three types, i.e., extrusion, briquetting and pelleting [168]. Pelleting of woody biomass is popular [165], and wood pellets are common secondary fuels for co-firing with coal in coal-fired boilers [163]. Pellets are also of interest for conversion via gasification [169]. The global production amount of wood pellets is 39.36 Mt and this accounts for 1.2 % of global wood production [170].

The particle size in powder influences the durability of pellets [171-173]. Small particle diameters (<2.0 mm) enhance the mechanical properties of the pellet. The smaller particle has big surface area, which results in stronger bonding in the pellet matrix [171]. On the other hand, small particles (<1 mm) can also dry out easily during pelletisation causing reduced strength. Feedstock with particle diameters below 0.5 mm, however, have a negative impact on pellet quality [165]. In practice, most pellet producers use powders that have between 2 to 4 mm particle diameters. Some studies have shown no differences in some pellet characteristics (e.g. bulk density) over this range [171].

1.5.4 Pulp and paper industry

Wood powder is widely used as organic filler in paperboard manufacture, such as duplex board [8], and in papermaking [9]. Utilisation of wood powders can reduce production cost by increasing the bulk and decreasing the consumption of steam [174]. Wood powders may play a role of enabling better remove the water. Thus, it can contribute to the reduction of steam use. Incorporation of wood powders also has a negative impact on strength properties of paper products, for example, burst strength, breaking length, stiffness and compressive strength [8, 175] but these can negotiated through modifying surface of the powders with starch [8]. Wood powder is also used as organic pigment [176]. Wood powder is used in filter paper and it increases the absorption and adsorption capacity of filter paper [177, 178]. Seo *et al.* [179] has conducted research on using wood powder as coating material in combination with calcium carbonate but brightness and strength

properties, except for stiffness, are poor. The authors have claimed that the use of <200-mesh screen wood powder can improve the properties. Application of wood powder as a filler instead of traditional inorganic filler can solve the problem of recycling, wearing of equipment parts and calendaring pressure in papermaking process [176].

The size of the powder is important if used as an organic filler in pulp and paper industry. The most likely size of wood powder for using as organic filler is 0.01 to 0.10 mm [12]. Sami *et al.* [176] has reported that the size of wood powder is 0.002 to 0.021 mm for employing as a pigment. Navarre *et al.* [177, 178] have concluded that the appropriate size of wood powder is 0.001 to 0.150 mm for applying as a filler in filter paper. To use as a coating material together with calcium carbonate, 200 mesh of wood powder is not good enough and the size should be more smaller than 200 mesh with bleaching for getting better brightness and strength results [179].

1.5.5 Feedstock for biorefining

A biorefinery is a facility, which is composed of equipment, methods and processes for the conversion of biomass (wood and non-wood) to chemicals, power and fuels [180]. Woody biomass is one of the most important lignocellulosic feedstock for biorefining [180]. The macromolecular components of wood, hemicellulose, cellulose and lignin, can be converted into different types of fuels and chemicals [180].

Biofuels

The pathways for the production of biofuels from woody biomass are fermentation after saccharification (acidic or enzymatic hydrolysis), pyrolysis and gasification after size reduction of wood [180].

Fermentation is the technique to convert sugar into ethanol by microorganism [180]; sugar is extracted from wood by acid hydrolysis [180] or enzymatic hydrolysis [115, 180, 181] of cellulose and hemicellulose of wood. On the other hand, cellulose is the main source of sugar in wood and well-studied in literature [182-184]. The lignin and hemicellulose content affect the enzymatic digestibility of wood [185-187]; the efficiency of enzymatic digestibility can be improved by removing hemicellulose [186] and lignin [106, 181, 184, 186, 188]. The removal of lignin entails the accessibility of enzyme to cellulose by creating pores and increasing internal surface [182]. On the other hand, Leu S.-Y. and Zhu [189] have concluded

that removal of hemicellulose is more effective than removal of lignin to create pores for enzyme to get access to cellulose. Cellulose crystallinity affects the hydrolysis of cellulose [106, 107, 182, 185, 187, 190-192], but the modification of cell wall of wood has a more positive impact on cellulose hydrolysis [182]. Particle size and milling type, which has contribution on size reduction and cellulose crystallinity, affect the digestibility of lignocellulosic biomass [107]. Smaller particle sizes increase the surface area and this increases the available surface area for reactions, causing a higher efficiency of hydrolysis [193-195]. The smaller the particle size of wood powder, the more decrease in cellulose crystallinity with higher surface area, which influence the hydrolysis of wood powder [15]. Effective hydrolysis requires a particle size of 1 to 2 mm [15]. Dasari and Berson [196] have observed a similar trend that finer red-oak (*Quercus rubra*) wood powder (sawdust) is better suited to enzymatic hydrolysis; 0.033 to 0.075 mm provided more glucose in comparison to larger sizes. Morphological variation in wood powder, for example, breakage of cellulose and lignin bonds, can enhance enzymatic hydrolysis [197].

In pyrolysis, wood is heated in the absence of oxygen and bio-oil is one of the products produced. It is used for the production of heat and electricity [180]. There are different types of pyrolysis, such as, bubbling fluidised bed, microwave pyrolysis and fixed bed fast pyrolysis. Fast pyrolysis of wood, at 500 ºC and 1 s, can yield 75 % bio-oil and smaller particles enhance the reaction [198]. Particle size and shape of wood powder influence the rate of heating, drying and reaction [109].

Gasification of wood is another process for producing biofuels [180, 199]. There are two types of gasifiers, i.e., fixed and fluidised-bed; the heating agents for gasification are air, oxygen and steam [180]. Gasification product is syngas (CO and H_2), which is used for producing fuels to generate power [169, 180]. Wood powder size and shape affect the gasification efficiency of gasifier [200]. The optimum size of wood powder is 3 to 50 mm for fixed bed gasifier, while the size restriction of wood powder is 0.1 to 5 mm but it can be 1 to 2 mm for fluidised-bed reactors [180].

In addition to these, hydrothermal liquefaction (HTL) is another technique to produce bio-oil from wood powders. In this case, the concentration of wood powder is 15 % (mixed with water) and pH is adjusted by adding Na_2CO_3. The mixture is heated up to 350 ºC with pressure 20 MPa

for 15 min and then, the bio-oil is extracted from the aqueous phase and solids [201].

Chemical products

Furfural and furans can be achieved by degradation of hemicellulose during hydrolysis of wood [184]. Tar is one of the chemical products of wood during pyrolysis of wood powder. The particle shape and size affect the yield of tar; near-spherical shape with similar mass and smaller size of all shapes wood powder increase the yield of tar [109]. The gasification of wood powder can also provide chemicals [169, 180]. Lignophenols are derived from grafting monomeric phenols with propane units of native lignin; these lignophenols are used for producing different type of value added products [202, 203]. Meanwhile, this native lignin is derived from milled wood [204]. For the extraction of lignin, smaller size is important; Funaoka and Fukatsu [205] and Funaoka *et al.* [206] have used 80 mesh and Radotić and Mićić [207] have mentioned the required size of wood powder for extracting lignin is 0.25 to 1.0 mm.

1.6 Potential applications of wood powder

As the bioeconomy evolves, wood powders will find more and more uses in consumer and smart products. Some potential future applications are presented in this section.

1.6.1 Source of food

Cellulose is the main component of wood and a plentiful global resource, which can be recycled from wood products and be a potential source of food for humanity. Superfine powders from woody biomass is the starting point on a pathway for functional food, an example dietary fibre [40].

1.6.2 3D printing

3D printing is a promising technology in the near future; low cost customised products can be printed and the process can be profitable as well [208]. Interest has been growing in 3D printing since 2013; it is the latest technology to use raw materials efficiently [209]. Wood powders can be used in the 3D printing process as an additive with others material, for example,

lignin, polyhydroxyalkanoate (PHA), nanocellulose, colour master batches, and talcum, to produce wood-based products, such as a wrist watch [209].

In previous studies, wood powder has been used as additive 3D printing [209-213]. The use of wood powder is cost effective and environmentally friendly by replacing synthetic origin resin [211]. The particle size of the powder should be small; powders with ultra-fine size are used as wood filled filament for 3D printing [209].

Kariz *et al.* [211, 212, 214] and Tao *et al.* [215] used 0.237 mm beech wood (*F. sylvatica* L.) and 0.014 mm aspen wood powder for 3D printing, respectivley; spruce wood powder (0.8 to 2 mm) as bulk material was used in 3D printing process [210]. As per findings, researchers reported that the physical properties, for instance, moisture content, swelling and mechanical properties, such as, modulus of elasticity were degraded using wood powder as an additive [212]. On the other hand, Kariz *et al.* [214] observed that a smaller portion (10 %) of wood powder helped to get higher tensile strength in the product. Tao *et al.* [215] observed the lower temperature of thermal degradation with wood powders, although without affecting the melting temperature. Poor strength properties stems from the formation of voids and clusters of powder within the bulk of the structure [214]. Tisserat *et al.* [213] have observed poor internal bonding between wood powder (*Maclura pomifera* and *Paulownia sp.* wood) and polylactic acid, which reduces the tensile strength of filaments for 3D printing. However, the effect of printing parameters and wood particle quality, including wood species, need to be better characterised to identify suitable composition for wood powder used as 3D printing filaments [214].

1.6.3 Water treatment

There is great interest in developing cheap water treatment [216] and renewable lignocellulosic materials may permit a low cost for water treatment chemicals [216, 217]. Wood powder (saw dust) has been widely studied for removal of organic pollutants, such as, fats [218] and inorganic pollutant, for example PB (II), Ni (II), Cd (II) [219], U, Co, As, V, Sb, Ni [220], NO_3^- [216, 220, 221], SO_4^{2-} [220], Cr (VI) [222], Cu, Zn, Fe [223]. Authors have used pine (*Pinus sylvestris* L.), red fir (*Abies magnifica*), spruce (*Picea abies* Karst. L), oak (*Quercus sp.*), poplar (*Populus sp.*), cherry (*Prunus avium*), ash (*Fraxinus excelsior*), hornbeam (*Carpinus betulus*), balsa (*Ochroma pyramidale*), lauan (*Toona calantas*) and walnut (*Juglans*

sp.) powders. Ucun *et al.* [224] and Bagherifam *et al.* [225] have also used ground cone pine wood and pine wood, respectively to measure the efficiency of removing Cr (VI) and U (IV) from solution. The physical and chemical characteristics of wood are responsible for the absorption of pollutants from water [217, 218]. The presence of carboxylic, phenolic and hydroxyl groups are the key mechanisms for absorption of heavy metals [219, 222, 223, 226]. Surface modification has also been carried out to absorb pollutants from water [216, 218, 221, 225]. The absorption efficiency is dependent on the properties of wood powder; particle size and surface area of wood powder are the key parameters for the efficacy of absorption of water pollutants [6]. The used particle sizes in previous studies is in the range of 0.09 to <2 mm [6]. Reported surface areas of wood powders range from 0.72 to 1.44 m^2 g^{-1} [6, 222, 225].

1.6.4 Nanocellulose production

Wood powder is also a potential feedstock in the emerging field of nanocomposites. Research on extracting nanocellulose to develop bio-based nanocomposites for advanced applications have been carried out. For example, nanocellulose obtained from <60 mesh poplar (*Populus ussuriensis*) wood powder was used to develop conductive nanocomposite [227]. In another study, nanocellulose extracted from 60-0 mesh poplar wood powder was used to apply in wound dressing and tissue engineering [228]. A bio-based adhesive was made from nanocellulose obtained from <0.2 mm beech and spruce wood [229]. Jonasson *et al.* [230] characterised the nanocellulose produced from hybrid aspen (*Populus tremula* x *tremuloides*) wood powder.

1.7 Experimental design and statistical analysis

Statistical tools have been used to study the size reduction of wood and to illuminate relationships between size reduction process parameters and resulting powder characteristics. Jiang *et al.* [22] studied the impact of feedstock moisture content on powder PSD using Tukey's model with SAS 9.0 software. Others have looked at the correlation and model fitness for energy consumption, Hausner ratio, and Carr-compressibility index concerning particle size using Levenberg-Marquardt's non-linear regression model [28]. The relationship between energy consumption, powder moisture

content and particle size have also been studied using backpropagation (Levenberg-Marquardt) algorithms in artificial neural network (ANN) models [26].

1.7.1 Design of experiment

The design of experiment (DOE) method is used to minimise the number of tests to perform in order to obtain useful data for resolving issues. DOE is considered for the screening, optimisation and robustness testing. The most contributing factors along with their ranges are identified in the screening design. The combined effect of influential factors for optimising the operation conditions is analysed by the optimisation design. The influence of changing of factors setting on the desired result is investigated using robust design.

DOE facilitates the experimenter to conduct the research in an organised way. It supports to set up the experiments based on the objectives. Although it offers a number of experiments, it provides accurate information by the interaction effects of the factors. The model accuracy confirms the influence of factors and the intensity is described by the regression coefficients. Contour plots assists the explanation from a range of possible settings. A screening design with DOE can add value to detect the factors and target settings for further investigation in details.

1.7.2 Modelling

A liner regression model explains the relationship between a single independent and dependent variable. A multi-linear regression (MLR) model, on the other hand, expresses the relationship between the multiple independent variables and dependent variable (often denoted as *response*) [231, 232]. It also known as multiple regression. It develops a single equation using the used variables to predict the intensity of independent variables [232]. It considers the linear relationship between independent and dependent variables and non-correlation between independent variables. The independency between observations, equal variance of independent variables and normal distribution of errors are also considered during developing MLR model. MLR interprets the results with coefficients, R^2 (coefficient of determination) values, significance, confidence intervals and residuals. Coefficient is the change of dependent variable with the changing of independent variable. R^2 values indicates the explanation of variability of

dependent variables by the independent variables. The p-values measures the level of significant of model and coefficient. Confidence intervals is the range of values where the true population should be. Residuals are the values obtained from the difference between predicted and actual values and it should be normally distributed for a good fit of the model.

Projections to latent structures or partial least squares (PLS) is used to make a model using all the independent and dependent variables [233]. It can accept the collinearity among the variables. In general, a design unfit for MLR can be analysed by PLS. MLR relies on the orthogonality while PLS can handle if it is distorted. The condition number represents the model behaviour and it ranges from 10 to 20. Beyond this range, the model is unfit for MLR and PLS can be used to generate a well explained model. Furthermore, PLS can manage the missing values of responses but it is not possible for MLR. PLS model is interpreted using scores, loadings and variable importance of the projections (VIP). Scores represent the general trend, outliers and groups of observations. Loadings express the correlation between two variables. VIP uses all variables with weighted summary [234]. Principal component analysis (PCA) is an unsupervised method that studies the maximum differences in variability of the X variables. PLS/OPLS models iteratively the co-variance between an X variable matrix and one or more responses. In orthogonal projections to latent structures (OPLS), the systematic variation are separated into correlated (predictive towards a response) while the uncorrelated (orthogonal) variation is left out. This enables easier interpretation since all co-variation is collected in one predictive component. Additional information of the analysed system can be gained by studying the orthogonal components which can include systematic variation unrelated to the studied response. Orthogonal projections to latent structures discriminant analysis (OPLS-DA) model provides the class information. It explains the difference between two groups and possible reasons are responsible between the variables [235].

1.8 Objectives of the study

The overall objective of thesis was to investigate the milling performance of a multi-blade shaft mill and to characterise the wood powders produced using this new technology. The specific research objectives were to:

- Describe the influence of the milling parameters and the moisture content of wood input material on the resulting powder properties using a series of designed experiments
- Investigate the energy consumption of the mill in relation to the obtained particle size distributions of powders and how the shape of input materials affects energy consumption
- Develop valid multilinear regression models to describe the mill performance
- Characterise particle size distributions of produced powders using mechanical sieving and other physical properties using standard methods and compare them to powders produced using a hammer mill
- Characterise particle size distributions and particle shape properties using two-dimensional image analysis
- Describe and compare the characteristics of MBSM and hammer powders using staining methods and light microscopy

2. Materials and methods

2.1 Preparation of raw material

Scots pine (*Pinus sylvestris* L.) thinned trees of 22 to 32 year-old were procured from a plantation forest, Vindeln, Sweden in September 2019. Defect-free, straight, and similar diameter trees were selected from the site and delivered to the Biomass Technology Center (BTC), Swedish University of Agricultural Sciences, Umeå, Sweden (Figure 2).

Figure 2: Procurement of trees.

From the procured trees, 47 (27 for MBSM and 20 for hammer mill) were selected based on diameter, straightness, and presence of similar type of knots (Figure 3).

Figure 3. Grading (a) and selection (b) of trees.

Logs of 1.7 m length were cut from the bottom of the selected trees to minimise the tapering of the stem. The range of stem diameter between top and bottom was 10 to was used to debark the log. This was done carefully to avoid 14 cm. To avoid contamination, i.e., chain-oil, a hand saw was used. A drawknife removing stem wood (Figure 4). To adjust the log moisture content for experiments, drying at 25 ºC was carried out on selected logs in a drying cabinet (Elvärmedetaljer, Skurup, Sweden). The moisture content of cross-sectional discs which were cut from either end of the log were used to setup the experimental design. Three moisture content (MC) levels were defined; 11 to 24 %, 26 to 31 %, and 38 to 51 % wet basis (wb). The logs were wrapped in plastic to preserve the MC level. The final log length used in the experiments was 1.6 m.

Figure 4. Debarking using a drawknife (a) and the debarked log (b).

Ten pine (*P. sylvestris* L.) boards were obtained from a local sawmill (Sävar såg, Norra Timber, Umeå, Sweden). Their average age was 60 (standard deviation = 18) years, determined by counting the annual growth rings. The boards were resized to

a dimension of approximately 1100 × 150 × 50 mm. Selected boards were dried and stored as mentioned above. The defined MC levels were 13 to 16 %, 20 to 24 %, and 21 to 33 % (wb).

2.2 Milling technology

The prototype multi-blade shaft mill (MBSM) (Klingmill AB, Torshälla, Sweden) had a roller table, a feeding section, and outlet for the collection of the produced powder (Figure 5a). The mill accepted log diameters up to 280 mm. The milling principle relies on two 350 mm-wide bladed shafts, each driven by an electric motor with a rated power of 55 kW and speed of 1480 rpm. The blades on the first and second shaft consisted of eight and 24 teeth, respectively. The blades' teeth clearance angle was 18°, rake angle 5° and kerf 4.2 mm for the first shaft. For the second shaft, rake angle and kerf were 15° and 3 mm, respectively. For all the experiments, the feeding direction was constant, whereby the lower edge of the log was tangential to the perimeter of the blades on the first shaft (Figure 5b).

For comparative purposes, a hammer mill (Bühler Hammermill Vertica, Switzerland (DFZK 1) was used. It consisted of a vertical grinding shaft, an electric motor, floating hammers, and a 2 mm circular sieve. The motor capacity was 55 kW at 1480 rpm. The hammer configuration was 12 × 4.

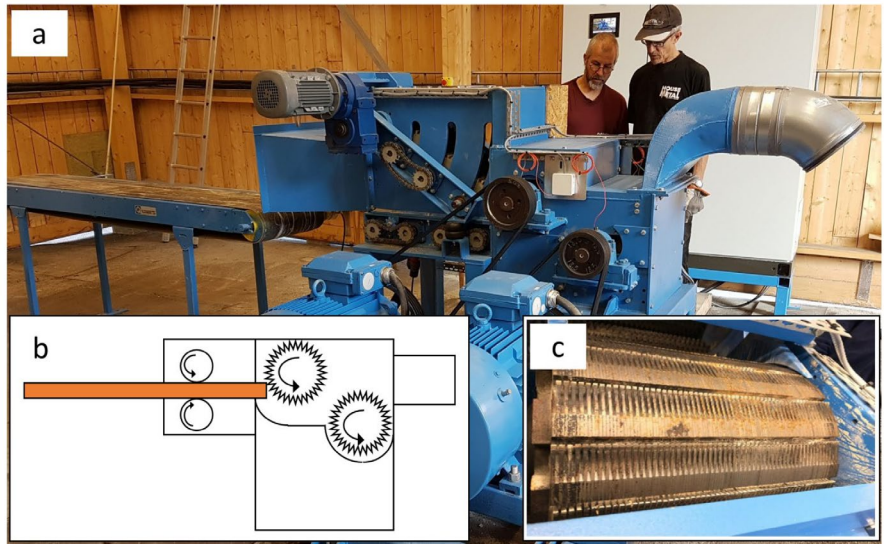

Figure 5. (a) The prototype multi-blade shaft mill (MBSM) without its housing enclosure. The roller table, feeder and the two shafts connected to the motors are visible. The sample collector is not fitted to the outlet in the photograph. (b) The principle of operation of the MBSM and (c) the multi-blade shaft (Paper I).

2.3 Experimental design and procedure

A full factorial (two-level) experimental screening design with one centre point having three replications was used for the milling experiments. There were three variable factors, MC, feeding speed, and sawblade speed (Table 1). The ranges of MC, feeding speed, and sawblade speed for log milling were 10 to 50 % (wb), 1.3 to 2.6 m min^{-1}, and 52 to 72 m s^{-1}, respectively. For board milling, the ranges of MC, feeding speed (FS), and sawblade speed (BS) were 13 to 33 % (wb), 1.3 to 2.3 m min^{-1}, and 52 to 72 m s^{-1}, respectively. The responses for log milling were specific milling energy (kWh t^{-1} DM), the wood powder particle size distribution (PSD, mass %), and the wood powder bulk density (kg m^{-3} DM) while it was solely specific milling energy (kWh t^{-1} DM) for board milling. A method of trial and error was applied to set the range of experimental factors.

The milling was performed according to a random run order from the experimental design, ensuring that the centre point experiments were

dispersed; one at the start, one near the middle, and one at the end. Before milling, each log/board was weighed and its length recorded and a bag was installed for sample collection. The logs/boards were fed via the roller table to the centre of the MBSM feeding section. A data acquisition system (INTAB PC-logger 3100) was used to record the electrical power (kW) and mill setting factors at 1 Hz frequency. After each milling, the sample bag was removed, sealed, and weighed followed by a cleaning of the mill. The mass of the remaining (unmilled) log/board end was recorded to obtain the correct mass balance. The length of the milled log/board (with end length subtracted) was used to determine feeding speed.

For hammer mill experiments, 20 logs were debarked and fed to a chipper (Edsbyhuggen, Woxnadalens Energi AB, Sweden). The chips were dried in an in-house-built flat-bed dryer to obtain a moisture content of 7.2% (wb). The chips were then screened (EO554, Fredrik Mogensen AB, Sweden) to an accepted size of 1.9 to 16 mm. The chips were then hammer milled with a 2 mm screen. The electrical power (kW) of the chipper and hammer mill was recorded at 1 Hz by a power logger (Fluke 1735, Fluke Corporation Everett, WA USA). An overview of the procedure is shown in Figure 6.

Table 1. Experimental design.

Experiment Name	Run Order	Factors		
		Moisture content (%)	Feeding speed (m min^{-1})	Blade speed (m s^{-1})
N1	21	13.1	1.32	52
N2	5	46.4	1.32	52
N3	14	13.6	2.28	52
N4	23	41.7	2.16	52
N5	25	16.8	1.26	72
N6	9	44.0	1.32	72
N7	8	16.0	2.64	72
N8	11	41.8	2.28	72
N12	18	13.8	1.38	52
N13	6	46.3	1.32	52
N14	28	13.8	2.22	52
N15	7	51.4	2.22	52
N16	20	13.0	1.44	72
N17	10	42.0	1.32	72
N18	22	13.2	2.4	72
N19	16	38.1	2.64	72
N20	5	11.8	1.38	52
N22	15	30.7	1.86	62
N23	17	11.0	1.38	52
N24	4	42.6	1.32	52
N25	13	24.0	2.28	52
N26	27	43.3	2.16	52
N27	24	13.0	1.38	72
N28	3	45.4	1.38	72
N29	12	15.5	2.28	72
N30	19	41.3	2.28	72
N31	29	28.9	1.8	62
N33	2	25.6	1.86	62

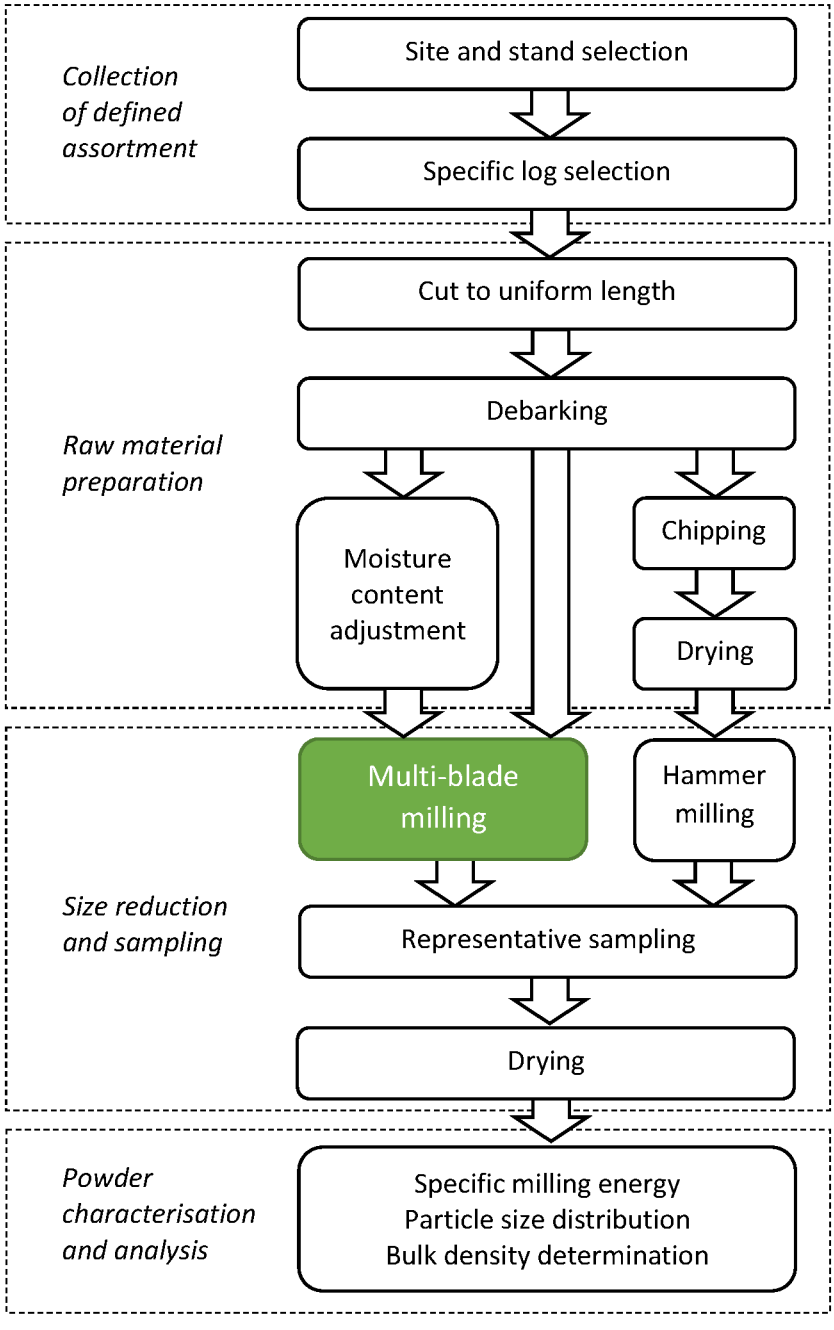

Figure 6. An overview of the experimental procedure used in the study (Paper I).

2.4 Sampling

All wood powders were collected and sampling was carried out using the systematic coning and quartering method (SS-EN ISO 14780:2017). All samples were dried at 105 ºC overnight within 20 minutes of milling except those for extractive, micromorphological, and cytochemical analyses (including cross-sectional discs) which were stored at -20 ºC. The dried samples were sealed in the plastic bag separately for further analysis. The MC of wood powder was used for determining the log MC.

2.5 Analysis of powder properties

2.5.1 Particle size distribution

The particle size distribution (PSD) was measured based on the mass per cent according to the standard method (EN 15149–2:2010) using sieves (Cisa, Spain) with a sieve shaker (Analysette 3, Fritsch, Germany). The standard (ISO-3310.1) sieve sizes were 0.063, 0.125, 0.25, 0.5, 1.0, 1.4, 2.0, 2.8, 3.15, 8.0 and 16.0 mm. A 0.5 to 0.7 L wood powder sample was used and the shaker was set at 1.5 mm amplitude for 10 min, selected by trial and error. The total mass of wood powder and the mass of each fraction were measured. These were used to calculate the mass per cent of each size fraction. PSD was determined in triplicates for each of the 27 MBSM samples and hammer-milled samples.

2.5.2 Powder bulk density

The bulk density (BD) (kg m^{-3} DM) of oven-dried wood powders was determined following the standard method (EN 15103:2009). Both the loose and tapped bulk densities were measured. A 5.4 L cylindrical vessel was used for measuring the bulk densities. For tapped density, the wood powder was compacted using the sieve shaker using an amplitude of 1.5 mm for 20 min. The Hausner ratio (HR) is the ratio of the tapped density to the loose bulk density.

2.5.3 Image and BET analysis

The powder samples used in image analysis and Brunauer-Emmett-Teller (BET) surface area analysis were screened to exclude particles larger than 1.0 mm using a sieve shaker (Analysette 3, Fritsch, Germany) and were then

divided with a rotary sample divider. The used amplitude and duration for the screening were 1.5 mm and 10 min, respectively.

A 2D image analyser (Camsizer XT Particle Analyser, Microtrac Retsch GMBH, Germany) with software (Camsizer XT 6.3.10, Microtrac Retsch GMBH, Germany) was used to determine powder PSD and particle shape at the Department of Engineering Sciences and Mathematics, Luleå University of Science and Technology, Luleå, Sweden. The used size detection range was 0.001 to 3 mm. Analysis was carried out in triplicate using sample sizes of 2.8 to 6.1 g.

BET analysis was performed by Celignis Analytical, Ireland, using a surface area and pore size analyser (NOVA 2200e series, Quantachrome Instruments, Boynton Beach, USA). These measurements were carried out on two MBSM powders, those having the highest and lowest bulk density, and hammer mill powder. The sample size was 1.1 to 1.3 g.

2.5.4 Micromorphology and extractive distribution

A variety of microscopical histochemical techniques was applied to analyse the extractive distribution in produced powders and their morphological properties. Stains were used for visual analysis of micromorphology and extractives; Saffranin for micro-morphological, Nile blue for neutral triglycerides, Sudan black B for total lipids and osmium tetroxide for unsaturated fats. The extent of Micro-structural distortions in powders was analysed using polarized light microscopy.

Saffranin for morphological analysis

Non-dried powder samples were removed from the storage (– 20 ºC) 15 to 20 minutes before preparation at room temperature. Samples were submersed in a 0.1% Saffranin solution for 3 to 5 minutes and the excess stain was removed by pipette. Samples were then rinsed three times with ultra-pure water, the excess being removed with pipette. The samples were placed on glass slides, and glycerol-gelatin was added. A cover slide was placed over each sample.

Nile blue staining for triglycerides

Non-dried powder samples were removed from the storage (– 20 ºC) 15 to 20 minutes before preparation at room temperature. The wood discs were removed from the storage (– 20 ºC) 2 h before preparation at room

temperature. Wood blocks (approx. 1 × 1 × 1 cm) were cut by hand saw and soaked in ultra-pure water before sectioning (7 to 10 µm) using a microtome. Solutions of 1% aqueous Nile blue, ultra-pure water and 1% acetic acid were heated separately at 37 ºC for 10 to 15 minutes. Each sample was submersed in Nile blue and heated at 37 ºC for 5 minutes followed by excess removal with pipette. It was then rinsed three times with hot ultra-pure water followed by removing the excess with pipette. AA was added to the mixture, which was then heated at 37 ºC for 30 s with removal of the excess with pipette. Finally, it was rinsed three times with hot ultra-pure water followed by excess removal. The samples were placed on glass slides and mounted with glycerol-gelatin followed by covering with a slide. Light microscopic analysis was done following the similar methods discussed above.

Sudan black B for total lipids

Samples and sections were rinsed with a 70 % ethanol solution for a few seconds and the excess ethanol was removed with pipette. Samples were then submersed in Sudan black B/ethanol solution (70 %) and the mixture was left to stand for 25 minutes. The excess was then removed with pipette followed by rinsing with 70 % ethanol solution for 1 minute followed by excess removal. It was then rinsed once with 50 % ethanol and twice with ultra-pure water. Excess ethanol and water were removed. Samples were mounted with glycerol-gelatin as above.

Osmium tetroxide for unsaturated fats

Samples and sections were submersed in a 1% aqueous osmium tetroxide solution (w/v) for one hour. The excess osmium tetroxide solution was removed with pipette. Rinsing was done four times with ultra-pure water with excess removal. The samples were mounted as above.

Micro-structural deformation

For micro-structural distortions within fibre walls, wood powders were processed using the above method except any staining applied. Samples were submersed in ultra-pure water for five minutes, followed by removing the excess amount of water with pipette. They were mounted as above using glycerol-gelatin.

All prepared slides were visually analysed by light microscope (Leica DMLB). Analysis of fibre cell wall deformations used a polarised light

source. Digital images of the samples were taken using Infinity X-32 digital camera and processed using Leica IM50 Image Manager software.

2.5.5 Angle of repose

The apparatus used to determine angle of repose has been described [28] and consists of a graduated vertical wall attached at right angles to a horizontal plate. Powders were fed to the apparatus through a funnel above a vibrating channel. Particles fall from the channel onto a chute attached with funnel, at 45 ° to the plate, and pile up on a plate to form a half cone whose height and base radius are used to calculate angle of repose. Powder samples were first screened using a 1.0 mm sieve to avoid flow interference from oversized particles. The powder sample size used for measuring the angle of repose was 60 to 65 g. The angle of repose (AoR) is calculated using Equation 1 in which h_p (mm) is the height and r_p (mm) is the radius of the pile of powder.

$$AoR\ (^o) = Degrees\left[ATAN\left\{\left(h_p \times 4\right)/\left(r_p \times 2\right)\right\}\right] \quad (1)$$

2.6 Milling energy

The specific milling energy for MBSM milling e_M (kWh t^{-1} DM) was calculated using Equation 2, in which m_M (kg DM) is the dry mass of the milled log, t_M (s) is the log milling time, P_f (kW) is the feeding power of the log and P_m (kW) is the milling power of log.

$$e_M = m_M^{-1} \sum_{t_M} \left(P_f + P_m\right) t_M \quad (2)$$

The specific milling energy for hammer milling e_h (kWh t^{-1} DM) was calculated using Equation 3, in which m_h (kg DM) is the dry mass of the hammer-milled wood powder, t_c (s) is the chipping time, Pc (kW) is the chipping power, t_h (s) is the hammer-milling time and P_h (kW) is the hammer-milling power.

$$e_h = m_h^{-1}\left(\sum_{t_c}\left(P_c \times\ t_c\right) + \sum_{t_h}\left(P_h \times t_h\right)\right) \quad (3)$$

2.7 Powder yield

The yield of powder *Yp* (%) for MBSM milling was determined using Equation 4, in which D_{mp} (kg DM) is the dry mass of powder and D_{ml} is the dry mass of log.

$$Y_p(\%) = \left(\frac{D_{mp}}{D_{ml}}\right) \times 100 \quad (4)$$

2.8 Modelling and analysis

MODDE Pro-12 software (Umetrics Sartorius, Umeå, Sweden) was used to develop models based on responses and factors using multilinear regression (MLR) analysis. SIMCA 16 software (Umetrics, Umeå, Sweden) was used for evaluating the wood particle aspect ratio and its effect on bulk density based on orthogonal partial least squares (OPLS) projections to latent structures [233] and orthogonal partial least squares discriminant analysis (OPLS-DA) [235]. Aspect ratio data were selected for PSDs of 50 to 500 µm. Based on the manufacturer of the Camsizer, values outside of this range were not deemed statistically reliable. According to UV-scaling in SIMCA, all data were mean centred and scaled to equal variance. Aspect ratio was put in a vector (X) as factor and powder bulk density considered as a response was put in a vector (Y). There were two groups denoted as class 1 and 2 based on initial wood MC. General trends and patterns in the data and outlier detection were evaluated by an initial principal component analysis (PCA). R^2 (coefficient of determination, describing the amount of explained variation in X), Q^2 (coefficient of multiple determination, describing the amount of variation in the cross-validated subsets predicted by the model) and $RMSE_{CV}$ (root mean square error using cross-validation with seven cross validation groups and the same number of iterations) diagnostics were used to evaluate the calibration (OPLS) and discriminant models (OPLS-DA).

2.9 Summary

A summary of all methods used in the thesis is given in Table 2.

Table 2. An overview of used materials and methods in the thesis.

Resources and methodologies	Paper				
	I	II	III	IV	V
Materials					
Whole logs (*Pinus sylvestris* L.)	×				
Boards (*Pinus sylvestris* L.)		×			
Wood powder (*Pinus sylvestris* L.)			×	×	
Multi-blade shaft mill (MBSM)	×	×	×	×	
CAMSIZER XT			×		
NOVA 2200e series			×		
M205FA, Leica	×				
Leica DMLB				×	
Software					
MODDE Pro-12	×	×			
SIMCA			×		
Experimental design					
Screening	×	×			
Model					
Multilinear regression (MLR)	×	×			
Orthogonal partial least squares projections to latent structures (OPLS)			×		
Principal component analysis (PCA)			×		
Analysis technique					
Sieve	×				
Optical imaging	×				
Two-dimensional image			×		
Staining				×	
Light microscopy				×	
Analysis					
Particle size distribution (PSD)	×		×		
Bulk density	×				
Sphericity			×		
Aspect ratio			×		
Surface area			×		
Porosity			×		
Morphology	×		×	×	
Extractive distribution					
Energy consumption	×	×			

3. Results and discussion

3.1 Particle size distribution

The cumulative PSDs from all experiments are shown in the Figure 7 and the fraction of particles below 1.0 mm for each experiment is presented in Table 3. The MBSM prototype produced a substantially greater amount of fine particles compared to the hammer mill. The fraction of particles <0.5 mm was 55 to 80 % while it was 41 % for hammer-milled powders (Figure 7b). All MBSM powders had 80 to 95 % of their particles below 1.0 mm. The finest PSD (95 % <1.0 mm) was observed when milling wood with high MC at high BS and low FS.

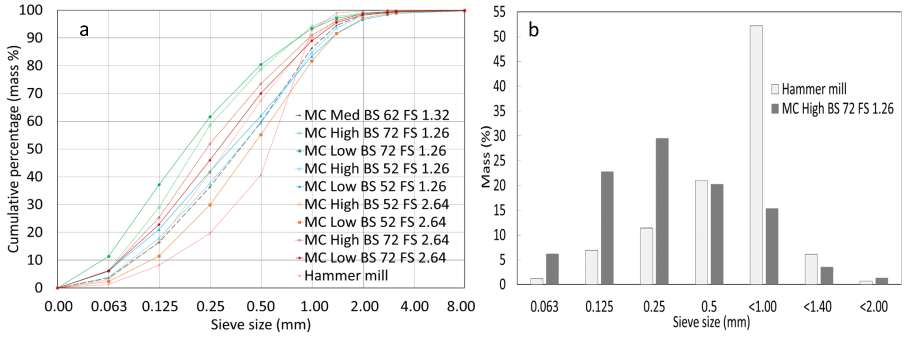

Figure 7. (a) Cumulative particle size distribution of powders obtained from the multi-blade shaft mill (MBSM) and hammer mill. (b) Specific particle size differences between finest MBSM powder and hammer mill. Label symbols refer to MC = moisture content, Med = medium, BS = blade speed and FS = feeding speed (Paper I).

Table 3. Obtained responses from the designed experiments.

Experiment Name	Run Order	Responses		
		Specific milling energy (kWh t^{-1} DM)	Wood particle <1 mm (%)	Bulk density (kg m^{-3} DM)
N1	21	146.6	81.9	257.9
N2	5	133.0	89.0	158.7
N3	14	98.6	63.5	245.1
N4	23	109.8	86.0	164.2
N5	25	231.6	93.2	232.2
N6	9	202.2	95.3	143.8
N7	8	130.6	93.1	215.5
N8	11	144.9	94.2	150.6
N12	18	175.1	80.0	242.7
N13	6	119.5	83.7	161.0
N14	28	114.5	82.2	243.9
N15	7	112.6	90.8	141.5
N16	20	192.4	95.0	141.8
N17	10	197.4	94.0	138.0
N18	22	132.1	86.9	236.8
N19	16	111.4	90.6	169.7
N20	5	142.5	87.4	234.0
N22	15	115.4	88.5	174.1
N23	17	120.7	84.0	220.3
N24	4	139.3	81.7	148.9
N25	13	127.9	81.1	154.9
N26	27	122.5	93.0	154.6
N27	24	197.2	92.1	264.4
N28	3	165.6	93.1	159.5
N29	12	160.8	86.9	229.4
N30	19	109.3	88.3	168.0
N31	29	150.4	86.3	183.5
N33	2	144.8	84.1	157.4

Note: *The values of particle size <1.0 mm of 63.5 % and bulk density of 141.2 kg m^{-3} DM were excluded from the model as those values were out layer among three replicates. It might be problem of inherent log quality. N20 is the fourth replication of one of the experimental set ups.

The produced MLR model (R^2 = 0.707 and Q^2 = 0.526) for PSD shows that BS and MC have a significant (<0.05) effect on the fraction of particles <1.0 mm while FS has no direct influence on the PSD (Figure 8b). However, a significant interaction effect (FS*BS) exists.

As depicted in the contour plot of the experimental design (Figure 9), the range of FS (Y-axis), MC (X-axis) and BS (secondary X-axis) for the finest PSD (Figure 9a) are 1.8 m min^{-1}, >48% and 72 m s^{-1}, respectively. From this result, the mass percentage of particles below 1.0 mm increased with increasing of wood MC and BS, and the decreasing of FS.

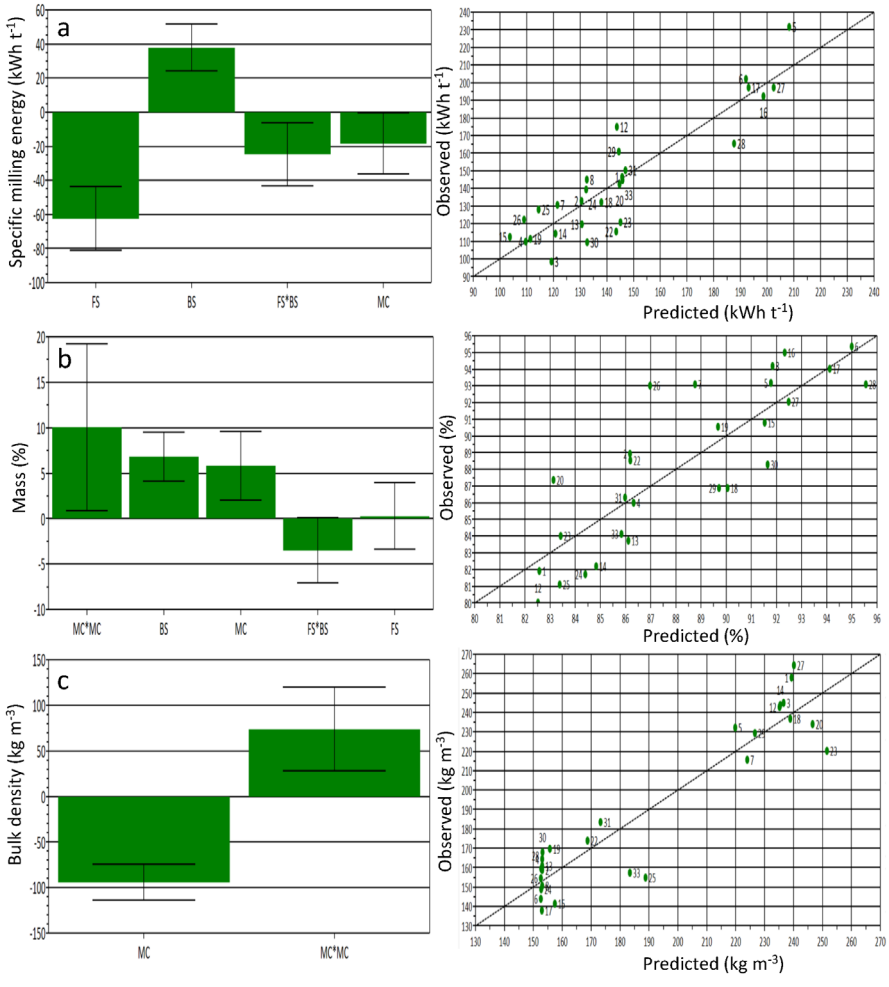

Figure 8. Effects of scaled and centred factors in the response models for the (a) specific milling energy: Y_E (kWh t^{-1}) = −0.46 MC + 65.72 FS + 5.38 BS – 1.79 FS*BS – 92.16 (b) amount of wood particles <1 mm: Y_{PSD} (mass %) = −0.62 MC + 15.93 FS + 0.84 BS + 0.01 MC*MC – 0.25 FS*BS + 41.56 (c) powder bulk density: Y_{BD} (kg m^{-3}) = −7.98 MC + 0.09 MC*MC + 328.28 when each individual factor is varied from its lowest to its highest value, keeping all other factors at their average values in the design. The error bars indicate 95% level of confidence. Symbols refer to MC = moisture content, BS = blade speed and FS = feeding speed (Paper I).

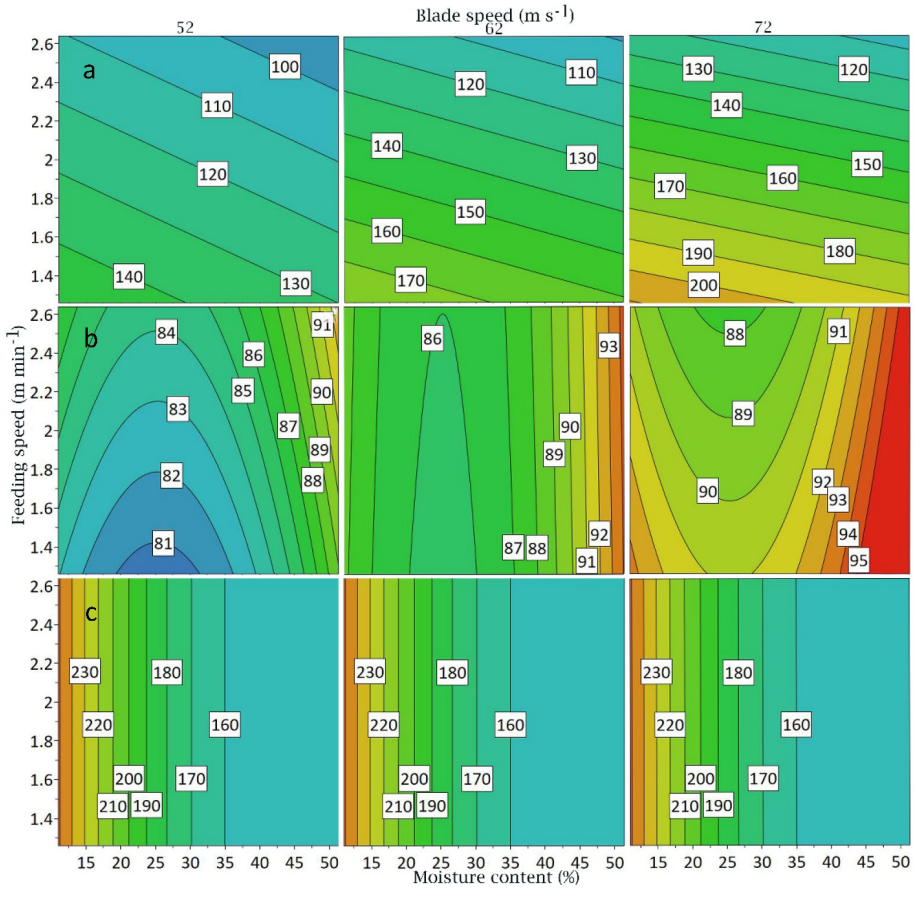

Figure 9. Contour plots of experimental design space showing the influence of the three experimental design factors (moisture content (%), blade speed (m s−1) and feeding speed (m min^{-1})) on the a) specific milling energy (kWh t^{-1} DM), b) particle size distribution (mass %) and c) bulk density (kg m^{-3} DM) of powders (Paper I).

3.2 Shape properties

The aspect ratio and sphericity of MBSM powders, determined by Camsizer, were higher compared to hammer-milled powders (Figure 10). Clear differences were also seen in MBSM powders milled from wood having MC above (green curves) and below (brown curves) the fibre saturation point. The aspect ratio and sphericity ranged from 0.54 to 0.61 and 0.51 to 0.75,

respectively. The corresponding ranges for hammer-milled powders were 0.36 to 0.44 and 0.50 to 0.61. The MBSM mill settings had little influence on the aspect ratio and sphericity. Using a light microscopy, shape differences between the two powder types could be observed (Figure 11).

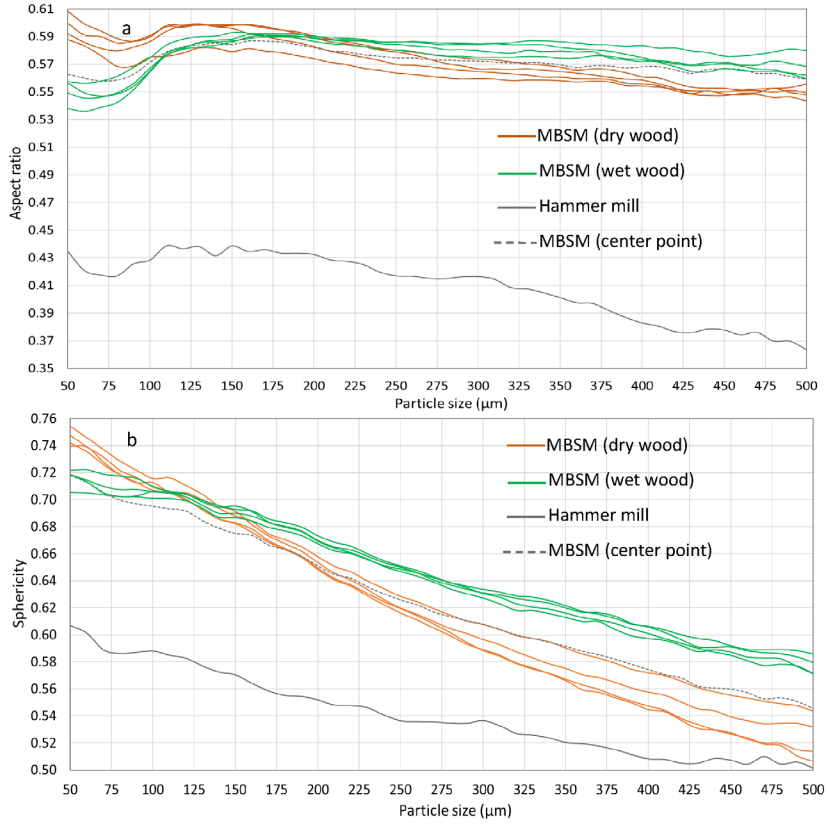

Figure 10. Aspect ratio (a) and sphericity (b) of multi-blade shaft mill (MBSM) and hammer mill powder (Paper III).

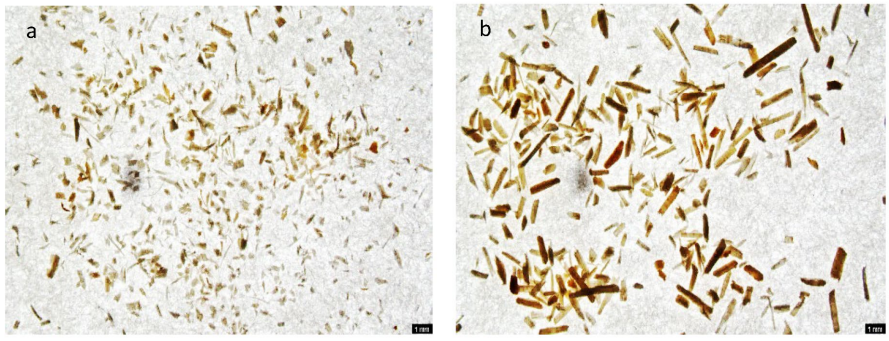

Figure 11. Optical image of powders passing through 0.5 mm sieve from (a) multi-blade shaft mill and (b) hammer mill. The black line length is 1 mm (Paper I).

At and below particle sizes of 200 µm (approx. 150 to 250 µm), wood having lower MC resulted in particles with larger shape factors. The opposite effect was observed for particles above this size. The mid-point of the experimental design (dotted line) was positioned between the groups of curves. The distribution of shape factors for hammer-milled powders displayed similar behaviour.

Due to the design of the experimental procedure, the differences in shape factors between the two groups of powders must be due to one of the following effects or combination of them: (i) the drying steps at 105 ºC after milling or (ii) the action of the MBSM blades during milling. Considering the first option, the presence of a MC gradient during drying causes internal stress and leads to wood deformation [236]. Similarly, pine wood particles showed more spherical shape and had greater porosity after rapid de-volatilisation [237], although the temperature used in drying was comparatively low. Considering the second option, the milling action may have been more effective when milling wet wood because the excess moisture acted like lubrication, which assists cutting and produces more spherical particles. Conversely, less effective cutting means more impact force and more elongated particles.

The range of aspect ratio and sphericity of MBSM powders were higher than those observed in previous studies. Hammer-milled Douglas fir (*P. menziesii*) powders had an aspect ratio range of 0.31 to 0.55 across a PSD of 0.07 to 0.78 mm [63]. Pine powder obtained from a vibration mill (rod and ball mill) had an aspect ratio range of 0.20 to 0.33 across a PSD of 0.02 to 0.5 mm [48].

3.3 Powder bulk density

The bulk density of MBSM pine wood powders (PSD of 63.5 to 95.3% <1.00 mm) was in the range of 138 to 264 kg m^{-3} DM (Table 3). The highest bulk density (264 kg m^{-3} DM) was observed for powders produced from wood having the lowest MC. Powders produced from green wood had the lowest bulk density (138 kg m^{-3} DM). For comparison, the hammer-milled powder showed a bulk density of 219 kg m^{-3} DM (PSD of 92.9% <1.00 mm). These ranges were comparable to those in the literature. For example, powders of pine, Douglas fir and poplar wood produced by knife and hammer mills had a range of 95 to 381 kg m^{-3} DM [13, 26, 58, 63, 89].

The MLR model (R^2 = 0.88 and Q^2 = 0.83) produced from the experimental data shows that MC is the only significant ($p<0.05$) factor on the bulk density; the milling of wood with high MC resulted in a low bulk density powder (Figure 8c and Figure 9c). This influence of wood MC was validated by OPLS analysis in which the obtained MBSM powders from green wood and dry wood were separated into two groups (Figure 12b).

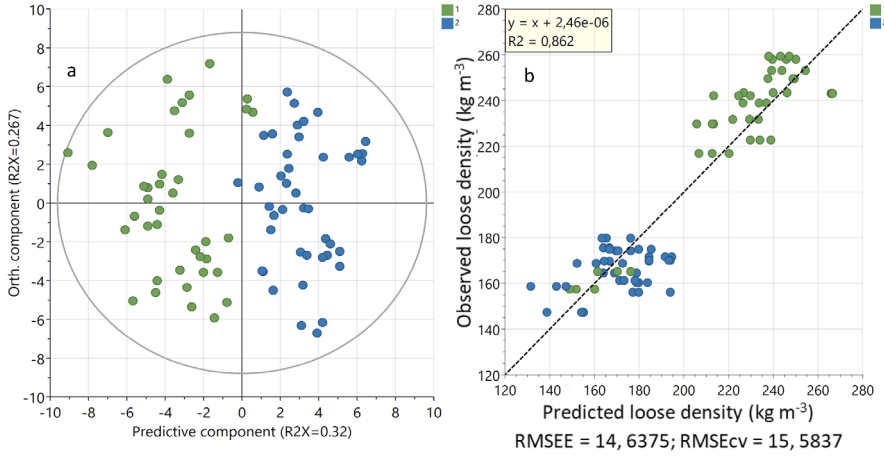

Figure 12. (a) Score plot derived from class discriminant analysis (OPLS-DA) of AR dependence on moisture content (dry (class 1, green) and wet (class 2, blue), and (b) OPLS calibration model for aspect ratio (X) and bulk density (Y) displaying measured bulk density (kg m^{-3}) versus model predicted bulk density (kg m^{-3}). (For interpretation of the references to colour in this figure legend, the reader is referred to the web version of this article.)

Using MLR analysis with the design data showed that the natural variations in the wood used in the study did not influence the results. For

example, the wood density, stem diameter, tree age and number of knots did not produce significant effects in the model; the wood MC was the main factor (Figure 13).

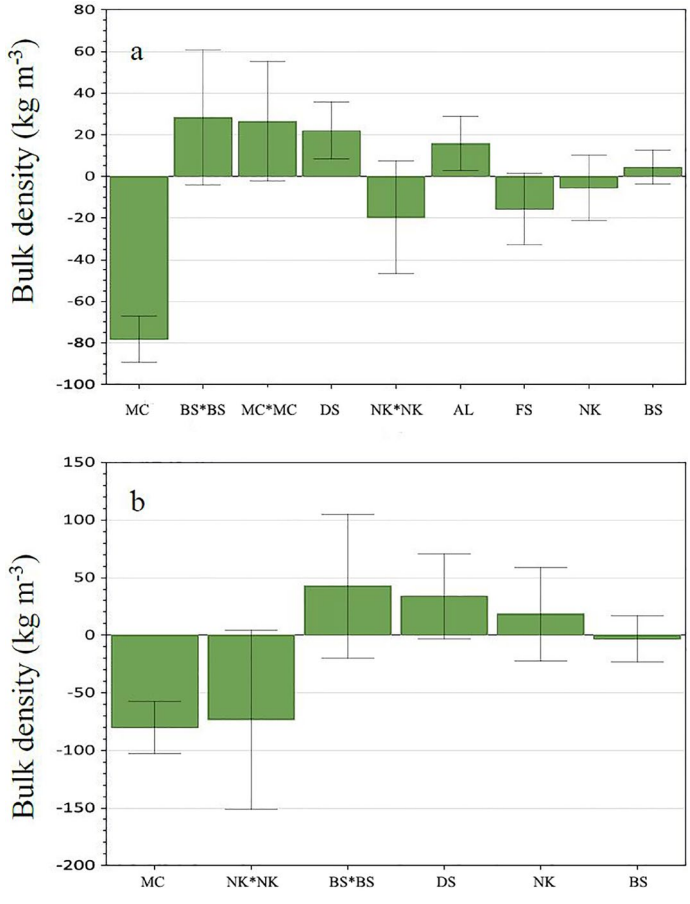

Figure 13. (a, b) Effects of scaled and centred factors in the response models for the powder bulk density when each individual factor is varied from its lowest to its highest value, keeping all other factors at their average values in the design. The error bars indicate 95% level of confidence. Symbols refer to MC = moisture content, BS = blade speed, FS = feeding speed, DS = wood basic density, NK = number of knots and AL = Aged of log.

In the initial study, an explanation was sought for the large difference in bulk densities, depending on the whether wood is above or below fibre saturation point (FSP). Dimensional changes of wood, i.e., shrinkage and swelling, occurs below the MC of the fibre saturation point (FSP) [238].

Drying temperature is an influential factor in shrinkage [236]. Tangential and radial shrinkage of wood veneers can be observed at 7.6 and 9.9 % and 5.4 and 5.7 % during drying at 60 and 150 ºC, respectively [239]. The hydrostatic tension occurs during wood drying, which causes internal checking and washboard depression in the wood [240].

The low wood MC used in the experimental design was adjusted to a MC under and around FSP by drying at 25 ºC before milling, while high wood MC was milled at above FSP. Consequently, the powders obtained from high wood MC had higher moisture levels resulting in higher vapour pressures in their wood matrix during drying at 105 ºC [241]. This led to higher dimensional changes in these powders. Drying temperature affects chemical composition and crystallinity [48] and influences shape and particle density. This may explain the low bulk density of powders obtained from high wood MC and the observed significant factor of MC in the model (Figure 8c).

Interpretation of more recent results, which characterise shape factors across the PSD, indicate that there may be several contributing factors behind the bulk density results. Firstly, the initial drying of the logs may cause cell collapse [242]. When this wood was milled, the particles formed no longer had the native structure. On the other hand, the cells in the green wood were saturated with water during milling which may have preserved their native structure. All the powders, from green and pre-dried wood were dried at 105 ºC thereafter. Whatever the explanation, the powders from green wood either had their microstructure preserved during milling or had their porosity enhanced from the drying.

BET analysis indicated that MBSM powders from green wood were indeed more porous. Their porosity, expressed as pore volume, (0.002759 $cm^3\ g^{-1}$) was 2.8 times greater than those obtained from dry wood (0.001035 $cm^3\ g^{-1}$) and 3.1 times greater than hammer-milled powders (0.001037 $cm^3\ g^{-1}$). Micropore diameter of MBSM powders sourced from green wood (4.52 nm) was also higher than that from dried wood (1.61 nm) and hammer-milled (1.48 nm) powders. It is clear that in comparing two powders with identical PSD, the one with more porous particles will have the lower bulk density. However, in the present study, the PSD of the powders and their shapes were also different. Both particle size and shape are important for the effective packing of powders. For example, small particles move easily and help fill the gaps between bigger ones, and particles with greater sphericity have fewer points of contact with their nearest neighbours [26]. In the particle size

range of 20 to 150 µm, the number of particles was greater in powders obtained from dry wood (67,000 particles g^{-1}) compared to powders obtained from green wood (38,000 particles g^{-1}). Powders from dry wood were also more spherical. Therefore, a difference in porosity, number of smaller particles and the particle shape can explain the large variations observed in bulk density. According to the OPLS model, there are good correlations between aspect ratio and bulk density (R^2 = 0.86, Q^2 = 0.84 and RMSEcv = 15.58) (Figure 12b) and particle number and bulk density (R^2 = 0.87, Q^2 = 0.80 and RMSEcv = 17.31).

In addition, the micromorphlogy and wood extractive distribution of wood powders can attribute to difference in bulk density. The content of extractive and fracture of wood powders can vary due to the difference of wood MC. Microscopic and topochemistry analyses can help to investigate the findings of considerable factors.

3.4 Powder micromorphology

3.4.1 Effects on surface and fibre properties

The surface of powders obtained from MBSM (GMP, FMP and DMP) in both the non-dried and dried cases was smooth (Figure 14a-f), while the hammer mill powders (HMP) had rough surfaces (Figure 14g and h). There is an indication that fibre defibration, fibrillation and separation/release of fibres occurs less frequently or not at all for GMP, FMP and DMP powders (Figure 14a-f). HMP powders, on the other hand, showed fibre defibration (Figure 14g and h, red arrows), fibrillation (Figure 14g and h, green arrows) and release of fibres (Figure 14g and h, black arrows) in the non-dried and dried cases. There was also a broken fibre wall observed for dried HMP powders (Figure 14h, blue arrow).

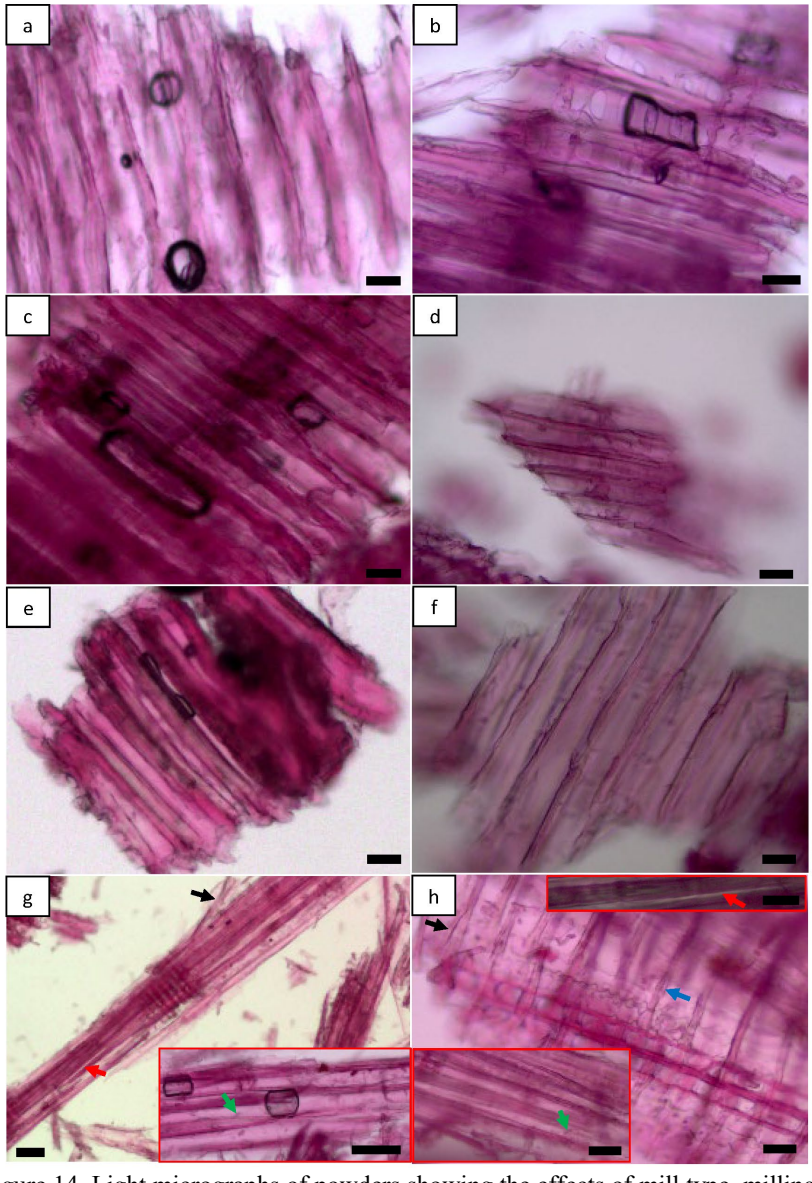

Figure 14. Light micrographs of powders showing the effects of mill type, milling parameters and drying on the surface and fibre properties. MBSM powders (a-f) and hammer mill powders (g and h) are shown where (a) Non-dried MBSM powder from green wood, (b) Dried MBSM powder from green wood, (c) Non-dried MBSM powder from wood at fibre saturation point, (d) Dried MBSM powder from wood at fibre saturation point, (e) Non-dried MBSM powder from dry wood, (f) Dried MBSM powder from dry wood, (g) Non-dried hammer mill powder and (h) Dried hammer mill powder. Scale bars represent 30 µm (a-f, h and h inset top right), 50 µm (g and h inset bottom left) and 100 µm (g inset).

3.4.2 Effects on micro-structural deformation

Images from polarised light microscopy are shown in Figure 15. The non-dried MBSM powders of GMP, FMP and DMP showed comparatively less damage in their cellulose fibril structure (Figure 15a, c and e). The observed continuous, sharp and less disrupted brightness of the fibre walls is likely an indication of a more intact native crystalline cellulosic structure. In dried MBSM powders (i.e., GMP, FMP and DMP), however, the disrupted brightness along the fibre wall (Figure 15b, d and f, red arrows) indicated some degree of deformation/damage to their cellulose fibril structure. However, all HMP powders (Figure 15g and h) were found to contain considerable defects (e.g. fibre wall breakage, dislocations etc.) in their fibre wall suggesting the presence of induced non-crystalline structures.

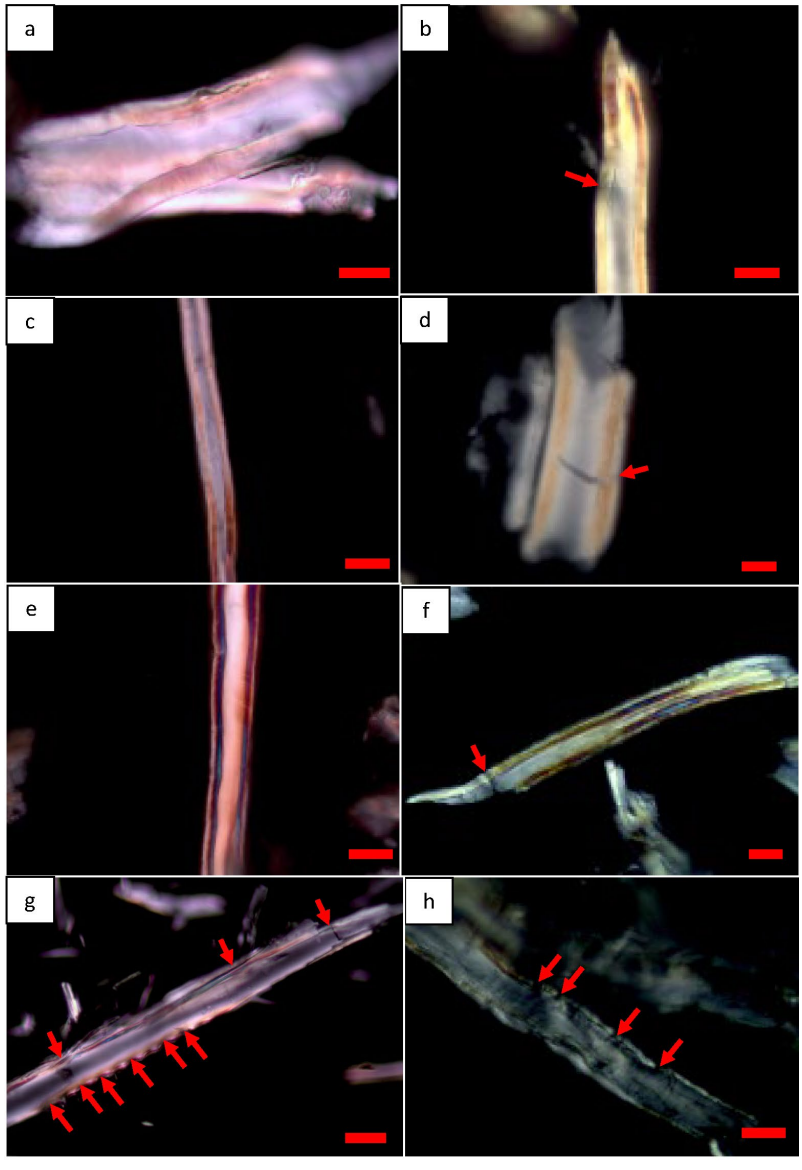

Figure 15. Effect of mill type, milling parameters and drying on the micro-structural deformation. MBSM powders (a-f) and hammer mill powders (g and h) are shown where (a) Non-dried MBSM powder from green wood, (b) Dried MBSM powder from green wood, (c) Non-dried MBSM powder from wood at fibre saturation point, (d) Dried MBSM powder from wood at fibre saturation point, (e) Non-dried MBSM powder from dry wood, (f) Dried MBSM powder from dry wood, (g) Non-dried hammer mill powder and (h) Dried hammer mill powder. Scale bars represent 20 µm (a-c, e and h), 10 µm (d), 30 µm (f, g).

3.4.3 Effects on triglyceride distribution

The non-dried and dried powders obtained from MBSM (Figure 16a-f) and hammer mill (Figure 16g and h) showed different micro-morphological features of extractives and their micro-distribution. There were also variations among the MBSM powder types. In general, staining showed comparatively strong responses (higher staining intensity) for non-dried MBSM powders (Figure 16a, c and e) compared to dried MBSM powders (GMP, Figure 16b) and HMP (Figure 16g and h) powders. Triglycerides, which were stained red/pink in colour, redistributed on the fibre surface as globules mainly in the bordered pits area (Figure 16a, red arrow) for non-dried GMP. They appeared intact in the cell lumen of ray parenchyma cells (Figure 16c, green arrow) for non-dried FMP and epithelial cells (Figure 16e, blue arrow) for non-dried DMP. For HMP, however, triglycerides were redistributed over the particle surface for non-dried (Figure 16g, black arrows) and dried (Figure 16h, black arrows) powders. MBSM dried powders (i.e., FMP and DMP) had mostly clear surfaces (Figure 16d and f) where as GMP showed small globules of triglyceride close to the bordered pit region of the fibres (Figure 16b, red arrow).

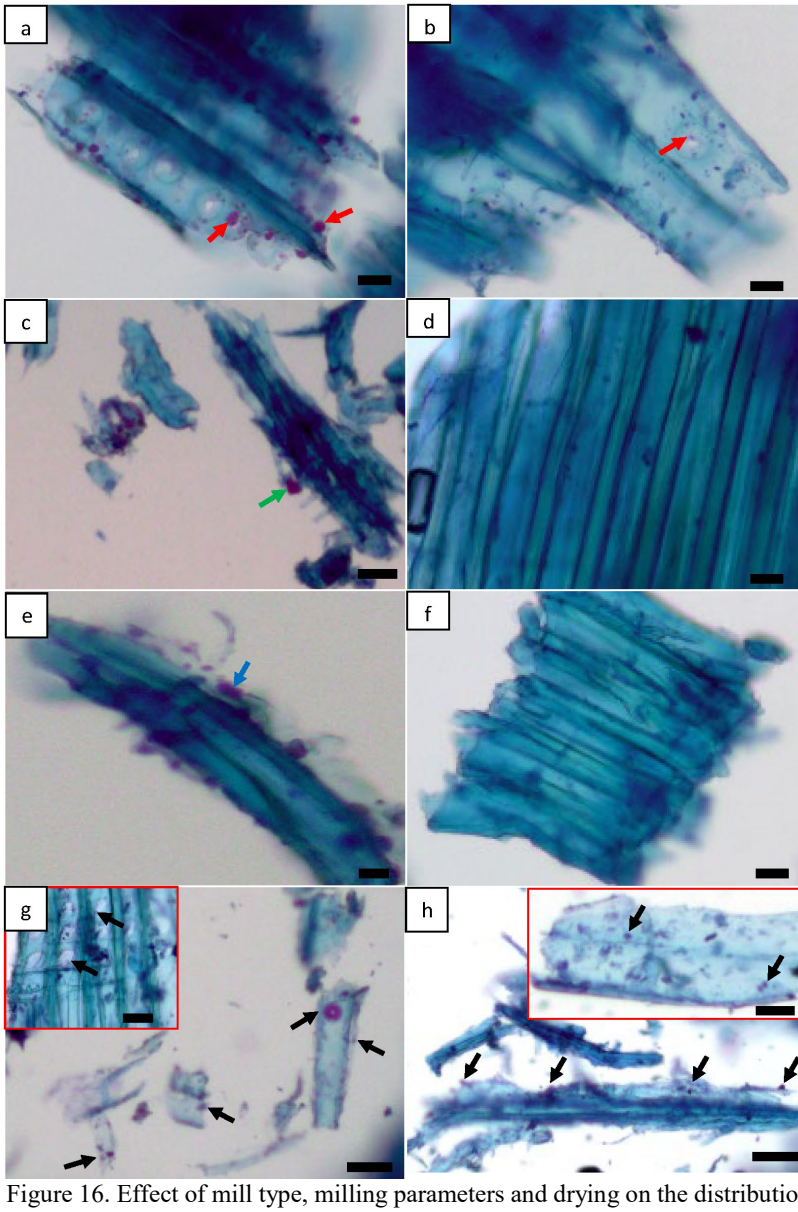

Figure 16. Effect of mill type, milling parameters and drying on the distribution of neutral triglycerides (red/pink staining) in the cellular system of pine wood powder using Nile blue (NB). MBSM powders (a-f) and hammer mill powders (g and h) are shown where (a) Non-dried MBSM powder from green wood, (b) Dried MBSM powder from green wood, (c) Non-dried MBSM powder from wood at fibre saturation point, (d) Dried MBSM powder from wood at fibre saturation point, (e) Non-dried MBSM powder from dry wood, (f) Dried MBSM powder from dry wood, (g) Non-dried hammer mill powder and (h) Dried hammer mill powder. Scale bars represent 30 µm (a, b, d, f and h inset), 70 µm (c), 10 µm (e), 50 µm (g, g inset and h).

3.4.4 Effects on lipids distribution

Generally, all dried MBSM powders exhibited a mostly clear surface, indicating the absence of lipids (Figure 17b, d and f). Small blue-black globules were observed sparsely dispersed especially in the ray regions of GMP powders (Figure 17a, red arrows) indicating the presence of lipids (i.e. fats/free FAs). Lipids were also distributed as small globules and in small quantity on the particle surface for non-dried FMP (Figure 17c, green arrows) and DMP (Figure 17e, blue arrow). They were distributed as large globules on the particle surface for non-dried HMP (Figure 17g, black arrows) but appeared as small globules for dried HMP (Figure 17h, black arrows). The whole ray area can sometimes appears blue-black in colour, indicating dispersion of lipids across the whole ray cell for non-dried HMP (Figure 17g inset, red arrowhead).

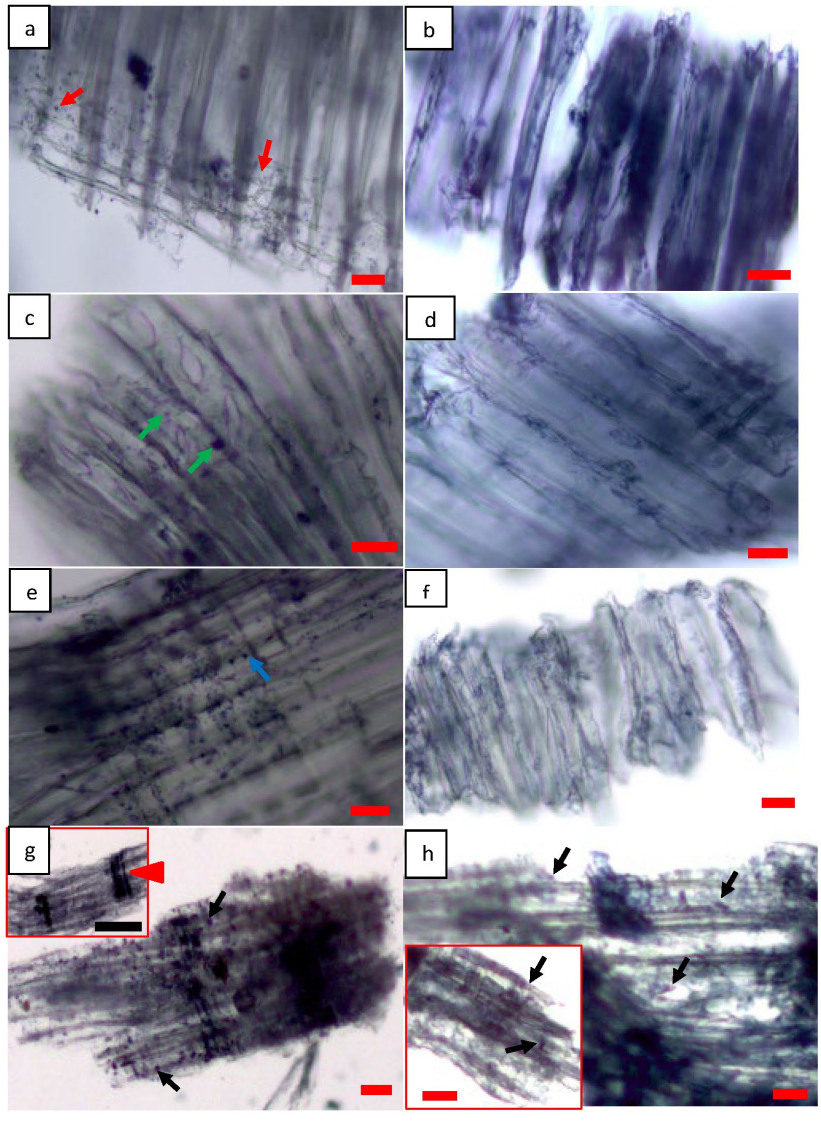

Figure 17. Effect of mill type, milling parameters and drying on the distribution of lipids (i.e. fats/free fatty acids) in pine wood powders using Sudan black B (SB). MBSM powders (a-f) and hammer mill powders (g and h) are shown where (a) Non-dried MBSM powder from green wood, (b) Dried MBSM powder from green wood, (c) Non-dried MBSM powder from wood at fibre saturation point, (d) Dried MBSM powder from wood at fibre saturation point, (e) Non-dried MBSM powder from dry wood, (f) Dried MBSM powder from dry wood, (g) Non-dried hammer mill powder and (h) Dried hammer mill powder. Scale bars represent 30 µm (a, d and f), 20 µm (b), 10 µm (c), 70 µm (e), 50 µm (g, h and h inset), 100 µm (g inset).

3.4.5 Effects on unsaturated fats distribution

Osmium tetroxide stained the cell lumen of parenchyma black in colour for non-dried GMP (Figure 18a, red arrow) indicating the retention of unsaturated fats/free FAs inside the ray cells. There were weakly stained parenchyma cells for non-dried FMP (Figure 18c, green arrow) and DMP (Figure 18e, blue arrow) confirming the presence of unsaturated fats/free FAs but likely with lesser amounts. Dried MBSM powders (i.e., GMP, FMP and DMP), on the other hand, showed mostly clear particle surfaces (Figure 18b, d and f). For hammer mill powders, they were redistributed as small globules on the particle surface (Figure 18g and h, black arrows) and inside the bordered pits (Figure 18g and h, green arrowheads) for both non-dried and dried HMP. For the former, they were also seen dispersed across ray parenchyma cells (Figure 18g, red arrowhead).

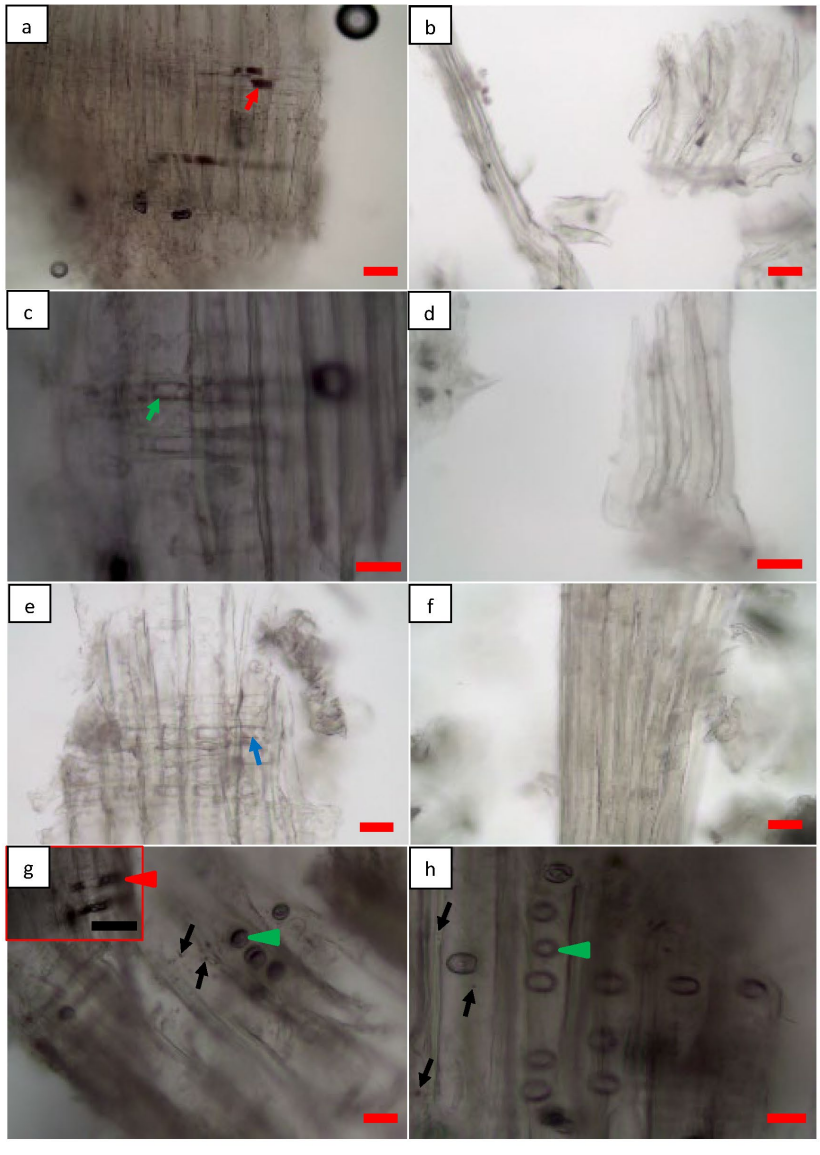

Figure 18. Effect of mill type, milling parameters and drying on the distribution of unsaturated fats in pine wood powder using osmium tetroxide. MBSM powders (a-f) and hammer mill powders (g and h) are shown where (a) Non-dried MBSM powder from green wood, (b) Dried MBSM powder from green wood, (c) Non-dried MBSM powder from wood at fibre saturation point, (d) Dried MBSM powder from wood at fibre saturation point, (e) Non-dried MBSM powder from dry wood, (f) Dried MBSM powder from dry wood, (g) Non-dried hammer mill powder and (h) Dried hammer mill powder. Scale bars represent 30 µm (a, b and e-h), 20 µm (c and d), 100 µm (g inset).

Based on the above observations, there are clear differences in the micromorphology of the MBSM powders examined compared to HM powders. A likely explanation of these are the fundamentally different mechanisms at work during size reduction. The mechanism for the MBSM is primarily a cutting or swing force using sharp metal blades (Paper I and Paper II) while the hammer mill acts on wood using impact and shear forces [32]. These differences result in differences in particle surface and fibre properties. MBSM powders were more likely to have intact structure at their cell wall levels while HM powders appeared to exhibit more disrupted. Stresses during drying can also enhance deformation or defects in fibre walls [236] and increases the microfibril angle [243]. Both have been observed but HM powder showed comparatively greater effects. The impact and shearing forces in hammer milling can be responsible for the destruction of parenchyma and epithelial cells leading to liberating extractives out of the cells and spreading over particle surfaces. In contrast, MBSM powders tended to have intact parenchyma and/or unbroken cells retaining their extractive content.

3.5 Powder flowability

Using the angle of repose of produced powders as a response, it was not possible to make a valid MLR model ($R^2 = 0.25$ and $Q^2 = 0.045$). In other words, the flowability of all powder types (including hammer mill powders) was the same and can be classified as very cohesive [63]. The flowability according to the Hausner ratio (1.2 to 1.3) was moderate to good [244] yet the MLR model produced has poor correlation ($R^2 = 0.68$ and $Q^2 = 0.59$) with the MC, BS and FS factors. Larger scales and powder amounts may enable greater accuracy in the determination of the flowability.

3.6 Energy consumption

The calculated specific milling energy for all MBSM experiments is listed in Table 3. It ranged from 99 to 232 kWh t^{-1} DM and was 1.2 to 2.7 times higher than the hammer mill value (86 kWh t^{-1} DM). The lowest milling energy (99 kWh t^{-1} DM) produced the fewest fraction of particles <1.0 mm (63.5 %). The highest milling energy (232 kWh t^{-1} DM) produced the greatest fraction of particles <1.0 mm (93.2%). A direct comparison between the energy used

with these two milling technologies is challenging for two reasons; (i) the input materials had different forms and (ii) the final PSDs were not equivalent. The MBSM accepts whole stems whereas the hammer mill accepts only chips (Figure 6). The production of fine powders necessitates greater energy expenditure than coarse powders both in theory [29] and in practice [12]. A true comparison of milling energy must start with the same input material and end with the same PSD.

An alternate method of comparison is to evaluate size reduction by the amount of generated surface area on the particles when going from input material to powder. BET analysis showed that the surface area of produced powders was 1.38 and 0.429 $m^2\ g^{-1}$ for green wood MBSM and hammer-milled powders, respectively. Using the specific milling energy, the surface area generated from MBSM milling was 6981 $m^2\ kWh^{-1}$ while the hammer mill it was 4990 $m^2\ kWh^{-1}$. MBSM powders produced from dry wood had surface area of 0.557 $m^2\ g^{-1}$ and surface area generation of 2826 $m^2\ kWh^{-1}$. The MLR model (R^2 = 0.82 and Q^2 = 0.73) of milling energy showed a significant ($p<0.05$) positive effect from BS while FS and MC have significant ($p < 0.05$) negative effects (Figure 8a). From Figure 9a, it can be seen that the increment of specific milling energy occurs with increasing BS and decreasing FS and MC. The highest modelled milling energy occurs for a BS of 72 m s^{-1} and a FS of <1.5 m min^{-1}.

The effect of MC on the milling energy is consistent with the understanding of hydrogen bonding between wood polymers; the lower the MC in the wood cell wall the greater number of hydrogen bonds [23, 24]. This means the required milling energy should be greater for dry wood. At and above the fibre saturation point (FSP), the cell is saturated and extra water contributes to a lubrication effect during milling.

The specific milling energy in MBSM milling is comparable to that of other mill types. For example, a two-stage hammer mill uses a 150 kWh t^{-1} DM to produce <1.0 mm 95% powders from pine (*Pinus sylvestris* L.) chips [13]. For producing 0.71 mm powders from pine chips, a knife mill consumes 238 kWh t^{-1} [89] while an oscillatory type ball mill has a milling energy range of 100–380 kWh t^{-1} for 0.02–0.10 mm powders from spruce (*Picea abies*) sawdust. Importantly, these studies used small input sizes of wood but the input materials for the MBSM was the whole log.

From the designed experiment with rectangular pine boards, the specific milling energy range was 60 to 172 kWh t^{-1}, which was much less than

milling with cylindrical logs. The differences between the two materials were the shape of the work piece (50 × 150 mm rectangular cross-section vs 100 to 140 mm diameters cylinders), the average age of the wood (60 vs 29 years) and the MC range (13 to 33 % vs 11 to 51 %).

The observed differences in milling energy is ascribed to the differences in the number of teeth engaged, the angle of engagement and the travelled path length for the teeth through the kerf [245]. In the board milling, fewer teeth were engaged in the vertical plane and more teeth in the horizontal plane with differences in the angle of engagement (Figure 19). In the stem milling, the longer path travelled by the teeth increases the energy consumption. These results show that the energy needed to produce powders with the MBSM can be reduced by selecting materials of the right shape or geometry.

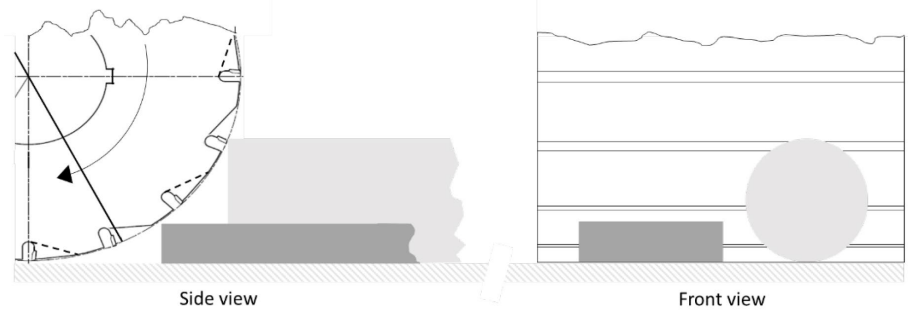

Figure 19. Side and front views of the main shaft of the multi-blade shaft mill. The thickness and width of the boards (A) and stems (B) influence the engagement angle and the number of teeth engaged, both in the vertical (left) and horizontal (right) planes (Paper II).

4. Implications

This thesis explored a new concept of milling wood while green, something not technically possible with conventional size reduction technologies. MBSM technology enables wood to be stored in its preferred natural form (i.e. as a stem) until the moment of utilisation. The single-step process is fast and eliminates the intermediate steps (i.e., chipping, drying and handling) needed when producing powders from hammer milling. In addition to saving time, there is also a potential savings in emissions associated with these operations.

Tailor-made PSD that are possible with the MBSM are expected to be more compatible with downstream biorefining processes, which use biomass powders. Especially green powders may be attractive for biochemical applications where the native chemical profile of the feedstock is intact. Milling green biomass will enhance the efficiency of bioconversion and development of bioproducts (e.g. biopolymers, nanocellulose and ethanol) due to better surface area and porosity of powders. For example, this was observed in the manufacturing of bioplastic from wood powders via chemical routes and additive manufacturing (Figure 20). This development supports the desired to utilise bio-based materials in consumer products in order to replace fossil feedstock and reduce environmental impacts. As with all new technologies, it is difficult to predict the range of future applications, which may immerge for MBSM powders.

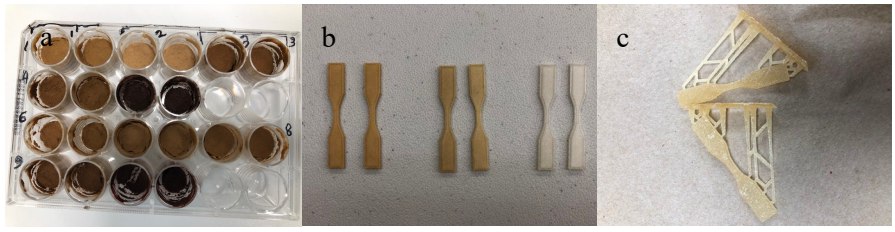

Figure 20. Manufactured bioplastic (a) deep eutectic solvent (DES) treatment, (b) fused deposition modelling (FDM) and (c) stereolithography (SLA) from wood powders obtained from MBSM.

5. Future outlook

There are still research questions to be answered regarding the performance of the MBSM. This thesis worked exclusively with pine but mill performance using other wood species (e.g., *Betula sp.*, *Picea abies*, *Eucalyptus sp.*, *Acacia sp.*), important non-wood species, (e.g., bamboo, hemp, jute stick) and common agricultural residues (e.g., straw, bagasse, grasses) are also of interest. Some of the above feedstock (e.g., straw, grass) have a large inorganic content compared to pine, which may inhibit milling performance. As pine has relatively high extractive content, feedstock with low extractive content may help isolate the effects of extractives through comparison. Powders from the above feedstock should also be characterised as they may exhibit unique properties especially when they are milled green.

Future work will generate large data sets on energy consumption using several feedstock types and attempt to adapt the results to milling theories for biomass. The influence of work piece shape on specific milling energy needs to be studied in detail to understand how to reduce energy use through optimising of angle of engagement between feedstock and blade teeth. The potential influence of these on powder quality will also be studied. Analysis of PSDs from a full industrial installation (e.g. complete with a vacuum enclosure) of the MBSM is necessary to quantify the finest airborne particles.

Applications involving the use of MBSM powders are obvious future topics for investigations. The preliminary results carried out show potential benefits of using the powders in 3D printing (e.g., fused deposition modelling) and renewable bioplastic production (deep eutectic solvent treatment) (Figure 20). These efforts will continue. As a chemical production route, how MBSM powders influence the efficiency of biochemical extraction (e.g., bioethanol) is also interesting.

Finally, there are practical question to answer about the capital and maintenance costs of the mill, including the determination of blade lifetime. Therefore, a techno economic analysis with energy and emission balance is desirable in order to place the technology within the context of a sustainable bioeconomy.

6. Conclusions

This thesis investigated, for the first time, a new type of milling technology, the multi-blade shaft mill (MBSM). The mill performance was successfully characterised through milling of Scots pine (*Pinus sylvestris* L.) wood both above and below its fibre saturation point (FSP). Analyses of the produced powders showed distinct differences compared to conventional powders obtained using a hammer mill (HM).

The mill allowed more control over particle size distributions (PSD) through selection of studied parameters. Without exception, much narrower PSDs were observed in MBSM powders and they consisted of significantly finer particles than in HM powder. Particles in MBSM powders exhibited less elongated shape compared to those in HM powder at all operational settings. Based on these findings, it can be stated that particles with high aspect ratio and sphericity are a characteristic of MBSM technology. This is valid for wood both above and below its FSP.

Powders produced from green wood showed evidence of higher specific surface area, larger pore volume and greater micropore diameter than those from HM powder. Microscopic examination indicated that cell walls in MBSM powders were more likely to retain their original native wood structure. Consequently, their extractive content was predominantly intact. This was in contrast to HM powder and it may reflect the differences between these two milling actions.

The specific milling energy of the MBSM was higher than conventional HM milling but was within the range of other established size reduction technologies. However, the elevated energy consumption observed in this study was compensated through resulting particle size, which contributed to significantly greater surface area. Furthermore, the results indicate that milling energy is a function of the wood shape to be milled. The existence of

this effect, influenced by teeth engagement, and the dependence of milling energy on the wood moisture content indicate that MBSM milling is akin to the process of sawing wood and unlike impact-based milling.

References

1. Fritsche, U., et al., *Future transitions for the Bioeconomy towards Sustainable Development and a Climate-Neutral Economy - Foresight Scenarios for the EU bioeconomy in 2050, Borzacchiello, M. T., Stoermer, E. and Avraamides, M. editor(s), Publications Office of the European Union, Luxembourg, 2021, ISBN 978-92-76-28413-0, doi:10.2760/763277, JRC123532*, M.T. Borzacchiello, E. Stoermer, and M. Avraamides, Editors. 2021: Publications Office of the European Union, Luxembourg, .
2. Zhang, M., et al., *Biofuel manufacturing from woody biomass: effects of sieve size used in biomass size reduction.* J Biomed Biotechnol, 2012. **2012**: p. 581039.
3. da Silva Barbosa Ferreira, E., et al., *Polypropylene/wood powder/ethylene propylene diene monomer rubber-maleic anhydride composites: Effect of PP melt flow index on the thermal, mechanical, thermomechanical, water absorption, and morphological parameters.* Polymer Composites, 2021. **42**(1): p. 484-497.
4. Renner, K., et al., *Micromechanical deformation processes in PP/wood composites: Particle characteristics, adhesion, mechanisms.* Composites Part A: Applied Science and Manufacturing, 2010. **41**(11): p. 1653-1661.
5. Das, A.K., et al., *A review on wood powders in 3D printing: processes, properties and potential applications.* Journal of Materials Research and Technology, 2021. **15**: p. 241-255.
6. Keränen, A., et al., *Preparation of novel anion exchangers from pine sawdust and bark, spruce bark, birch bark and peat for the removal of nitrate.* Chemical Engineering Science, 2013. **98**: p. 59-68.
7. Šillerová, H., et al., *Brewers draff as a new low-cost sorbent for chromium (VI): Comparison with other biosorbents.* Journal of Colloid and Interface Science, 2013. **396**: p. 227-233.
8. Kim, S.Y., et al., *Surface modifications of organic fillers to improve the strength of paperboard.* BioResources, 2015. **10**(1): p. 1174-1185.
9. Shin, T.-G., et al., *Fundamental study on developing lignocellulosic fillers for papermaking (I).* Journal of Korea Technical Association of The Pulp and Paper Industry, 2008. **40**(2): p. 8-15.
10. Agar, D.A., et al., *A systematic study of ring-die pellet production from forest and agricultural biomass.* Fuel Processing Technology, 2018. **180**: p. 47-55.

11. McDonough, T.J., *Wood chemistry - fundamentals and applications - Sjostrom, E.* J Am Chem Soc, 1983. **105**: p. 4503.
12. Karinkanta, P., et al., *Fine grinding of wood – Overview from wood breakage to applications.* Biomass and Bioenergy, 2018. **113**: p. 31-44.
13. Esteban, L.S. and J.E. Carrasco, *Evaluation of different strategies for pulverization of forest biomasses.* Powder Technology, 2006. **166**(3): p. 139-151.
14. Gil, M. and I. Arauzo, *Hammer mill operating and biomass physical conditions effects on particle size distribution of solid pulverized biofuels.* Fuel Processing Technology, 2014. **127**: p. 80-87.
15. Kratky, L. and T. Jirout, *Biomass Size Reduction Machines for Enhancing Biogas Production.* Chemical Engineering and Technology, 2011. **34**(3): p. 391-399.
16. Alakoski, E., et al., *From wood pellets to wood chips, risks of degradation and emissions from the storage of woody biomass - A short review.* Renewable & Sustainable Energy Reviews, 2016. **54**: p. 376-383.
17. Wihersaari, M., *Energy consumption and greenhouse gas emissions from biomass production chains.* Energy Conversion and Management, 1996. **37**(6-8): p. 1217-1221.
18. Fougere, J.D., et al., *Impact of mechanical downsizing on the physical structure and enzymatic digestibility of pretreated hardwood.* Energy and Fuels, 2014. **28**(4): p. 2645-2653.
19. Stenström, S., *Drying of biofuels from the forest—A review.* Drying Technology, 2017. **35**(10): p. 1167-1181.
20. Paulrud, S. and C. Nilsson, *The effects of particle characteristics on emissions from burning wood fuel powder.* Fuel, 2004. **83**(7-8): p. 813-821.
21. Falk, J., et al., *Mass flow and variability in screw feeding of biomass powders - Relations to particle and bulk properties.* Powder Technology, 2015. **276**: p. 80-88.
22. Jiang, J., et al., *Microstructure change in wood cell wall fracture from mechanical pretreatment and its influence on enzymatic hydrolysis.* Industrial crops and products, 2017. **97**: p. 498-508.
23. Green, D.W., J.E. Winandy, and D.E. Kretschmann, *Mechanical Properties of Wood*, in *Wood Handbook.* 1999, Forest Products Laboratory, USDA Forest Service, USA
24. Rowell, R., *How the environment affects lumbar design.* Forest Products Laboratory ReportUSDA, Forest Service, 1980.
25. Winandy, J.E. and R.M. Rowell, *11 chemistry of wood strength.* Handbook of wood chemistry and wood composites, 2005. **303**.
26. Gil, M., I. Arauzo, and E. Teruel, *Influence of input biomass conditions and operational parameters on comminution of short-rotation forestry poplar*

and corn stover using neural networks. Energy and Fuels, 2013. **27**(5): p. 2649-2659.
27. Morita, T., *Corrosive-wear characteristics of diamond-coated cemented carbide tools.* Journal of Wood Science, 1999. **45**(6): p. 463-469.
28. Rezaei, H., et al., *Size, shape and flow characterization of ground wood chip and ground wood pellet particles.* Powder Technology, 2016. **301**: p. 737-746.
29. Voller, V.R., *A note on energy-size reduction relationships in comminution.* Powder Technology, 1983. **36**(2): p. 281-286.
30. Repellin, V., et al., *Energy requirement for fine grinding of torrefied wood.* Biomass and Bioenergy, 2010. **34**(7): p. 923-930.
31. Yokoyama, T. and Y. Inoue, *Chapter 10 Selection of Fine Grinding Mills*, in *Handbook of Powder Technology*, A.D. Salman, M. Ghadiri, and M.J. Hounslow, Editors. 2007, Elsevier Science B.V. p. 487-508.
32. Mayer-Laigle, C., et al., *Comminution of Dry Lignocellulosic Biomass: Part II. Technologies, Improvement of Milling Performances, and Security Issues.* Bioengineering, 2018. **5**(3): p. 50.
33. Tamura, M., et al., *Grinding and combustion characteristics of woody biomass for co-firing with coal in pulverised coal boilers.* Fuel, 2014. **134**: p. 544-553.
34. Schell, D.J. and C. Harwood, *Milling of lignocellulosic biomass.* Applied Biochemistry and Biotechnology, 1994. **45**(1): p. 159-168.
35. Gil, M., et al., *Handling behavior of two milled biomass: SRF poplar and corn stover.* Fuel Processing Technology, 2013. **112**: p. 76-85.
36. Cadoche, L. and G.D. López, *Assessment of size reduction as a preliminary step in the production of ethanol from lignocellulosic wastes.* Biological Wastes, 1989. **30**(2): p. 153-157.
37. Tavares, L.M., *Chapter 1 Breakage of Single Particles: Quasi-Static*, in *Handbook of Powder Technology*, A.D. Salman, M. Ghadiri, and M.J. Hounslow, Editors. 2007, Elsevier Science B.V. p. 3-68.
38. Chuetor, S., et al., *Analysis of ground rice straw with a hydro-textural approach.* Powder Technology, 2017. **310**: p. 74-79.
39. Kobayashi, N., et al., *Efficient pulverization technique of woody biomass by a multiple tube vibration mill.* Journal of the Japan Institute of Energy, 2011. **90**(11): p. 1024-1030.
40. Zhao, X.-Y., et al., *Application of superfine pulverization technology in Biomaterial Industry.* Journal of the Taiwan Institute of Chemical Engineers, 2009. **40**(3): p. 337-343.
41. Karinkanta, P., M. Illikainen, and J. Niinimäki, *Impact-based pulverisation of dried and screened Norway spruce (Picea abies) sawdust in an oscillatory ball mill.* Powder Technology, 2013. **233**: p. 286-294.

42. Karinkanta, P., M. Illikainen, and J. Niinimäki, *Pulverisation of dried and screened Norway spruce (Picea abies) sawdust in an air classifier mill.* Biomass and Bioenergy, 2012. **44**: p. 96-106.
43. Karinkanta, P., M. Illikainen, and J. Niinimäki, *Effect of different impact events in fine grinding mills on the development of the physical properties of dried Norway spruce (Picea abies) wood in pulverisation.* Powder Technology, 2014. **253**: p. 352-359.
44. Tassinari, T. and C. Macy, *Differential speed two roll mill pretreatment of cellulosic materials for enzymatic hydrolysis.* Biotechnol Bioeng, 1977. **19**(9): p. 1321-30.
45. Tassinari, T., et al., *Energy requirements and process design considerations in compression-milling pretreatment of cellulosic wastes for enzymatic hydrolysis.* Biotechnology and Bioengineering, 1980. **22**(8): p. 1689-1705.
46. Tassinari, T.H., C.F. Macy, and L.A. Spano, *Technology advances for continuous compression milling pretreatment of lignocellulosics for enzymatic hydrolysis.* Biotechnology and Bioengineering, 1982. **24**(7): p. 1495-1505.
47. Kobayashi, N., et al., *A new pulverized biomass utilization technology.* Powder Technology, 2008. **180**(3): p. 272-283.
48. Kobayashi, N., et al., *Evaluation of wood powder property pulverized by a vibration mill.* Nihon Enerugi Gakkaishi/Journal of the Japan Institute of Energy, 2007. **86**(9): p. 730-735.
49. Retsch, *Retsch Ultra Centrifugal Mill ZM 200, with 900 ml Cassette , 230 V, 50/60 Hz*. 2023: https://www.retsch.com/products/milling/rotor-mills/zm300/?gclid=EAIaIQobChMIoJW2jNfy_gIVCSIYCh02GwJXEAAYASAAEgLskPD_BwE
50. ZPS, Z., *Principle of operation*. 2023: https://www.hosokawa-alpine.com/powder-particle-processing/machines/classifiermills/zirkoplex-zps/.
51. Peukert, W. and L. Vogel, *Comminution of Polymers – An Example of Product Engineering.* Chemical Engineering & Technology, 2001. **24**(9): p. 945-950.
52. Motte, J.-C., et al., *Elastic properties of packing of granulated cork: Effect of particle size.* Industrial Crops and Products, 2017. **99**: p. 126-134.
53. Bridgeman, T.G., et al., *An investigation of the grindability of two torrefied energy crops.* Fuel, 2010. **89**(12): p. 3911-3918.
54. Hardgrove, R.M., *Discussion: "The Relative Grindability of Coal" (Sloman, H. J., and Barnhart, A. C., 1934, Trans. ASME, 56, pp. 773-779).* Journal of Fluids Engineering, Transactions of the ASME, 1935. **57**(4): p. 190-191.
55. Agus, F. and P.L. Waters, *Determination of the grindability of coals, shales and other minerals by a modified Hardgrove-machine method.* Fuel, 1971. **50**(4): p. 405-431.

56. Joshi, N.R., *Relative grindability of bituminous coals on volume basis.* Fuel, 1979. **58**(6): p. 477-478.
57. Temmerman, M., P.D. Jensen, and J. Hébert, *Von Rittinger theory adapted to wood chip and pellet milling, in a laboratory scale hammermill.* Biomass and Bioenergy, 2013. **56**: p. 70-81.
58. Miao, Z., et al., *Energy requirement for comminution of biomass in relation to particle physical properties.* Industrial Crops and Products, 2011. **33**(2): p. 504-513.
59. Holtzapple, M.T., A.E. Humphrey, and J.D. Taylor, *Energy requirements for the size reduction of poplar and aspen wood.* Biotechnol Bioeng, 1989. **33**(2): p. 207-10.
60. Gryc, V., et al., *Basic density of spruce wood, wood with bark, and bark of branches in locations in the czech republic.* Wood Research, 2011. **56**(1): p. 23-32.
61. Gryc, V., H. Vavrčík, and Š. Gomola, *Selected properties of European beech (Fagus sylvatica L.).* Journal of Forest Science, 2008. **54**(9): p. 418-425.
62. Karinkanta, P., M. Illikainen, and J. Niinimaki, *Effect of mild torrefaction on pulverization of Norway spruce (Picea abies) by oscillatory ball milling: particle morphology and cellulose crystallinity.* Holzforschung, 2014. **68**(3): p. 337-343.
63. Tannous, K., et al., *Physical properties for flow characterization of ground biomass from douglas fir wood.* Particulate Science and Technology, 2013. **31**(3): p. 291-300.
64. Dai, J.J. and J.R. Grace, *Biomass granular screw feeding: An experimental investigation.* Biomass & Bioenergy, 2011. **35**(2): p. 942-955.
65. Demirbas, A., A. Sahin-Demirbas, and A.H. Demirbas, *Briquetting properties of biomass waste materials.* Energy Sources, 2004. **26**(1): p. 83-91.
66. Geldart, D., *Estimation of basic particle properties for use in fluid particle process calculations.* Powder Technology, 1990. **60**(1): p. 1-13.
67. Lam, P.S., et al., *Effect of Temperature, Time, Particle size and Moisture content on Physical and Chemical Properties of Steam Exploded Woody Biomass*, in *2010 Pittsburgh, Pennsylvania, June 20 - June 23, 2010*. 2010, ASABE: St. Joseph, MI.
68. Mandø, M. and L. Rosendahl, *On the motion of non-spherical particles at high Reynolds number.* Powder Technology, 2010. **202**(1): p. 1-13.
69. Paulrud, S., J.E. Mattsson, and C. Nilsson, *Particle and handling characteristics of wood fuel powder: Effects of different mills.* Fuel Processing Technology, 2002. **76**(1): p. 23-39.

70. Ryu, C., et al., *Effect of fuel properties on biomass combustion: Part I. Experiments - fuel type, equivalence ratio and particle size.* Fuel, 2006. **85**(7-8): p. 1039-1046.
71. Clarke, K.L., T. Pugsley, and G.A. Hill, *Fluidization of moist sawdust in binary particle systems in a gas-solid fluidized bed.* Chemical Engineering Science, 2005. **60**(24): p. 6909-6918.
72. Mujumdar, A.S., *Principles, classification, and selection of dryers*, in *Handbook of Industrial Drying, Fourth Edition*. 2014. p. 3-30.
73. Austin, L.G., *A treatment of impact breakage of particles.* Powder Technology, 2002. **126**(1): p. 85-90.
74. Austin, L.G., *A preliminary simulation model for fine grinding in high speed hammer mills.* Powder Technology, 2004. **143**: p. 240-252.
75. Wadell, H., *Volume, Shape, and Roundness of Quartz Particles.* The Journal of Geology, 1935. **43**(3): p. 250-280.
76. Mohsenin, N.N. *Physical Properties of Plant and Animal Materials: v. 1: Physical Characteristics and Mechanical Properties*. 2020.
77. Lam, P.S., et al., *Bulk density of wet and dry wheat straw and switchgrass particles.* Applied Engineering in Agriculture, 2008. **24**(3): p. 351-358.
78. Zou, R.P. and A.B. Yu, *Wall effect on the packing of cylindrical particles.* Chemical Engineering Science, 1996. **51**(7): p. 1177-1180.
79. Santomaso, A., P. Lazzaro, and P. Canu, *Powder flowability and density ratios: The impact of granules packing.* Chemical Engineering Science, 2003. **58**(13): p. 2857-2874.
80. Zou, R.P., et al., *Packing of cylindrical particles with a length distribution.* Journal of the American Ceramic Society, 1997. **80**(3): p. 646-652.
81. Barletta, B.J., K.M. Knight, and G.V. Barbosa-CÁNovas, *Compaction characteristics of agglomerated coffee during tapping.* Journal of Texture Studies, 1993. **24**(3): p. 253-268.
82. Sokhansanj, S. and W.G. Lang, *Prediction of kernel and bulk volume of wheat and canola during adsorption and desorption.* Journal of Agricultural Engineering Research, 1996. **63**(2): p. 129-136.
83. Chevanan, N., et al., *Effect of particle size distribution on loose-filled and tapped densities of selected biomass after knife mill size reduction.* Applied Engineering in Agriculture, 2011. **27**(4): p. 631-644.
84. Geldart, D., et al., *Characterization of powder flowability using measurement of angle of repose.* China Particuology, 2006. **4**(3): p. 104-107.
85. Fasina, O.O., *Flow and physical properties of switchgrass, peanut hull, and poultry litter.* Transactions of the ASABE, 2006. **49**(3): p. 721-728.
86. Tabil Jr, L.G. and S. Sokhansanj, *Bulk properties of alfalfa grind in relation to its compaction characteristics.* Applied Engineering in Agriculture, 1997. **13**(4): p. 499-505.

87. Jayas, D.S., S. Sokhansanj, and N.D.G. White, *Bulk density and porosity of two Canola species.* Transactions of the American Society of Agricultural Engineers, 1989. **32**(1): p. 291-294.
88. Sokhansanj, S. and J.J. Fenton. *Cost benefit of biomass supply and pre-processing*. 2006.
89. Phanphanich, M. and S. Mani, *Impact of torrefaction on the grindability and fuel characteristics of forest biomass.* Bioresource Technology, 2011. **102**(2): p. 1246-1253.
90. Mattsson, J.E. and P.D. Kofman, *Method and apparatus for measuring the tendency of solid biofuels to bridge over openings.* Biomass & Bioenergy, 2002. **22**(3): p. 179-185.
91. Hausner, H.H. *Friction conditions in a mass of metal powder*. International Journal of Powder Metallurgy.1967. **3**: p. 7-13.
92. Ileleji, K.E. and B. Zhou, *The angle of repose of bulk corn stover particles.* Powder Technology, 2008. **187**(2): p. 110-118.
93. Zhou, Y.C., et al., *An experimental and numerical study of the angle of repose of coarse spheres.* Powder Technology, 2002. **125**(1): p. 45-54.
94. Baxter, J., et al., *Stratification in poured granular heaps [11].* Nature, 1998. **391**(6663): p. 136.
95. Makse, H.A., *Stratification instability in granular flows.* Physical Review E - Statistical Physics, Plasmas, Fluids, and Related Interdisciplinary Topics, 1997. **56**(6): p. 7008-7016.
96. Frette, V., et al., *Avalanche dynamics in a pile of rice.* Nature, 1996. **379**(6560): p. 49-52.
97. Jaeger, H.M., C.H. Liu, and S.R. Nagel, *Relaxation at the angle of repose.* Physical Review Letters, 1989. **62**(1): p. 40-43.
98. Lee, J., *Avalanches in (1 + 1)-dimensional piles: a molecular dynamics study.* J. Phys. I France, 1993. **3**(10): p. 2017-2027.
99. Buchholtz, V. and T. Pöschel, *Numerical investigations of the evolution of sandpiles.* Physica A: Statistical Mechanics and its Applications, 1994. **202**(3): p. 390-401.
100. Dury, C.M., et al., *Boundary effects on the angle of repose in rotating cylinders.* Physical Review E - Statistical Physics, Plasmas, Fluids, and Related Interdisciplinary Topics, 1998. **57**(4): p. 4491-4497.
101. Jullien, R., P. Meakin, and A. Pavlovitch, *Particle Size Segregation by Shaking in Two-Dimensional Disc Packings.* Europhysics Letters, 1993. **22**(7): p. 523.
102. Carstensen, J.T. and P.-C. Chan, *Relation between particle size and repose angles of powders.* Powder Technology, 1976. **15**(1): p. 129-131.
103. Carrigy, M.A., *Experiments on the angles of repose of granular materials.* Sedimentology, 1970. **14**(3-4): p. 147-158.

104. Van Burkalow, A., *Angle of repose and angle of sliding friction: An experimental study.* Bulletin of the Geological Society of America, 1945. **56**(6): p. 669-707.
105. Adams, T.N., D.R. Raymond, and C. Schmid, *Optimization of a swirl burner for pulverized-wood fuels.* Tappi Journal, 1988. **71**(5): p. 91-96.
106. Chang, V.S. and M.T. Holtzapple, *Fundamental factors affecting biomass enzymatic reactivity.* Applied Biochemistry and Biotechnology - Part A Enzyme Engineering and Biotechnology, 2000. **84-86**: p. 5-37.
107. Hendriks, A.T.W.M. and G. Zeeman, *Pretreatments to enhance the digestibility of lignocellulosic biomass.* Bioresource Technology, 2009. **100**(1): p. 10-18.
108. Kociszewski, M., et al., *Effect of industrial wood particle size on mechanical properties of wood-polyvinyl chloride composites.* European Journal of Wood and Wood Products, 2012. **70**(1-3): p. 113-118.
109. Lu, H., et al., *Effects of particle shape and size on devolatilization of biomass particle.* Fuel, 2010. **89**(5): p. 1156-1168.
110. Reuther, J.J., G.G. Karsner, and S.T. Jack, *Plane flame furnace combustion studies of pulverized wood*, in *Fundamentals of thermochemical biomass conversion*, R.P. Overend, T.A. Milne, and L.K. Mudge, Editors. 1985, Springer Netherlands: Dordrecht. p. 793-810.
111. Stark, N.M. and R.E. Rowlands, *Effects of wood fiber characteristics on mechanical properties of wood/polypropylene composites.* Wood and Fiber Science, 2003. **35**(2): p. 167-174.
112. Sun, Y. and J. Cheng, *Hydrolysis of lignocellulosic materials for ethanol production: A review.* Bioresource Technology, 2002. **83**(1): p. 1-11.
113. Takatani, M., et al., *Effect of lignocellulosic materials on the properties of thermoplastic polymer/wood composites.* Holzforschung, 2000. **54**(2): p. 197-200.
114. Zhang, M., et al. *Effects of mechanical comminution on enzymatic conversion of cellulosic biomass in biofuel manufacturing: A review*. in *ASME 2010 International Manufacturing Science and Engineering Conference, MSEC 2010*. 2010.
115. Zhu, J.Y., et al., *Sulfite pretreatment (SPORL) for robust enzymatic saccharification of spruce and red pine.* Bioresource Technology, 2009. **100**(8): p. 2411-2418.
116. Cosereanu, C., et al., *Effect of particle size and geometry on the performance of single-layer and three-layer particleboard made from sunflower seed husks.* BioResources, 2015. **10**(1): p. 1127-1136.
117. Veigel, S., et al., *Particle board and oriented strand board prepared with nanocellulose- reinforced adhesive.* Journal of Nanomaterials, 2012. **2012**.

118. Wolcott, M.P., *Wood–Plastic Composites*, in *Encyclopedia of Materials: Science and Technology*, K.H.J. Buschow, et al., Editors. 2001, Elsevier: Oxford. p. 9759-9763.
119. FAO, *Global forest products / Facts and figures*. 2016: http://www.fao.org/3/i7034en/i7034en.pdf.
120. Ichazo, M.N., et al., *Polypropylene/wood flour composites: Treatments and properties.* Composite Structures, 2001. **54**(2-3): p. 207-214.
121. Astari, L., K.W. Prasetiyo, and L. Suryanegara. *Properties of Particleboard Made from Wood Waste with Various Size*. in *IOP Conference Series: Earth and Environmental Science*. 2018.
122. Dunky, M., *Urea–formaldehyde (UF) adhesive resins for wood.* International Journal of Adhesion and Adhesives, 1998. **18**(2): p. 95-107.
123. İstek, A., U. Aydin, and İ. Özlusoylu, *The effect of chip size on the particleboard properties,*, in *International Conference on Engineered and Life Sciences (ICELIS)Kastamonu/Turkey*. 2018. p. 439 – 444.
124. Lias, H., et al. *Influence of board density and particle sizes on the homogenous particleboard properties from kelempayan (Neolamarckia cadamba)*. 2014.
125. Nuryawan, A., et al., *Urea-formaldehyde resins: production, application, and testing.* IOP Conference Series: Materials Science and Engineering, 2017. **223**(1): p. 012053.
126. He, S., T. Liu, and M. Di, *Preparation and Properties of Wood Flour Reinforced Lignin-Epoxy Resin Composite.* BioResources, 2016. **11**(1): p. 2319-2333.
127. Oduor, N.M., P. Vinden, and P.C.S. Kho. *Dimensional Stability of Particle Board and Radiata Pine Wood (Pinus radiata D. Don) Treated with Different Resins*. 2013.
128. Vital, B.R., J.B. Wilson, and P.H. Kanarek, *Parameters affecting dimensional stability of flakeboard and particleboard.* Forest Products Journal, 1980. **30**(12): p. 23-29.
129. Bengtsson, M., P. Gatenholm, and K. Oksman, *The effect of crosslinking on the properties of polyethylene/wood flour composites.* Composites Science and Technology, 2005. **65**(10): p. 1468-1479.
130. Chen, H.C., T.Y. Chen, and C.H. Hsu, *Effects of wood particle size and mixing ratios of HDPE on the properties of the composites.* Holz als Roh - und Werkstoff, 2006. **64**(3): p. 172-177.
131. Clemons, C., *Raw materials for wood-polymer composites*, in *Wood-Polymer Composites*. 2008. p. 1-22.
132. Gozdecki, C., et al., *Mechanical properties of wood-polypropylene composites with industrial wood particles of different sizes.* Wood and Fiber Science, 2012. **44**(1): p. 14-21.

133. Gozdecki, C., et al., *Effect of wood particle size on mechanical properties of industrial wood particle-polyethylene composites.* Polimery/Polymers, 2011. **56**(5): p. 375-380.
134. Izekor, D., S.O. Amiandamhen, and O.S. Agbarhoaga, *Effects of geometric particle sizes of wood flour on strength and dimensional properties of wood plastic composites.* Journal of Applied and Natural Science, 2013. **5**: p. 194-199.
135. Jaya, H., et al., *Effect of Particle Size on Mechanical Properties of Sawdust-High Density Polyethylene Composites under Various Strain Rates.* Bioresources, 2016. **11**: p. 6489-6504.
136. Khalil, H.P.S.A., et al., *Recycle Polypropylene (RPP) - Wood Saw Dust (WSD) Composites - Part 1: The Effect of Different Filler Size and Filler Loading on Mechanical and Water Absorption Properties.* Journal of Reinforced Plastics and Composites, 2006. **25**(12): p. 1291-1303.
137. Khonsari, A., et al., *Study on the effects of wood flour geometry on physical and mechanical properties of wood-plastic composites.* Maderas: Ciencia y Tecnologia, 2015. **17**(3): p. 545-558.
138. Maiti, S.N. and K. Singh, *Influence of wood flour on the mechanical properties of polyethylene.* Journal of Applied Polymer Science, 1986. **32**(3): p. 4285-4289.
139. Rasat, M.S.M., et al., *Influence of wood particle size on strength properties of wood plastics composite (Wpc) from laran species.* Journal of Applied Sciences Research, 9 (2013) 2585 – 2590, 2013. **9**(4): p. 2585 – 2590.
140. Rimdusit, S., et al., *Highly filled polypropylene rubber wood flour composites.* Engineering Journal, 2011. **15**(2): p. 17-30.
141. Stark, N.M. and M.J. Berger. *Effect of Particle Size on Properties of Wood-Flour Reinforced Polypropylene Composites*. 1998.
142. Gu, K., J. Huang, and K. Li, *Preparation and evaluation of particleboard bonded with a soy flour-based adhesive with a new curing agent.* Journal of Adhesion Science and Technology, 2013. **27**(18-19): p. 2053-2064.
143. Kajikawa, S., et al. *Molding of wood powder with a natural binder*. in *Procedia Engineering*. 2017.
144. Ashori, A., et al., *Wood-wool cement board using mixture of eucalypt and poplar.* Industrial Crops and Products, 2011. **34**(1): p. 1146-1149.
145. Badejo, S.O.O., *Effect of flake geometry on properties of cement-bonded particleboard from mixed tropical hardwoods.* Wood Science and Technology, 1988. **22**(4): p. 357-369.
146. Frybort, S., et al., *Cement bonded composites - A mechanical review.* BioResources, 2008. **3**(2): p. 602-626.
147. Meneéis, C.H.S.D., V.G. De Castro, and M.R. De Souza, *Production and properties of a medium density wood-cement boards produced with oriented*

strands and silica fume. Maderas: Ciencia y Tecnologia, 2007. **9**(2): p. 105-115.
148. Moslemi, A.A., J.F. Garcia, and A.D. Hofstrand, *Effect of various treatments and additives on wood-portland cement-water systems.* Wood and Fiber Science, 2007. **15**: p. 164-176.
149. Moslemi, A.A. and S. Pfister, *The influence of cement/wood ratio and cement type on bending strength and dimensional stability of wood-cement composite panels'.* Wood and Fiber Science, 1987. **19**: p. 165-175.
150. Nasser, R.A., et al., *Effects of tree species and wood particle size on the properties of cement-bonded particleboard manufacturing from tree prunings.* Journal of Environmental Biology, 2014. **35**(5): p. 961-971.
151. Sudin, R., *Cement bonded particleboard from Acacia mangium: a preliminary study.* J Trop For Sci, 1990. **2**: p. 267-273.
152. Hashim, R., et al., *Effect of particle geometry on the properties of binderless particleboard manufactured from oil palm trunk.* Materials and Design, 2010. **31**(9): p. 4251-4257.
153. Miyamoto, K., S. Nakahara, and S. Suzuki, *Effect of particle shape on linear expansion of particleboard.* Journal of Wood Science, 2002. **48**(3): p. 185-190.
154. Sackey, E.K., et al., *Improving core bond strength of particleboard through particle size redistribution.* Wood and Fiber Science, 2008. **40**(2): p. 214-224.
155. Chaudemanche, S., et al., *Properties of an industrial extruded HDPE-WPC: The effect of the size distribution of wood flour particles.* Construction and Building Materials, 2018. **162**: p. 543-552.
156. Leu, S.-Y., et al., *Optimized material composition to improve the physical and mechanical properties of extruded wood–plastic composites (WPCs).* Construction and Building Materials, 2012. **29**: p. 120-127.
157. Dai, J., H. Cui, and J.R. Grace, *Biomass feeding for thermochemical reactors.* Progress in Energy and Combustion Science, 2012. **38**(5): p. 716-736.
158. Pallarés, J., et al., *Numerical study of co-firing coal and Cynara cardunculus in a 350 MWe utility boiler.* Fuel Processing Technology, 2009. **90**(10): p. 1207-1213.
159. Steer, J., et al., *Biomass co-firing trials on a down-fired utility boiler.* Energy Conversion and Management, 2013. **66**: p. 285-294.
160. van Loo, S. and J. Koppejan, *The handbook of biomass combustion and co-firing*. The Handbook of Biomass Combustion and Co-Firing. 2012. 1-442.
161. Ruben Sudhakar, D. and A.K. Kolar, *Experimental investigation of the effect of initial fuel particle shape, size and bed temperature on devolatilization of single wood particle in a hot fluidized bed.* Journal of Analytical and Applied Pyrolysis, 2011. **92**(1): p. 239-249.

162. Demirbas, A., *Potential applications of renewable energy sources, biomass combustion problems in boiler power systems and combustion related environmental issues.* Progress in Energy and Combustion Science, 2005. **31**(2): p. 171-192.
163. Gravelsins, R.J. and O. Trass, *Analysis of grinding of pelletized wood waste with the Szego Mill.* Powder Technology, 2013. **245**: p. 189-198.
164. Saastamoinen, J., et al., *Burnout of pulverized biomass particles in large scale boiler - Single particle model approach.* Biomass and Bioenergy, 2010. **34**(5): p. 728-736.
165. Stelte, W., et al., *Recent developments in biomass pelletization - a review.* BioResources, 2012. **7**(3): p. 4451-4490.
166. Gendek, A., M. Aniszewska, and K. Chwedoruk. *Bulk density of forest energy chips*. 2016.
167. Tumuluru, J.S., et al., *A review on biomass torrefaction process and product properties for energy applications.* Industrial Biotechnology, 2011. **7**(5): p. 384-401.
168. Tumuluru, J.S. and C.T. Wright, *A review on biomass densification technologie for energy application*. 2010: United States. p. Medium: ED.
169. Dai, J., et al., *Gasification of Woody Biomass.* Annual Review of Chemical and Biomolecular Engineering, 2015. **6**: p. 77-99.
170. Europe, U.N.E.C.f., *Forest Products Annual Market Review 2020-2021*. 2022: United Nations.
171. Bergström, D., et al., *Effects of raw material particle size distribution on the characteristics of Scots pine sawdust fuel pellets.* Fuel Processing Technology, 2008. **89**(12): p. 1324-1329.
172. Castellano, J.M., et al., *Study on the effects of raw materials composition and pelletization conditions on the quality and properties of pellets obtained from different woody and non woody biomasses.* Fuel, 2015. **139**: p. 629-636.
173. Lehtikangas, P., *Quality properties of pelletised sawdust, logging residues and bark.* Biomass and Bioenergy, 2001. **20**(5): p. 351-360.
174. Lee, J.Y., et al., *Fundamental study on developing wood powder as an additive of paperboard.* Tappi Journal, 2014. **13**(11): p. 17-22.
175. Park, J.H., et al., *Effects of Lignocellulosic Bulking Agents Made from Agricultural Byproducts on Physical Properties and Drying Energy Consumption of Duplex Board.* BioResources, 2015. **10**(4): p. 7889-7897.
176. Sami, T., et al., *Method for making organic pigment*, in *https://patents.google.com/patent/WO2009080894A1/en*. 2009: USA.
177. Navarre, F.-P., P. Girard, and J. Dussaud, *Filled paper for gas filtration*, in *https://patents.google.com/patent/US5965091*. 1999: USA.
178. Navarre, F.-P., et al., *Filter paper for laden liquids*, in *https://patents.google.com/patent/US6224768B1/en*. 2001.

179. Seo, Y.B., D.S. Kang, and J.S. Han, *Utilization of Calcium Carbonate-Coated Wood Flour in Printing Paper and Their Conservational Properties.* Sustainability, 2019. **11**(7): p. 1867.
180. Berntsson, T., et al. *What is a biorefinery*. 2012.
181. Sugimoto, T., et al., *Ozone pretreatment of lignocellulosic materials for ethanol production: Improvement of enzymatic susceptibility of softwood.* Holzforschung, 2009. **63**(5): p. 537-543.
182. Agarwal, U.P., J.Y. Zhu, and S.A. Ralph, *Enzymatic hydrolysis of loblolly pine: Effects of cellulose crystallinity and delignification.* Holzforschung, 2013. **67**(4): p. 371-377.
183. Kirsch, C., C. Zetzl, and I. Smirnova, *Development of an integrated thermal and enzymatic hydrolysis for lignocellulosic biomass in fixed-bed reactors.* Holzforschung, 2011. **65**(4): p. 483-489.
184. Schütt, F., J. Puls, and B. Saake, *Optimization of steam pretreatment conditions for enzymatic hydrolysis of poplar wood.* Holzforschung, 2011. **65**(4): p. 453-459.
185. Chandra, R.P., et al., *Substrate Pretreatment: The Key to Effective Enzymatic Hydrolysis of Lignocellulosics?*, in *Biofuels*, L. Olsson, Editor. 2007, Springer Berlin Heidelberg: Berlin, Heidelberg. p. 67-93.
186. Díaz, M.J., et al., *Organosolv pretreatment of olive tree biomass for fermentable sugars.* Holzforschung, 2011. **65**(2): p. 177-183.
187. Kumar, P., et al., *Methods for pretreatment of lignocellulosic biomass for efficient hydrolysis and biofuel production.* Industrial and Engineering Chemistry Research, 2009. **48**(8): p. 3713-3729.
188. Zhu, J.Y. and X.J. Pan, *Woody biomass pretreatment for cellulosic ethanol production: Technology and energy consumption evaluation.* Bioresource Technology, 2010. **101**(13): p. 4992-5002.
189. Leu, S.Y. and J.Y. Zhu, *Substrate-Related Factors Affecting Enzymatic Saccharification of Lignocelluloses: Our Recent Understanding.* Bioenergy Research, 2013. **6**(2): p. 405-415.
190. Walker, L.P. and D.B. Wilson, *Enzymatic hydrolysis of cellulose: An overview.* Bioresource Technology, 1991. **36**(1): p. 3-14.
191. Zhu, J.Y., X. Pan, and R.S. Zalesny Jr, *Pretreatment of woody biomass for biofuel production: Energy efficiency, technologies, and recalcitrance.* Applied Microbiology and Biotechnology, 2010. **87**(3): p. 847-857.
192. Zhu, L., et al., *Structural features affecting biomass enzymatic digestibility.* Bioresource Technology, 2008. **99**(9): p. 3817-3828.
193. Mansfield, S.D., C. Mooney, and J.N. Saddler, *Substrate and enzyme characteristics that limit cellulose hydrolysis.* Biotechnology Progress, 1999. **15**(5): p. 804-816.

194. Zhu, J.Y., et al., *Specific surface to evaluate the efficiencies of milling and pretreatment of wood for enzymatic saccharification.* Chemical Engineering Science, 2009. **64**(3): p. 474-485.
195. Zhu, L., et al., *Multiple linear regression model for predicting biomass digestibility from structural features.* Bioresource Technology, 2010. **101**(13): p. 4971-4979.
196. Dasari, R.K. and R. Eric Berson, *The effect of particle size on hydrolysis reaction rates and rheological properties in cellulosic slurries.* Applied Biochemistry and Biotechnology, 2007. **137-140**(1-12): p. 289-299.
197. Fukazawa, K., et al., *Relationship between ball milling and the susceptibility of wood to digestion by cellulase.* Wood Science and Technology, 1982. **16**(4): p. 279-285.
198. Bridgwater, A.V., *Review of fast pyrolysis of biomass and product upgrading.* Biomass and Bioenergy, 2012. **38**: p. 68-94.
199. Svoboda, K., et al., *Pretreatment and feeding of biomass for pressurized entrained flow gasification.* Fuel Processing Technology, 2009. **90**(5): p. 629-635.
200. Thunman, H., et al., *Combustion of wood particles - A particle model for Eulerian calculations.* Combustion and Flame, 2002. **129**(1-2): p. 30-46.
201. Berglin, E.J., C.W. Enderlin, and A.J. Schmidt, *Review and Assessment of Commercial Vendors/Options for Feeding and Pumping Biomass Slurries for Hydrothermal Liquefaction*. 2012: United States. p. Medium: ED; Size: PDFN.
202. Funaoka, M., *A new type of phenolic lignin-based network polymer with the structure-variable function composed of 1,1-diarylpropane units.* Polymer International, 1998. **47**(3): p. 277-290.
203. Funaoka, M., *Lignin: Its Functions and Successive Flow.* Macromolecular Symposia, 2003. **201**: p. 213-222.
204. Sarkanen, K. and C.H. Ludwig. *Lignins : occurrence, formation, structure and reactions*. 1971.
205. Funaoka, M. and S. Fukatsu, *Characteristics of lignin structural conversion in a phase-separative reaction system composed of cresol and sulfuric acid.* Holzforschung, 1996. **50**(3): p. 245-252.
206. Funaoka, M., et al., *Conversion of native lignin to a highly phenolic functional polymer and its separation from lignocellulosics.* Biotechnology and Bioengineering, 1995. **46**(6): p. 545-552.
207. Radotić, K. and M. Mićić, *Methods for Extraction and Purification of Lignin and Cellulose from Plant Tissues*, in *Sample Preparation Techniques for Soil, Plant, and Animal Samples*, M. Micic, Editor. 2016, Springer New York: New York, NY. p. 365-376.
208. Berman, B., *3-D printing: The new industrial revolution.* Business Horizons, 2012. **55**(2): p. 155-162.

209. Wimmer, R., et al., *3D printing and wood.* Pro Ligno, 2015. **11**(4): p. 144-149.
210. Henke, K. and S. Treml, *Wood based bulk material in 3D printing processes for applications in construction.* European Journal of Wood and Wood Products, 2013. **71**(1): p. 139-141.
211. Kariz, M., M. Sernek, and M.K. Kuzman, *Use of wood powder and adhesive as a mixture for 3D printing.* European Journal of Wood and Wood Products, 2016. **74**(1): p. 123-126.
212. Kariz, M., M. Sernek, and M.K. Kuzman, *Effect of humidity on 3D-printed specimens from wood-pla filaments.* Wood Research, 2018. **63**(5): p. 917-922.
213. Tisserat, B., et al., *3D printing biocomposites.* Society of plastics Engineers, Plastics Research Online, 2015: p. 1-3.
214. Kariz, M., et al., *Effect of wood content in FDM filament on properties of 3D printed parts.* Materials Today Communications, 2018. **14**: p. 135-140.
215. Tao, Y., et al., *Development and application of wood flour-filled polylactic acid composite filament for 3d printing.* Materials, 2017. **10**(4).
216. Keränen, A., et al., *Preparation of novel anion exchangers from pine sawdust and bark, spruce bark, birch bark and peat for the removal of nitrate.* Chemical Engineering Science, 2013. **98**: p. 59-68.
217. Igwe, J.C., *A Review of Potentially Low Cost Sorbents for Heavy Metal Removal and Recovery.* Terrestrial and aquatic environmental toxicology, 2007. **1**: p. 60 – 69.
218. Maurin, E., et al., *A feasibility study on the use of chemically modified sawdusts bearing fatty alkyl chains for removal of oleic acid and olive-oil from water.* Holz als Roh - und Werkstoff, 1999. **57**(4): p. 265-266.
219. Albadarin, A.B., et al., *Biosorption Characteristics of Sawdust for the Removal of Cd(II) Ions: Mechanism and Thermodynamic Studies.* Chemical engineering transactions, 2011. **24**: p. 1297-1302.
220. Keränen, A., et al., *Quaternized pine sawdust in the treatment of mining wastewater.* Environmental Technology (United Kingdom), 2016. **37**(11): p. 1390-1397.
221. Orlando, U.S., et al., *Chemical properties of anion-exchangers prepared from waste natural materials.* Reactive and Functional Polymers, 2003. **55**(3): p. 311-318.
222. Bryant, P.S., et al., *Sorption of heavy metals by untreated red fir sawdust.* Applied Biochemistry and Biotechnology, 1992. **34-35**(1): p. 777-788.
223. Balintova, M., S. Demcak, and B. Pagacova. *A study of sorption heavy metals by natural organic sorbents*. 2016.
224. Ucun, H., et al., *Biosorption of chromium(VI) from aqueous solution by cone biomass of Pinus sylvestris.* Bioresource Technology, 2002. **85**(2): p. 155-158.

225. Bagherifam, S., et al., *Uranium removal from aqueous solutions by wood powder and wheat straw.* Journal of Radioanalytical and Nuclear Chemistry, 2010. **283**(2): p. 289-296.
226. Bailey, S.E., et al., *A review of potentially low-cost sorbents for heavy metals.* Water Research, 1999. **33**(11): p. 2469-2479.
227. Yu, H., et al., *Effect of cellulose nanofibers on induced polymerization of aniline and formation of nanostructured conducting composite.* Cellulose, 2014. **21**(3): p. 1757-1767.
228. Lu, T., et al., *Composite aerogels based on dialdehyde nanocellulose and collagen for potential applications as wound dressing and tissue engineering scaffold.* Composites Science and Technology, 2014. **94**: p. 132-138.
229. Pinkl, S., et al., *Nanopaper Properties and Adhesive Performance of Microfibrillated Cellulose from Different (Ligno-)Cellulosic Raw Materials.* Polymers, 2017. **9**(8): p. 326.
230. Jonasson, S., et al., *Isolation and characterization of cellulose nanofibers from aspen wood using derivatizing and non-derivatizing pretreatments.* Cellulose, 2020. **27**(1): p. 185-203.
231. Ross, S.M., *Chapter 9 - REGRESSION*, in *Introduction to Probability and Statistics for Engineers and Scientists (Fourth Edition)*, S.M. Ross, Editor. 2009, Academic Press: Boston. p. 353-439.
232. Sinharay, S., *An Overview of Statistics in Education*, in *International Encyclopedia of Education (Third Edition)*, P. Peterson, E. Baker, and B. McGaw, Editors. 2010, Elsevier: Oxford. p. 1-11.
233. Trygg, J. and S. Wold, *Orthogonal projections to latent structures (O-PLS).* Journal of Chemometrics, 2002. **16**(3): p. 119-128.
234. Eriksson, L., et al., *Design of experiments.* Principles and Applications, Learn ways AB, Stockholm, 2000.
235. Bylesjo, M., et al., *OPLS discriminant analysis: combining the strengths of PLS-DA and SIMCA classification.* Journal of Chemometrics, 2006. **20**(8-10): p. 341-351.
236. Chai, H., et al., *Effects of pretreatment with saturated wet air and steaming on the high-frequency vacuum drying characteristics of wood.* BioResources, 2019. **14**(4): p. 9601-9610.
237. Trubetskaya, A., et al., *Effect of fast pyrolysis conditions on biomass solid residues at high temperatures.* Fuel Processing Technology, 2016. **143**: p. 118-129.
238. Bajpai, P., Chapter 2 - Wood and Fiber Fundamentals, 2018: p. 19-74.
239. Shen, Y., et al., *Spectral and thermal analysis of Eucalyptus wood drying at different temperature and methods.* Drying Technology, 2020. **38**(3): p. 313-320.

240. Dawson, B.S.W., et al., *Effect of supercritical CO2 treatment and kiln drying on collapse in Eucalyptus nitens wood.* European Journal of Wood and Wood Products, 2020. **78**(2): p. 209-217.
241. Hadjiski, M., N. Deliiski, and N. Tumbarkova, *Mathematical description of the latent heat of water vaporization in capillary porous materials.* Informa. Technol. Control, 2019. **1**: p. 2-8.
242. Langrish, T. and J.C.F. Walker, *Drying of timber*, in *Primary Wood Processing: Principles and Practice*. 2006, Springer Netherlands: Dordrecht. p. 251-295.
243. Lube, V., et al., *Wood microfibril angle variation after drying.* Holzforschung, 2016. **70**(5): p. 485-488.
244. Geldart, D., N. Harnby, and A.C. Wong, *Fluidization of cohesive powders.* Powder Technology, 1984. **37**(1): p. 25-37.
245. Orlowski, K.A., et al., *Application of fracture mechanics for energetic effects predictions while wood sawing.* Wood Science and Technology, 2013. **47**(5): p. 949-963.

Acknowledgements

I would like to thank and show my gratitude to my thesis supervisors, Magnus Rudolfsson, David A. Agar, Sylvia H. Larsson and Dinesh Fernando. You all supported me not only on the academic side of things but also in practical matters. I am lucky to have all of you in my supervisor group. You always tried to accommodate my requests and look out for my interests. Although it is difficult for me to rank your importance to the research, there are no words in my dictionary to show my gratitude to Magnus Rudolfsson and David A. Agar for your continuous help in every step of the work. As per my experiences from other parts of the world, I would not have expected so much from others and there is not enough space here to express my appreciation.

I am also thankful to Michael Finell for his kind permission to admit me as a PhD candidate in the department and helping to solve many practical issues. This thanks extends to Mikael Thyrel as he became Prefekt and for teaching me a new analysis tool and encouraging me even in challenging times. I also thank you both for a perfect working environment, it is one of a kind in my experience and it enabled me to work at my best. In the same vein, I thank Jenny Högström, Kristina Åberg and Malin Sandberg for their wonderful administrative support and always-timely help. I cannot forget Tobias Holdo with whom I started my research work at the Biomass Technology Centre (BTC). He was such a nice person to work with and I thank Sylvia H. Larsson for selecting him, for teaching me the tools in experimental design and for supporting my time at the BTC. Thank you also to Gunnar Kalén and Markus Segerström who I will never forget for all their assistance in the milling experiments and analysis. I even worked until midnight some days and you always supported me. Dimitris Athanassiadis is acknowledged for teaching me how to hunt for funds for collaborative

work in other parts of the world. The support from my close colleagues, especially Mikael Lundbäck, Marjan Bozaghian Bäckman and Carola Häggström, is also not possible to overlook. Our pleasant discussions and their kind suggestions were influential in my practical life. They had a positive impact on my academic career. I would like to thank our SBT laboratory for part of my work, Carina Jonsson and Calle Niemi for their kind help and support. The daily and weekly *fika* breaks were a platform to meet people. These allowed me to get to know my colleagues and their work. I thank all the SBT personnel for their kind interactions and good discussions over the last four years.

I would also thank Professor Kentaro Umeki of Luleå University of Technology for providing me with the opportunity to visit and use the CAMSIZER for image analysis. Technical consultation from Sven Bremenfeld and Ted Rönnevall of Microtrac Retsch GmbH to complete the image analysis is well appreciated. Technical support and assistance from Borislav Vujadinovic is also acknowledged. Marta Derba-Maceluch at the Department of Forest Genetics and Plant Physiology is acknowledged for support with the optical imaging. I am also thankful to my host at the University of Tennessee-Knoxville, Professor Arthur J. Ragauskas for my research visit and expanding my knowledge through working on 3D printing. Your generous invitation and arrangements for the visit to Oakridge National Laboratory are well appreciated. I learned many new techniques and applications for wood powders. To make it successful, Carmen Ghossein, provided so much administrative support and help with practicalities – thank you! Thanks to Shuyang Zhang for his guidance in the laboratory! Next, I say thank you to Professor Nonappa, at Tampere University for inviting me to your group and laboratory to work with methods for lignocellulosic bioplastics. I also thank Professor Md. Nazrul Isalm, at Khulna University, for collaborative research work and his inspired talk to me. To all of the above, I hope our collaboration will continue in future!

I also acknowledge the funders of my research and those that provided travel funds. I am grateful to the Swedish Energy Agency (Project number-46904-1), the Swedish Bio4Energy Strategic Research Environment and the Department of Forest Biomaterials and Technology for the financial support to conduct the research. Funding from Seth M Kempes, Anna-Britta and Vadim Söderström, Bröderna Edlund, SLU Travel grant and Stiftelsen fonden för skogsvetenskaplig forskning are also acknowledged.

Finally, I would like to thank my mother, Renuka Das, to whom I promised that I would do a PhD and it helped me to never give up hope, and my late father, Deb Prosad Das, who was my ideal to teach me the humanity and reality of life. Next, I would like to include my youngest uncle, Shyama Prosad Das, and elder brothers, Das Anup Kumar and Arup Kumar Das who supported me to move in the beginning of my academic life. My uncle, Pinaki Das, who was a secondary school teacher in mathematics also had a great influence on my life. He taught me how to think to solve problems myself and it helped me to earn money through private tuition and continue my higher studies. Last but not at the least, I would like to show my sincere gratitude to my better half, Suzata Sarkar and my beloved son, Gopal Das. My wife had a great contribution and allowed me to engage myself in my research work. She tried to shield me from unnecessary things, which permitted me to focus on my work. My son sacrificed my company to give me a chance to do more work. I am nothing without them. I would like to include Magnus Rudolfsson and David A. Agar name in this personal part also because both of you work as my family members rather than thesis supervisors in many ways. It is not possible to forget that since we are living thousands of miles away from our home and family but your support has made it easier.

I

Powder Technology 378 (2021) 593–601

Contents lists available at ScienceDirect

Powder Technology

journal homepage: www.elsevier.com/locate/powtec

Multi-blade milling from log to powder in one step – Experimental design and results

Atanu Kumar Das *, David A. Agar, Sylvia H. Larsson, Tobias Holdo, Dinesh Fernando, Magnus Rudolfsson

Swedish University of Agricultural Sciences, Department of Forest Biomaterials and Technology, SE-901 83 Umeå, Sweden

ARTICLE INFO

Article history:
Received 17 July 2020
Received in revised form 16 September 2020
Accepted 6 October 2020
Available online 9 October 2020

Keywords:
Multi-blade shaft mill (MBSM)
Experimental design
Wood powder
Particle size distribution (PSD)
Specific milling energy

ABSTRACT

This study investigated a new technique for obtaining wood powders from whole logs (*Pinus sylvestris* L.) in a single-step operation. The performance of a prototype multi-blade shaft mill (MBSM) was evaluated using a designed series of experiments including three input parameters, i.e., the moisture content of the log, milling blade speed and log feeding speed, combined with multilinear regression (MLR) analysis. The milling performance was characterised by specific milling energy, particle size distribution and bulk density of powder. For MBSM powders (80 to 95% particles <1.0 mm), the specific milling energy ranged from 99 to 232 kWh t^{-1} DM. The mass per cent of particles <0.5 mm in MBSM powders ranged from 55 to 80% compared to 41% from hammer-milled powders. Powder bulk density varied from 138 to 264 kg m^{-3} DM and the moisture content of the milled log was the only significant ($p < 0.05$) factor affecting the bulk density of resulting powders (dried). MLR models show that the milling energy is inversely proportional to the moisture content, which indicates that moisture influences MBSM milling in a similar way as in the sawing of wood and opposite to that of impact-based mills (i.e. hammer mills).

1. Introduction

Wood is an abundant and widely available renewable material, whose utilisation in industry fulfils political and societal aims for greater sustainable development [1]. In Sweden, the wood supply continues to grow and there is a large supply potential of small-diameter trees from the thinning of young forests [2]. As a structurally complex and multi-purpose raw material, wood has excellent potential in industrial applications and products. Wood powders (i.e. wood particulates with a diameter less than approximately 1 mm) are the starting point for many thermal conversion and biorefining applications including combustion [3], chemical, enzymatic [4] and thermochemical processes for energy and chemical production (e.g. gasification).

Wood is a product of living trees and after falling and delimbing, the stem wood (i.e. log) is a convenient and compact form in which to store wood before utilisation. The original chemical composition, including those compounds of interest in biorefining, are best preserved in the log form with original moisture content or stored underwater [5]. When the time comes for size reduction, there are many technologies for producing wood powders [6] and new ones continue to be developed (e.g. Kobayashi et al. [7]).

Mechanical production of pulp directly from logs is an old technology [8] but outside of wood pulping applications, common industrial size-reduction technologies for producing wood powders are impact-based or knife mills, which use hammers (i.e. hammer mills), swing beaters, discs or impellers to crush wood [6]. These mills create powders from wood chips (with lengths ranging from about 10–70 mm), which are mechanically cut from logs, screened to remove oversized particles and necessarily pre-dried to ease conveying and avoid clogging of screens. Typical particle sizes from the wood chip-hammer mill production route are in the range of 0.2–2.0 mm [9–11]. This strategy is partly based on the ease of handling but the storage of wood as chips also presents its own risks such as the potential for microbial degradation, dry matter losses and unwanted greenhouse gas emissions [12]. From a system perspective, the several steps in this tree-to-powder pathway necessitate intermediate handling operations [9], which prolong the turnaround time, consume monetary resources and influence the emission footprint of wood as a raw material in industrial applications [13].

Powders produced via common chipping and hammer milling have pathway-specific microstructure properties because the mill type [4] and the drying process [14] leave signature modifications on wood cell walls. This affects the particle morphology (i.e. aspect ratio, surface porosity and specific surface area) which contributes to powder bulk properties, the chemical distribution in wood powders and ultimately their potential use in wood-based industries. For example, the chipping, drying and pulping of green wood rapidly accelerate the resin oxidation reactions. For acid sulphite pulping, this is beneficial but in kraft pulping, the loss of extractive content diminishes by-product yields, such as turpentine and tall oil [5]. Green and dry wood also break differently. The

* Corresponding author.
E-mail address: atanu.kumar.das@slu.se (A.K. Das).

https://doi.org/10.1016/j.powtec.2020.10.026

Nomenclature

BD	Bulk density
BS	Blade speed
DM	Dry mass
FS	Feeding speed
FSP	Fibre saturation point
MBSM	Multi-blade shaft mill
MC	Moisture content
PSD	Particle size distribution
e_M	Specific milling energy (kWh t^{-1})
m_h	Mass of the hammer-milled powder (kg)
m_M	Mass of milled log (kg)
P_c	Chipping power (kW)
P_f	Log feeding power (kW)
P_h	Hammer-milling power (kW)
P_m	Log milling power (kW)
Q^2	Goodness of prediction
R^2	Goodness of fit
t_c	Chipping time (s)
t_h	Hammer-milling time (s)
t_M	Log milling time (s)
Y_{BD}	Modelled bulk density (kg m^{-3})
Y_E	Modelled specific milling energy (kWh t^{-1})
Y_{PSD}	Modelled particle size distribution (mass %)

location of fractures within the cell wall is a function of moisture content and affects the quality of the fracture surface; at low moisture content, fractures expose more lignin and at high moisture content, fractures expose more carbohydrates [15]. Such differences in particle morphology have measureable effects on the enzymatic digestibility of sugars in wood powders [4]. Particle shape and particle size distribution (PSD) also contribute to powder combustion behaviour [16], material handling [17] and bulk density [18], which is an important predictor of its feeding properties [19]. What these examples show is that pretreatment methods have high relevance for subsequent conversion and biorefinery processes using wood.

Size reduction of wood requires an energy input to generate the shear, compressional, impact and cutting forces that act to fragment, grind and lacerate wood fibres [6]. From a physiological perspective, size reduction results from the rupture of bonds within the cell walls of wood where moisture content strongly affects hydrogen bonding between organic polymers. As the amount of bound water increases in the cell wall, hydrogen bonding decreases [20,21] from dry wood up to the fibre saturation point (FSP), which is defined as the moisture content at which the onset of shrinkage begins, triggering incremental changes in strength properties compared to green conditions [22]. The FSP is a useful construct but difficult to generalise as it depends on tree species and method of measurement but is approximately 23% moisture content (wet basis) [23]. Water uptake causes a reduction in the strength properties of wood [24] and enhances the breakage required to produce wood powders. Based on this understanding, the energy required to mill near the FSP is lower than that of dry wood. Above the FSP, the presence of free water in cell cavities has no appreciable influence on wood's strength properties [24] but excess water certainly contributes to material behaviour during size reduction [18], shaping with tools and sawing [25]. On a physical basis, water affects density and the response of wood to applied forces [26] through altering the coefficients of friction (static and kinetic) and its large heat capacity and latent heat affect material temperature, a factor of the cutting force.

The most common theories postulate that milling energy is proportional to new surface area generated through the milling process or by the reduction of volume from the starting material [27]. What this means is that there is no free lunch in size reduction – the finer the powder, the greater the energy input. The purpose of size reduction is to produce a finer particle size distribution (PSD). The geometric surface area of a unit mass of powder increases rapidly as particle diameter decreases. Effective surface area also depends on particle morphology and porosity. Fine powders cost more in terms of milling energy but can provide enormous surface areas, which may be beneficial in certain applications (e.g. chemical, thermal and biological conversion).

Also in practice, the specific milling energy is a function of achieved particle size with finer powders requiring more energy [6,10,28]. From experimental studies on both sawing and attrition milling, moisture content, wood density, tree species [29], grain orientation and temperature [30] influence the energy requirements. Specific milling energy in sawing wood is also a function of moisture content. Contrary to attrition milling, the required sawing energy increases as wood becomes more dry below the FSP. In this hygroscopic range of wood, the energy needed to produce the cutting force is greater than above the FSP due to greater wood hardness, fracture toughness and modulus of elasticity [31]. Above the FSP and with a surplus of water, the sawing energy demands decrease further [25]. Therefore, the changes in the physical properties of wood, due to low moisture content, make sawing wood more energy intensive. Yet these same changes assist the destructive forces in the attrition milling wood.

With the resurgence of various wood-based applications in society and wood powder feedstock for bio-based industries, new size reduction technologies have the potential to improve utilisation through supplying better-suited wood powders for refining processes and products. Eliminating multistep pre-processing and thermal treatments could save time and unlock more benefits from the green chemical profile of wood.

The purpose of this study was to evaluate the performance of a novel prototype milling technology for the production of wood powders directly from whole tree stems. The performance analysis was based on characterised wood powder properties, which included the particle size distribution and bulk density as well as the measured specific milling energy in size reduction. Through analysis of the results, the study aimed to determine whether the prototype mill behaved more like a saw or more like attrition-based size-reduction technologies.

2. Materials and methods

2.1. General procedure

In this study, a novel multi-blade shaft mill (MBSM) was utilised to produce fine wood powders from whole pine logs in a single step. A full experimental design was set up for log milling. A hammer-milling procedure was used as a comparison and the performance of the MBSM milling technology was investigated with respect to specific energy consumption, particle size distribution and bulk density for produced powders.

2.2. Milling systems

The multi-blade shaft mill (Klingmill AB, Torshälla, Sweden) consisted of a roller table, a feeder, and two 350 mm wide shafts of packed blades driven by two separate electric motors (Fig. 1). The first shaft had 110 parallel-mounted blades, each having eight teeth with a clearance angle of 18°, a rake angle of 5° and kerf 4.2 mm. The second shaft had 137 parallel-mounted blades, each having 24 teeth with 15° rake angle and 3 mm kerf. Each motor had a rated power of 55 kW and speed of 1480 rpm. A sample collector was set up at the outlet of the mill. It consisted of a vacuum system, a filter, and a plastic bag where the produced powder was collected. According to the manufacturer, the feeder on this prototype can accept log diameters up to 280 mm.

Hammer-milling experiments were performed with a Bühler Hammermill Vertica, Switzerland, which was equipped with a vertical grinding shaft, a 55 kW electric motor of 1480 rpm, with 12 × 4 floating hammers and a 2 mm circular sieve.

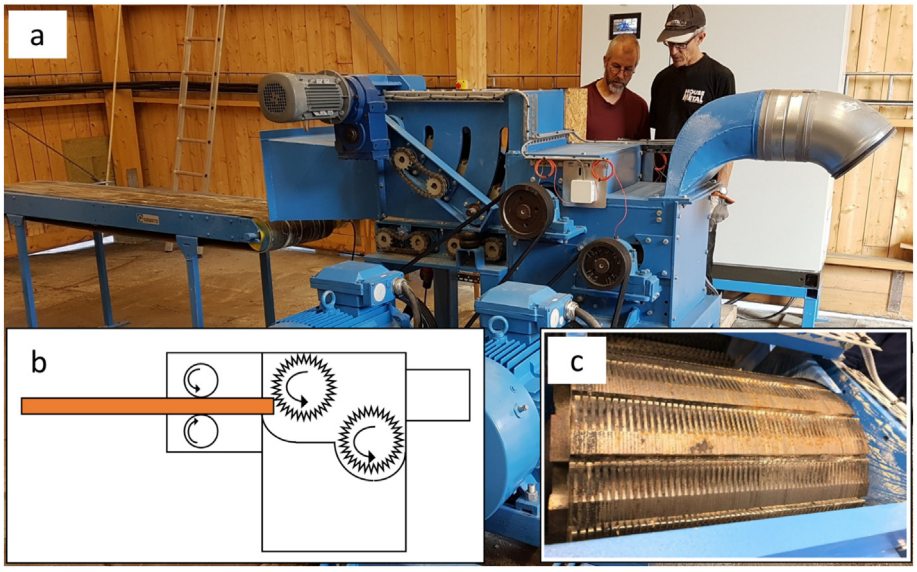

Fig. 1. (a) The prototype multi-blade shaft mill (MBSM) without its housing enclosure. The roller table, feeder and the two shafts connected to the motors are visible. The sample collector is not fitted to the outlet in the photograph. (b) The principle of operation of the MBSM and (c) the multi-blade shaft.

2.3. Experimental design

MSBM log milling was performed according to a full factorial (two-level) experimental screening design with one centre point varying three factors in their corresponding ranges: log moisture content (10 to 50%, wet basis), log feeding speed (1.3 to 2.6 m min^{-1}) and sawblade speed (52 to 72 m s^{-1}). The analysed responses were: the specific milling energy (kWh t^{-1} DM), the wood powder PSD (mass %) and the wood powder bulk density (kg m^{-3} DM). Experiments from each of the experimental design points were replicated three times, bring the total number of MBSM experiments for each response to 27. Settings, obtained factor values and response values are listed in Table S1 (Supplementary). The range of the three experimental factors was predefined by a method of trial and error.

Chipping and hammer milling were carried out at one single setting. The analysed responses were: the combined (chipper and hammer mill) specific milling energy (kWh t^{-1} DM), the wood powder PSD (mass %) and the wood powder bulk density (kg m^{-3} DM).

2.4. Material preparation

Defect-free Scots pine (*Pinus sylvestris* L.) trees were sourced from Vindeln, Sweden in September 2019. The trees, having an age of 22–32 years, were felled, delimbed and delivered next day to the Biomass Technology Centre, Swedish University of Agricultural Sciences, Umeå, Sweden. In total, 47 trees (27 for MBSM and 20 for hammer mill) were selected based on stem straightness and existence of knots. From the selected trees, 1.6 m logs were cut from the butt end aiming to minimise the extent of taper between the bottom and top, which ranged from approximately 10 to 14 cm in diameter. A handsaw was used to avoid chain-oil contamination. The logs were carefully debarked manually with drawknives as to not remove underlying stem wood. Drying was done at 25 °C in a drying cabinet (Elvärmedetaljer, Skurup, Sweden) to minimise changes in wood properties due to temperature. The dried and green logs were kept separate and wrapped in plastic to prevent changes in moisture content prior to experiments. An overview of the experimental procedure is depicted in Fig. 2.

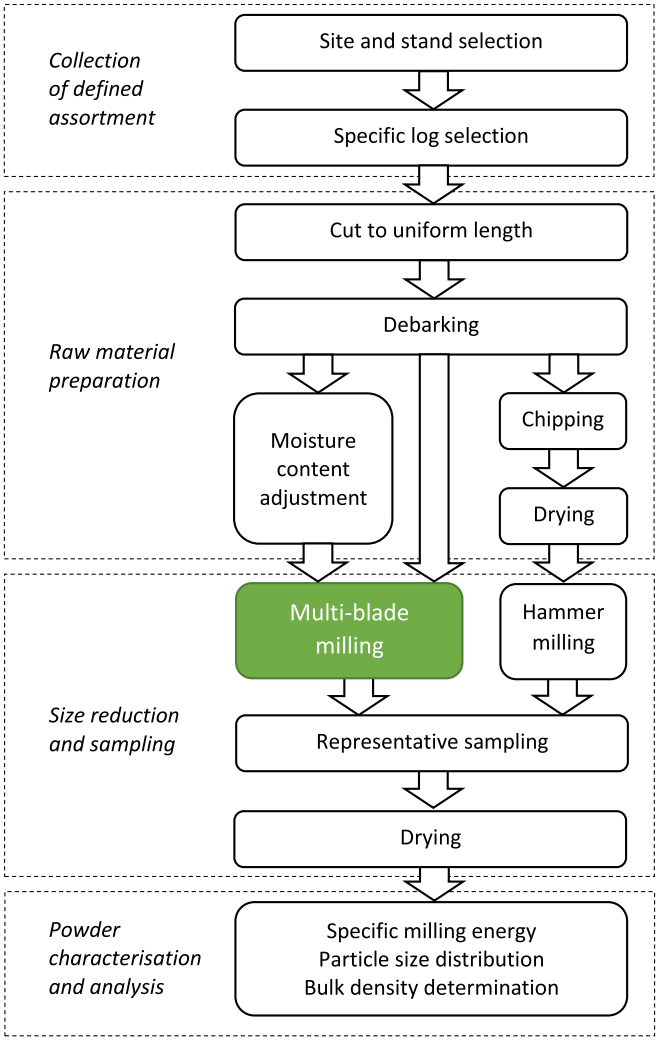

Fig. 2. An overview of the experimental procedure used in the study.

2.5. Milling procedure

The mass and length of the logs were measured and, within each moisture content level, ordered randomly with relation to the experimental design. Before each experiment, a plastic bag was fitted to the sample collector. The logs were then fed centrally via a roller table to the feeding section of the MBSM. During milling, the electric power (kW) and mill setting factors were recorded at 1 Hz frequency with a data acquisition system (INTAB PC-logger 3100). After the experiment, the sample bag was removed, sealed and weighed and the equipment thoroughly cleaned.

For the hammer mill experiment, 20 debarked logs were chipped (Edsbyhuggen, Woxnadalens Energi AB, Sweden) and then dried in an in-house-built flat-bed dryer to reach a moisture content of 7.2% (wet basis). The dry chips were screened (EO554, Fredrik Mogensen AB, Sweden) to obtain a 1.9–16.0 mm chip size range and this fraction was milled in the hammer mill. The electric power (kW) of the chipper and the hammer mill was logged at 1 Hz with a Fluke 1735 Power Logger (Fluke Corporation Everett, WA USA).

2.6. Sampling procedure

The sampling of wood powder from milling experiments was performed according to the standard method (SS-EN ISO 14780:2017 (E)) by systematically coning and quartering. Three samples were used for bulk density determination and one for sieve analysis. All powder samples were dried at 105 °C overnight, within approximately 20 min of milling and stored in sealed plastic bags for further analysis. The moisture content of the logs was measured from the powder moisture content.

2.7. Milling process performance

2.7.1. Specific milling energy

The specific milling energy e_M (kWh t^{-1} DM) for the MBSM milling was calculated according to Eq. (1):

$$e_M = m_M^{-1} \sum_{t_M} (P_f + P_m)\, t_M \tag{1}$$

in which m_M (kg DM) is the dry mass of the milled log, t_M (s) = log milling time, P_f (kW) = log feeding power and P_m (kW) = log milling power.

The specific milling energy e_h (kWh t^{-1} DM) for hammer milling was calculated according to Eq. (2):

$$e_h = m_h^{-1} \left(\sum_{t_c} (P_c \times t_c) + \sum_{t_h} (P_h \times t_h) \right) \tag{2}$$

in which m_h (kg DM) is the dry mass of the hammer-milled wood powder, t_c (s) = the chipping time, P_c (kW) = chipping power, t_h (s) = hammer-milling time and P_h (kW) = hammer-milling power.

2.7.2. Particle size distribution

The particle size distribution (PSD) was determined for the 27 MBSM samples and the hammer-milled samples using sieves following the standard method (EN 15149–2:2010). The sieving was done using a sieve shaker (Analysette 3, Fritsch, Germany) set at 1.5 mm amplitude for 10 min. The used sieves (Cisa, Spain) had standard (ISO-3310.1) sizes of 0.063, 0.125, 0.25, 0.5, 1.0, 1.4, 2.0, 2.8, 3.15, 8.0 and 16.0 mm. The amount of powder sample used in sieving was 0.5–0.7 L. The mass per cent of each size fraction was calculated from the total mass of sieved sample and the retained amount of powder on each sieve. The geometric mean (also known as Sauter) diameter was calculated using the equation from Tannous et al. [32]. Optical images of powders were taken using a stereo-microscope (model M205FA, Leica Microsystems, Germany) and a PLANAPO 0.63× lens at 4.92× magnification.

2.7.3. Powder bulk density

Determination of the bulk density (kg m^{-3} DM) of oven-dried wood powders was performed with a 5.4 L cylindrical vessel according to the standard method (EN 15103:2009).

2.8. Statistical analysis

Multilinear regression (MLR) analysis was utilised to build predictive models for the measured responses from input parameters. The modelling was performed with MODDE Pro-12 software (Umetrics Sartorius, Umeå, Sweden).

3. Results

A total of 27 MBSM experiments were performed at nine different settings according to the experimental design. The measured moisture content (% wet basis) of produced powders had ranges of high: 38–51, medium: 26–31 and low: 11–24 (Table S1).

3.1. Specific milling energy

The MSBM specific milling energy ranged from 99 to 232 kWh t^{-1} DM (Table S1) which is 1.2 to 2.7 times higher than that of the chipping and hammer-milling path (86 kWh t^{-1} DM). The MLR modelled effects and observed versus predicted plots are shown in Fig. 3a. The feeding speed (FS) and blade speed (BS) have significant ($p < 0.05$) negative and positive effects on milling energy, respectively. The moisture content (MC) has a significant ($p < 0.05$) negative effect on milling energy.

Within the range of the design, the specific milling energy was reduced by 62 kWh t^{-1} DM when the FS increased from its lowest to highest value, increased by 38 kWh t^{-1} DM when the BS was increased from its lowest to highest value, decreased by 25 kWh t^{-1} DM when the interaction term FS*BS increased from its lowest to highest value and decreased 18 kWh t^{-1} DM when MC increased from its lowest to highest value. The model has a R^2 value of 0.816 (Table 1), meaning that it can explain 81.6% of the variation in the experimental data. The Q^2 value of 0.733, which being above 0.5 indicates that the predictive ability of the model is good [33].

3.2. Particle size distribution

The cumulative PSDs of MBSM powders are shown in Fig. 4a along with the hammer mill PSD for comparison. The MBSM distributions are averages of the replicates at each experimental design point (Table S2 contains individual PSD data). The mass per cent of particles <0.5 mm in MBSM powders was much greater than in hammer-milled powders; ranging from 55 to 80% compared to 41%. The size specific differences are easily seen in the histogram (Fig. 4b) comparing the finest MBSM powder to that of the hammer mill.

All produced powders from the MBSM had a PSD within 80 to 95% particles <1.0 mm. The observed shape of MBSM powder particles, as seen in optical imaging (Fig. 5), was more spherical than in hammer mill powders. The highest mass per cent <1.0 mm was obtained with high BS and low FS using logs with high MC.

Regarding the model, which has a R^2 value of 0.707 and a Q^2 value of 0.526, the MC and BS factors have significant ($p < 0.05$) effect on the mass per cent of wood particle <1.0 mm (Fig. 3b). Square and interaction terms (MC*MC and FS*BS) also exist in the model. The share of particles <1.0 mm increased by approximately 7% and 6% when the BS and MC increased from their lowest to highest values, respectively.

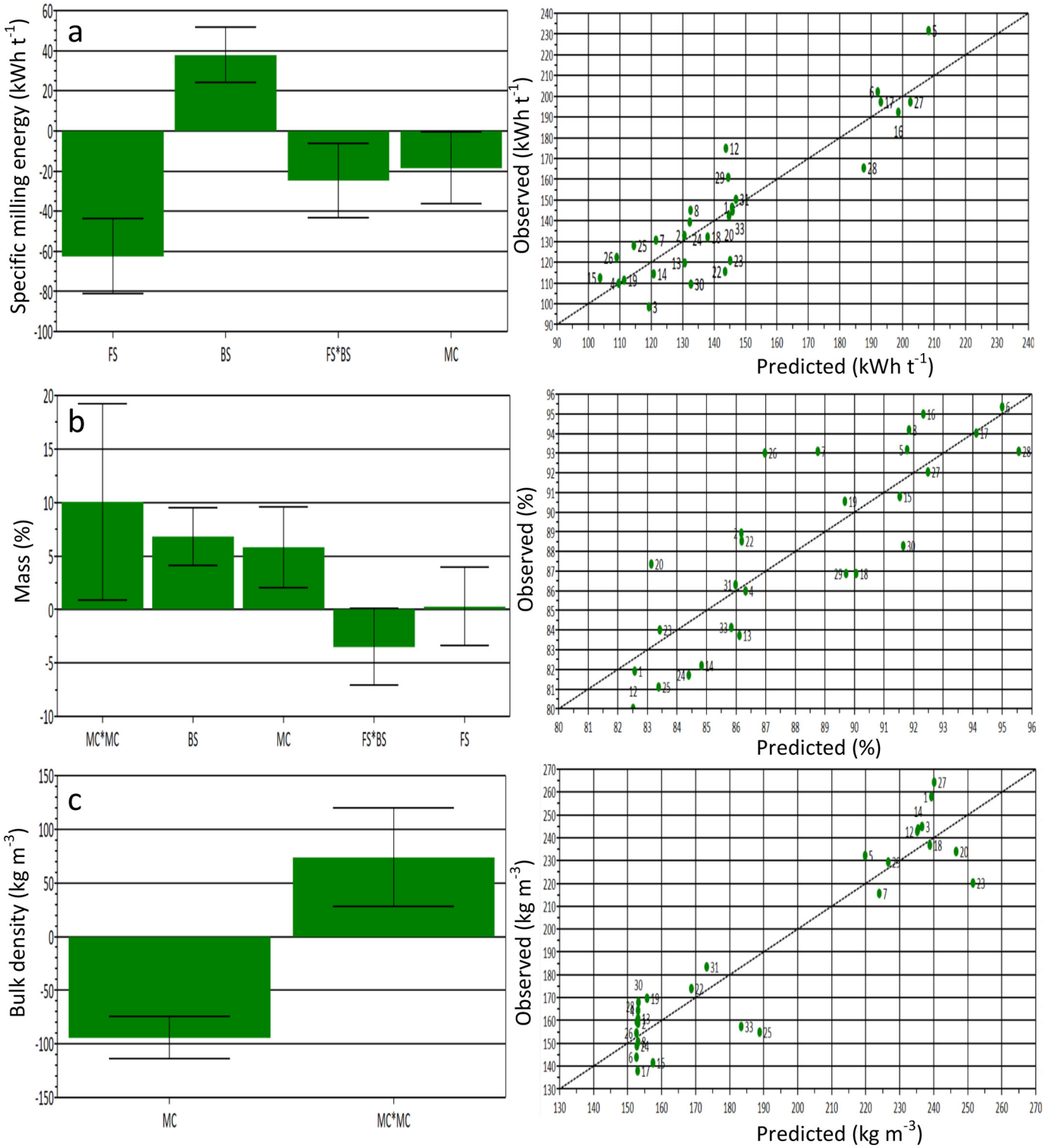

Fig. 3. Effects of scaled and centred factors in the response models for the (a) specific milling energy: Y_E (kWh t^{-1}) = −0.46 MC + 65.72 FS + 5.38 BS − 1.79 FS*BS − 92.16 (b) amount of wood particles <1 mm: Y_{PSD} (mass %) = −0.62 MC + 15.93 FS + 0.84 BS + 0.01 MC*MC − 0.25 FS*BS + 41.56 (c) powder bulk density: Y_{BD} (kg m^{-3}) = −7.98 MC + 0.09 MC*MC + 328.28 when each individual factor is varied from its lowest to its highest value, keeping all other factors at their average values in the design. The error bars indicate 95% level of confidence. Symbols refer to MC = moisture content, BS = blade speed and FS = feeding speed.

3.3. Powder bulk density

The bulk density of the MBSM powder varied from 138 to 264 kg m^{-3} DM (Table S1). According to the model, the MC of the milled log is the only significant ($p < 0.05$) factor affecting the bulk density of resulting dried powders. The bulk density decreases by 94 kg m^{-3} DM when MC increases from its lowest to highest value (Fig. 3c). The square effect of MC (i.e. the term MC*MC) has an opposite effect. The values of R^2 and Q^2 were 0.877 and 0.833 (Table 1), respectively.

Table 1
ANOVA of milling performance based on obtained responses.

Response	Model component					
	N	DF	R^2	Q^2	F	p
Specific milling energy (kWh t^{-1} DM)	28	23	0.816	0.733	25.50	0.00
Particle size distribution (mass %)	27	21	0.707	0.526	10.13	0.00
Bulk density (kg m^{-3})	27	24	0.877	0.833	85.44	0.00

Symbols are defined as: N = number of experiment, DF = degrees of freedom, R^2 = goodness of fit, Q^2 = goodness of prediction, F = ratio of explained to unexplained variance, p = probability of result.

4. Discussion

The influence of the three design factors on the responses (i.e. specific milling energy, wood particles <1.0 mm and bulk density) are shown as contour plots (Fig. 6).

4.1. Specific milling energy

The modelled specific milling energy increases with increasing BS and decreases with FS and the MC (Fig. 6a). The highest milling energy occurs for a BS of 72 m s^{-1} and a FS less than 1.5 m min^{-1}. Moisture content has a significant effect on the milling energy. A physical explanation is that water uptake up to the FSP (i.e. increasing amount of cell wall bound water) reduces hydrogen bonding between wood polymers [20,21] and weakens the strength properties of wood [24]. The result is that the breakage of wood to obtain wood powders is easier with higher MC up to the FSP. Above this level of moisture, the lower milling energy and greater amount of particles <1.0 mm may be due to a lubrication effect from surplus water during milling. The relatively large amount of extractives in pine (thinnings) have been reported to negatively affect the specific milling energy in attrition milling [34]. Without a comparative species in the present study, however, the influence of the extractive content on MBSM milling is not clear.

Based on this observation, the effect of MC in MBSM milling is similar to its influence in the sawing of wood. The lowest MBSM milling energy (99 kWh t^{-1} DM) was measured for powders having the largest PSD (63.5% <1.0 mm) and vice versa for highest milling energy (232 kWh t^{-1} DM) and smallest PSD (93.2% <1.0 mm). Comparison of the calculated geometric mean diameters reflects these differences in PSD (Table S2). While the specific milling energy was higher for the MBSM than for hammer-mill path, the powders produced were also substantially finer, which is what is expected from milling theory [27].

Considering previous studies with similar PSDs, the specific milling energy with the MBSM was comparable to ranges reported in literature. Esteban and Carrasco [9] produced powder 95% <1.0 mm from pine (*Pinus sylvestris L.*) chips using a two-stage hammer mill and a milling energy of 150 kWh t^{-1} DM. Phanphanich and Mani [35] used a knife mill to grind pine chips (21–71 × 15–40 × 1.9–4.9 mm) to geometric mean sized powder 0.71 mm with milling energy 238 kWh t^{-1}. Karinkanta et al. [36,37] milled spruce (*Picea abies*) sawdust with feed size 1–2 mm to obtain 0.02–0.10 mm median sized powder with a milling energy range of 100–380 kWh t^{-1} by oscillatory ball mill. Herein, the input material size (i.e. logs) was much higher than in previous

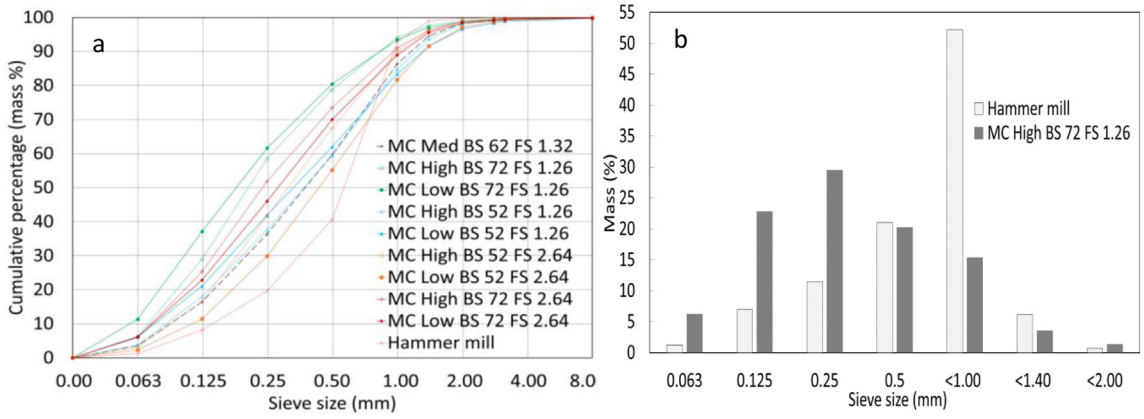

Fig. 4. (a) Cumulative particle size distribution of powders obtained from the multi-blade shaft mill (MBSM) and hammer mill. (b) Specific particle size differences between finest MBSM powder and hammer mill. Label symbols refer to MC = moisture content, Med = medium, BS = blade speed and FS = feeding speed.

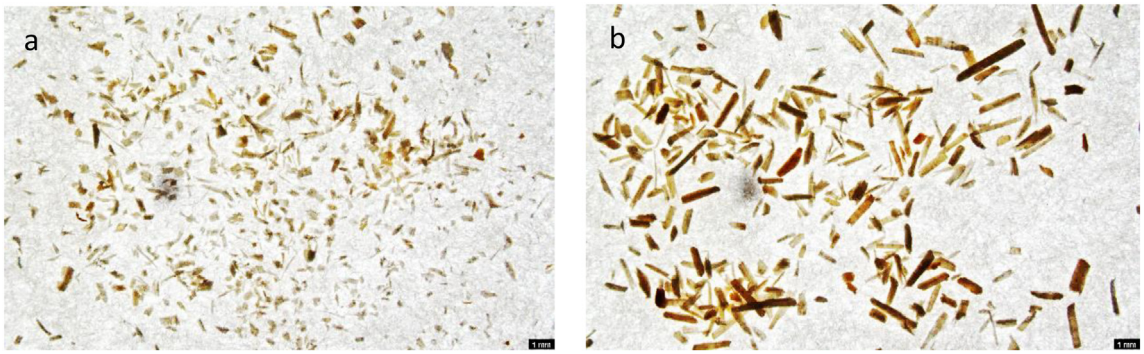

Fig. 5. Optical image of powders passing through 0.5 mm sieve from (a) multi-blade shaft mill and (b) hammer mill. The black line length is 1 mm.

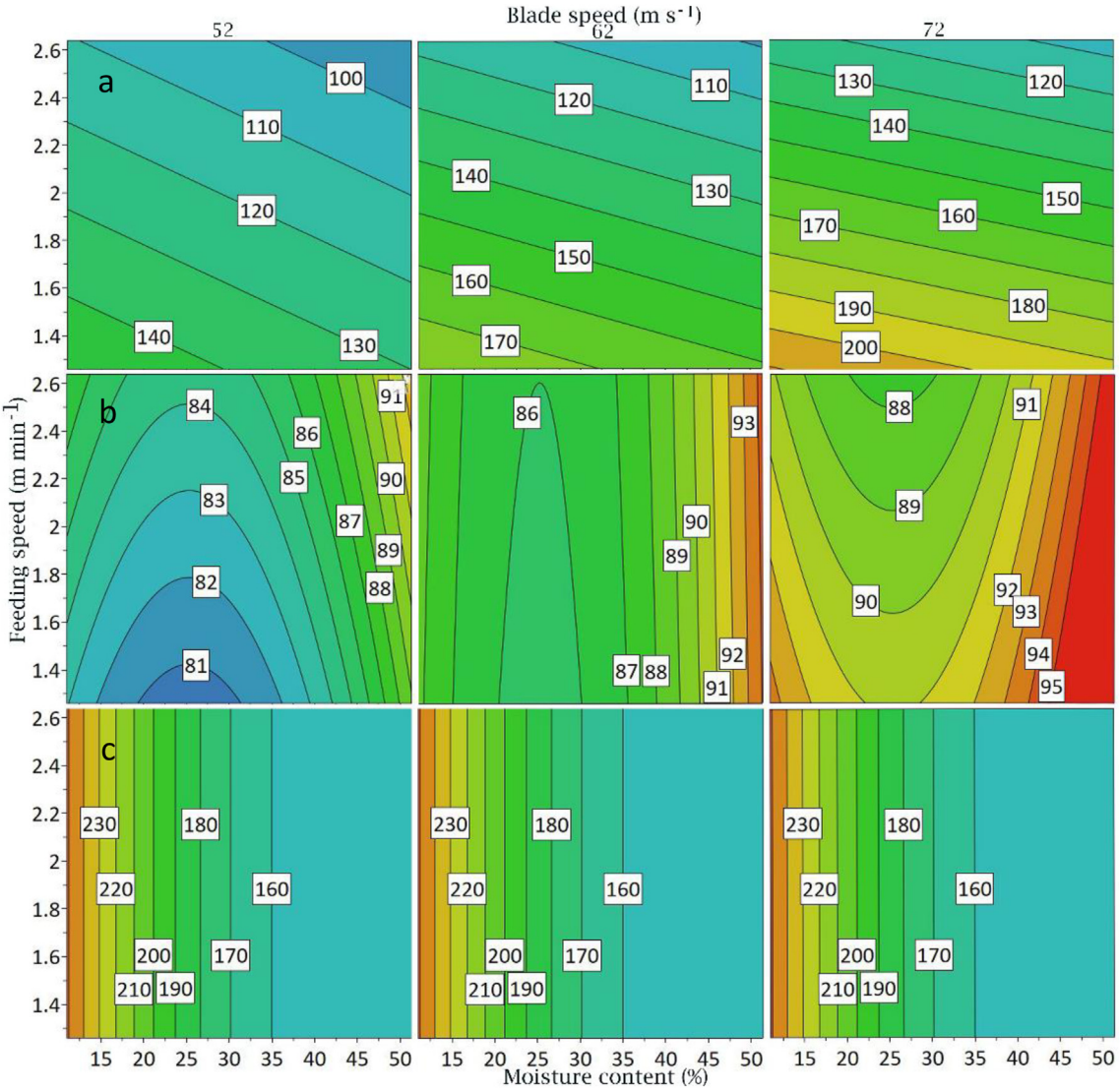

Fig. 6. Contour plots of experimental design space showing the influence of the three experimental design factors (moisture content (%), blade speed (m s^{-1}) and feeding speed (m min^{-1})) on the a) specific milling energy (kWh t^{-1} DM), b) particle size distribution (mass %) and c) bulk density (kg m^{-3} DM) of powders.

studies and the determined fine fraction of MBSM powders was also greater than in earlier work.

As the possibility to mill green wood is one of the key features of the MBSM, it is important to clarify the effect of MC on specific milling energy for other technologies. Attrition milling studies have found that MC dramatically affects milling energy; Liu et al. [38] and Gil et al. [18] have studied the effect using a hammer mill. They have shown that wetter wood required much greater (two to three times) the specific milling energy to produce comparable size wood powders. As indicated by the authors, hammer milling wetter materials makes the outlet screen more susceptible to blockages and this decreases the throughput of the mill (i.e. milling efficiency). Consequently, the mill must operate for longer duration with longer particle residence time and higher specific energy use.

One can conclude that comparing wet and dry materials in attrition mills is not a specific milling energy comparison but rather a comparison of how well the mill functions with moisture content variations. With size reduction using the MBSM, the length of time that the material is in the mill is known with precision and does not differ between wet and dry wood. In this regard, the action of milling with the MBSM seems analogous to sawing timber, only with multiple blades on the shaft working in parallel. This is supported by the influence of FS on milling energy. A higher FS reduces the milling energy of sawing wood because the duration of sawing is less (i.e. there is a higher throughput of material). This has been observed during band sawing of pine wood and it corresponded to a smaller sawdust particle size for lower FS [39]. Within the design space, decreasing FS with the MBSM shows the same result for high BS (Fig. 6a and 3a) but the opposite effect at low BS. Despite this observation, the significant effect of MC in the milling energy model indicates that the MBSM behaves more like sawing than like hammer milling.

4.2. Particle size distribution

Comparing the results, the hammer mill PSD was 92.9% <1.0 mm. With the MBSM, a high MC combined with higher BS increases the percentage of finer wood powders. The percentage of <1.0 mm particles increased with the increasing of MC and BS (Fig. 6b). The highest amount of <1.0 mm particles is achieved with a BS of 72 m s^{-1}, a feeding speed <1.8 m min^{-1} and a moisture content >48%. In general, these PSDs are a shift to finer wood powders compared to the studies in the literature cited above.

The model contains a MC quadratic term (i.e. MC*MC) which can indicate that the aforementioned role of MC in the milling energy is active

also indirectly here for the production finer powder (i.e. high MC lowers required milling energy, leading to more fine particles in the PSD and smaller geometric mean diameter) (Fig. 3b). Although FS is a non-significant term in the model, it has a significant interaction with BS (i.e. the term FS*BS).

It was observed that some powder material exits the improvised enclosure of the prototype mill during operation. PSD analysis of leaked powder showed that it had 2–10% higher fines content in the range of 0.25–0.50 mm. Therefore, it can be assumed that further development of the mill enclosure in future prototypes will assist in obtaining even finer PSDs.

4.3. Bulk density

The bulk density was in the range of 138 to 264 kg m^{-3} DM for 63.5 to 95.3% <1.00 mm MBSM pine wood powders while it was 219 kg m^{-3} for 92.9% <1.00 mm hammer-milled powders. BS and FS have no effect on bulk density (Fig. 6c). The highest bulk density occurs at low MC. The bulk density of MBSM and hammer-milled powders was in the range of previous studies (95–381 kg m^{-3} DM) from pine, Douglas fir and poplar wood produced using knife and hammer mills [9,18,32,35,40].

The factors that affect the bulk density of a powder are particle size distribution [28], particle length [28,41–43] and particle density [28]. Hook-shaped particles have an interlocking tendency [44] and larger biomass particles commonly have this shape [45]. Although bulk density is a function of particle size [40] and there is some evidence that finer particles result from the milling of high MC wood, less spherical shapes have more points of contact in the bulk and this worsens particle packing efficiency and decreases bulk density. Vice versa, smaller size particles have shapes that are more spherical and contribute to better packing by filling gaps, leading to higher bulk density [18].

Dimensional changes in wood (i.e. shrinkage and swelling) only occur when the moisture content falls below the FSP [46]. The extent of shrinkage and cracking in wood is a function of the drying temperature [47]. Shrinkage occurs in all three dimensions and can be significant. For example, in wood veneers shrinkage can be 7.6 and 9.9% tangentially and 5.4 and 5.7% radially when dried at 60 and 150 °C, respectively [48]. Drying of green wood to low moisture content then generates hydrostatic tension contributing to cellular collapse, internal checking and washboard depression in wood [49].

The experimental design used logs of low and high moisture content. An important difference in the experimental procedure (Fig. 2) was that low MC logs had their MC level adjusted by partial drying at 25 °C before milling but high MC logs were milled above their FSP so that their powders required more drying than powders from the low MC logs. Powders from the green logs had a higher vapour pressure within the wood matrix during drying at 105 °C [50]. Their powders experienced greater dimensional and chemical compositional changes because they had more water (high vapour pressure) within their cells. Due to this and the fact that drying temperature is also known to alter wood's chemical composition and cellulose crystallinity [48], it is plausible that the different conditions affected the particle shape and density in produced powders (i.e. that particles from high MC logs had shape or density that decreased their packing efficiency). These differences could explain why powders milled from high MC logs had a lower bulk density and why MC is the only significant factor in the model (Fig. 3c).

Referring to the model of bulk density, there is a squared effect of MC (i.e. MC*MC). The screening design in MODDE software does not justify the use of quadratic terms but it can be seen that it fits a physical explanation of fibre saturation in the wood (Fig. 6c). Above the FSP, there is a saturation behaviour of the model, which can be seen as the saturation of the wood itself. Since the extent of shrinkage above FSP does not depend on MC [46] there is no dimensional change at MC above this point.

Further study using imaging techniques will allow more accurate characterisation of particle size, morphology and topochemistry and illuminate how these factors affect the bulk density of MBSM powders. In addition, the relationship between milling factors, milling energy and effective surface area of powders needs further investigation.

Current practice in industry in size reduction technology is reliant on the use of wood chips rather than whole tree stems. Hammer mills have inherent technical limitations for producing wood powders, as they can accept neither all sizes nor all moisture content ranges of chips. Chips storage brings risks of biological degradation, dry-matter losses and undesirable emissions that presenting health risks. Milling with the MBSM prototype bypasses these limitations while at the same time produces powders with much finer particles. The MBSM can mill a wide range of diameters and moisture content logs meaning it can mill green wood directly after felling the tree. It also provides more possibilities to tailor the particle size distribution to the powder application of interest. Smaller particle sizes enhance available surface area, leading to better penetration of chemicals and enzymes in pre-processing for biofuel production. The technology enables wood storage in its preferred green form, thereby better preserving its chemical composition, up until the log is utilised. Moreover, MBSM technology may provide benefits from a supply chain perspective by shortening the tree-to-powder pathway in turnaround time and resource use. Further study is needed to characterise powders (chemical analysis and microstructure) from the MBSM and investigate the milling of other wood species.

5. Conclusions

In this study, wood powders were produced successfully from whole pine logs in a single step using a novel multi-blade shaft mill (MBSM). The specific milling energy of the MBSM was higher than conventional hammer milling but the MBSM produced significantly higher fractions of finer particles. According to the MLR model, the milling energy was inversely proportional to moisture content of wood both above and below the fibre saturation point. This indicates that moisture influences MBSM milling in a similar way as in the sawing of wood and opposite to impact-based milling.

Supplementary data to this article can be found online at https://doi.org/10.1016/j.powtec.2020.10.026.

Funding

This study was funded in part by the Swedish Energy Agency (Project number- 46904-1) and Swedish Bio4Energy Strategic Research Environment.

Declaration of Competing Interest

The authors declare that they have no known competing financial interests or personal relationships that could have appeared to influence the work reported in this paper.

Acknowledgements

The authors would like to thank Gunnar Kalén, for assistance and suggestions during milling and wood powder analysis, and Markus Segerström for his help in tree collection and milling assistance. Borislav Vujadinovic and KlingMill AB are also acknowledged for technical support and assistance. The authors also thank Marta Derba-Maceluch at the Department of Forest Genetics and Plant Physiology for support with optical imaging.

References

[1] United Nations, Transforming our world: the 2030 Agenda for Sustainable Development, sustainabledevelopment.un.org 2015 (pp. 41).

[2] R. Fernandez-Lacruz, F. Di Fulvio, D. Athanassiadis, D. Bergstrom, T. Nordfjell, Distribution, Characteristics and Potential of Biomass-Dense Thinning Forests in Sweden, Silva Fennica, 49, 2015.

[3] S. van Loo, J. Koppejan, The Handbook of Biomass Combustion and Co-Firing, Taylor & Francis Group, London, Routledge, 2012.
[4] J.D. Fougere, M. Lynch, J. Zhao, Y. Zheng, K.C. Li, Impact of mechanical downsizing on the physical structure and enzymatic digestibility of pretreated hardwood, Energy Fuel 28 (2014) 2645–2653.
[5] T.J. McDonough, Wood chemistry - fundamentals and applications – Sjostrom, E, J. Am. Chem. Soc. 105 (1983) 4503.
[6] P. Karinkanta, A. Ammala, M. Illikainen, J. Niinimaki, Fine grinding of wood - overview from wood breakage to applications, Biomass Bioenergy 113 (2018) 31–44.
[7] N. Kobayashi, P. Guilin, J. Kobayashi, S. Hatano, Y. Itaya, S. Mori, A new pulverized biomass utilization technology, Powder Technol. 180 (2008) 272–283.
[8] L.I. Salminen, S. Liukkonen, M.J. Alava, Ground wood Fiber length distributions, Bioresources 9 (2014) 1168–1178.
[9] L.S. Esteban, J.E. Carrasco, Evaluation of different strategies for pulverization of forest biomasses, Powder Technol. 166 (2006) 139–151.
[10] M. Gil, I. Arauzo, Hammer mill operating and biomass physical conditions effects on particle size distribution of solid pulverized biofuels, Fuel Process. Technol. 127 (2014) 80–87.
[11] L. Kratky, T. Jirout, Biomass size reduction Machines for Enhancing Biogas Production, Chem. Eng. Technol. 34 (2011) 391–399.
[12] E. Alakoski, M. Jamsen, D. Agar, E. Tampio, M. Wihersaari, From wood pellets to wood chips, risks of degradation and emissions from the storage of woody biomass - a short review, Renew. Sust. Energ. Rev. 54 (2016) 376–383.
[13] M. Wihersaari, Energy consumption and greenhouse gas emissions from biomass production chains, Energy Convers. Manag. 37 (1996) 1217–1221.
[14] S. Stenstrom, Drying of biofuels from the forest-a review, Dry. Technol. 35 (2017) 1167–1181.
[15] J.X. Jiang, J.W. Wang, X. Zhang, M. Wolcott, Microstructure change in wood cell wall fracture from mechanical pretreatment and its influence on enzymatic hydrolysis, Ind. Crop. Prod. 97 (2017) 498–508.
[16] S. Paulrud, C. Nilsson, The effects of particle characteristics on emissions from burning wood fuel powder, Fuel 83 (2004) 813–821.
[17] S. Paulrud, J.E. Mattsson, C. Nilsson, Particle and handling characteristics of wood fuel powder: effects of different mills, Fuel Process. Technol. 76 (2002) 23–39.
[18] M. Gil, I. Arauzo, E. Teruel, Influence of input biomass conditions and operational parameters on comminution of short-rotation forestry poplar and corn Stover using neural networks, Energy Fuel 27 (2013) 2649–2659.
[19] J. Falk, R.J. Berry, M. Brostrom, S.H. Larsson, Mass flow and variability in screw feeding of biomass powders - relations to particle and bulk properties, Powder Technol. 276 (2015) 80–88.
[20] D.W. Green, J.E. Winandy, D.E. Kretschmann, Mechanical Properties of Wood, Wood Handbook Chapter 4, Forest Products Laboratory, USDA Forest Service, USA, 1999.
[21] R.M. Rowell, How the environment affects lumbar design, in: D.E.A.G. Lyon (Ed.), Forest Products Laboratory ReportUSDA, Forest Service, 1980.
[22] W.W. Barkas, Fibre saturation point of wood [9], Nature 135 (1935) 545.
[23] S. Glass, S.L. Zelinka, Moisture relations and physical properties of wood, Wood Handbook—Wood as an Engineering Material, US Department of Agriculture, Forest Service, Forest Products Laboratory, Madison, WI, USA, 2010.
[24] J.E. Winandy, R.M. Rowell, Chemistry of wood strength, Handbook of Wood Chemistry and Wood Composites Chapter 11, CRC Press, N.W. Corporate Blvd., Boca Raton, Florida 334312005, 2000.
[25] T. Morita, K. Banshoya, T. Tsutsumoto, Y. Murase, Corrosive-wear characteristics of diamond-coated cemented carbide tools, J. Wood Sci. 45 (1999) 463–469.
[26] L. Cristovao, M. Ekevad, A. Gronlund, Industrial sawing of Pinus sylvestris L.: power consumption, Bioresources 8 (2013) 6044–6053.
[27] V.R. Voller, A note on energy-size reduction relationships in comminution, Powder Technol. 36 (1983) 281–286.
[28] H. Rezaei, C.J. Lim, A. Lau, S. Sokhansanj, Size, shape and flow characterization of ground wood chip and ground wood pellet particles, Powder Technol. 301 (2016) 737–746.
[29] V. Repellin, A. Govin, M. Rolland, R. Guyonnet, Energy requirement for fine grinding of torrefied wood, Biomass Bioenergy 34 (2010) 923–930.
[30] V. Nasir, J. Cool, A review on wood machining: characterization, optimization, and monitoring of the sawing process, Wood Mater. Sci. Eng. 15 (2020) 1–16.
[31] J. Nordstrom, J. Bergstrom, Wear testing of saw teeth in timber cutting, Wear 250 (2001) 19–27.
[32] K. Tannous, P.S. Lam, S. Sokhansanj, J.R. Grace, Physical properties for flow characterization of ground biomass from Douglas fir wood, Part. Sci. Technol. 31 (2013) 291–300.
[33] L. Eriksson, E. Johansson, N. Kettaneh-Wold, C. Wikström, S. Wold, Design of Experiments: Principles and Applications, Umeå Learnways AB, Stockholm, 2008.
[34] D. Fernando, J. Hafren, J. Gustafsson, G. Daniel, Micromorphology and topochemistry of extractives in scots pine and Norway spruce thermomechanical pulps: a cytochemical approach, J. Wood Sci. 54 (2008) 134–142.
[35] M. Phanphanich, S. Mani, Impact of torrefaction on the grindability and fuel characteristics of forest biomass, Bioresour. Technol. 102 (2011) 1246–1253.
[36] P. Karinkanta, M. Illikainen, J. Niinimaki, Impact-based pulverisation of dried and screened Norway spruce (*Picea abies*) sawdust in an oscillatory ball mill, Powder Technol. 233 (2013) 286–294.
[37] P. Karinkanta, M. Illikainen, J. Niinimaki, Pulverisation of dried and screened Norway spruce (*Picea abies*) sawdust in an air classifier mill, Biomass Bioenergy 44 (2012) 96–106.
[38] Y. Liu, J. Wang, J.C. Barth, K.R. Welsch, V. McIntyre, M.P. Wolcott, Effects of multistage milling method on the energy consumption of comminuting forest residuals, Ind. Crop. Prod. 145 (2020) 111955.
[39] M. Bariska, Z. Pasztory, The optimum log feed speed with bandsaw, Eur. J. Wood Wood Prod. 73 (2015) 245–250.
[40] Z. Miao, T.E. Grift, A.C. Hansen, K.C. Ting, Energy requirement for comminution of biomass in relation to particle physical properties, Ind. Crop. Prod. 33 (2011) 504–513.
[41] N. Chevanan, A.R. Womac, V.S. Bitra, S. Sokhansanj, Effect of particle size distribution on loose-filled and tapped densities of selected biomass after knife mill size reduction, Appl. Eng. Agric. 27 (2011) 631–644.
[42] P.S. Lam, S. Sokhansanj, X. Bi, C.J. Lim, L.J. Naimi, M. Hoque, S. Mani, A.R. Womac, X.P. Ye, S. Narayan, Bulk density of wet and dry wheat straw and switchgrass particles, Appl. Eng. Agric. 24 (2008) 351–358.
[43] R.P. Zou, X.Y. Lin, A.B. Yu, P. Wong, Packing of cylindrical particles with a length distribution, J. Am. Ceram. Soc. 80 (1997) 646–652.
[44] J.E. Mattsson, P.D. Kofman, Method and apparatus for measuring the tendency of solid biofuels to bridge over openings, Biomass Bioenergy 22 (2002) 179–185.
[45] M. Gil, D. Schott, I. Arauzo, E. Teruel, Handling behavior of two milled biomass: SRF poplar and corn Stover, Fuel Process. Technol. 112 (2013) 76–85.
[46] P. Bajpai, Wood and Fiber fundamentals, Biermann's handbook of pulp and paper, 3rd edition, volume 1: raw material and pulp making, chapter 2, Amsterdam, Netherlands, Elsevier (2018) 19–74.
[47] H.J. Chai, C. Xu, J. Li, F.X. Kong, Y.C. Cai, Effects of pretreatment with saturated wet air and steaming on the high-frequency vacuum drying characteristics of wood, Bioresources 14 (2019) 9601–9610.
[48] Y.H. Shen, Z.Z. Gao, X.F. Hou, Z.Y. Chen, J.Y. Jiang, J. Sun, Spectral and thermal analysis of Eucalyptus wood drying at different temperature and methods, Dry. Technol. 38 (2020) 313–320.
[49] B.S.W. Dawson, H. Pearson, M.O. Kimberley, B. Davy, A.R. Dickson, Effect of supercritical CO_2 treatment and kiln drying on collapse in Eucalyptus nitens wood, Eur. J. Wood Wood Prod. 78 (2020) 209–217.
[50] M. Hadjiski, N. Deliiski, N. Tumbarkova, Mathematical description of the latent heat of water vaporization in capillary porous materials, Informa. Technol. Control 1 (2019) 2–8.

II

Available online at www.sciencedirect.com

ScienceDirect

journal homepage: www.elsevier.com/locate/issn/15375110

Research Note

Investigating the influence of work piece geometry on the specific energy use in size reduction with a multi-blade shaft mill

Atanu Kumar Das[*], *David A. Agar*, *Sylvia H. Larsson*, *Magnus Rudolfsson*

Swedish University of Agricultural Sciences, Department of Forest Biomaterials and Technology, SE-901 83 Umeå, Sweden

ARTICLE INFO

Article history:
Received 21 December 2020
Received in revised form
22 June 2021
Accepted 4 July 2021
Published online 22 July 2021

Keywords:
Comminution
Wood powder technology
MBSM
Fine grinding
Experimental design
Milling

This study investigated the specific milling energy of rectangular pine (*Pinus sylvestris* L.) boards using a new size reduction technology, which can produce fine wood powders in a single-step operation. Multilinear regression (MLR) analysis was used to model the milling energy of a multi-blade shaft mill through a designed series of experiments having three input parameters: the moisture content of the board, milling blade speed and board feeding speed. The observed specific milling energy ranged from 60 to 172 kWh t^{-1} [DM] and the MLR model showed it was proportional to the blade speed and the moisture content. The results suggest that multi-blade shaft milling is a two-dimension extension of singular circular blade milling with regard to work piece shape and sawblade teeth engagement effects. The findings were compared with the specific milling energy of pine logs obtained in a previous study.

1. Introduction

With the resurgence of various wood-based applications in society and wood powder feedstock for bio-based industries, new size reduction technologies have the potential to improve utilisation by supplying better-suited wood powders for refining processes and products (Karinkanta et al., 2018). Eliminating multistep pre-processing and thermal treatments saves time and unlocks more benefits from the green chemical profile of wood.

A new size reduction technology, known as the multi-blade shaft mill (MBSM), has recently been assessed for the production of wood powders in a single-step milling operation from whole tree stems (Das et al., 2021). As the MBSM uses a packed shaft of circular cutting blades, which can be viewed as a parallel combination of rotary-blade sawing processes, the observation that moisture content is negatively correlated to milling energy appeared reasonable in an earlier study. Models showed that milling energy was inversely proportional to the moisture content of the wood and the log feeding speed, whilst being directly proportional to the blade speed.

* *Corresponding author.*
E-mail address: atanu.kumar.das@slu.se (A.K. Das).
https://doi.org/10.1016/j.biosystemseng.2021.07.002

Nomenclature

MBSM	Multi-blade shaft mill
BS	Blade speed
DM	Dry mass
FS	Feeding speed
MC	Moisture content
w.b.	Wet basis
e_M	Specific milling energy (kW h t^{-1})
m_M	Mass of milled board (kg)
P_f	Board feeding power (kW)
P_m	Board milling power (kW)
Q^2	Goodness of prediction
R^2	Goodness of fit
t_M	Board milling time (s)
Y_E	Modelled specific milling energy (kW h t^{-1})

High moisture content in wood generally lowers the energy required for sawing (Moradpour et al., 2013; Morita et al., 1999) since every increment of moisture content up to fibre saturation point decreases the modulus of elasticity, fracture toughness and hardness of wood (Nordstrom & Bergstrom, 2001). Power consumption in single-blade circular sawing is analysed using two contributions; the applied power needing to generate the cutting force and the power used in chip formation (i.e. sawdust) and removal from the work piece (Cristovao et al., 2013). Both these contributions are functions of MC and a number of other factors (Orlowski et al., 2013) whose influence can be difficult to evaluate because the experimenter only observes the total power of the sawing process. Moisture content plays a dual role in power consumption as water in wood can lower the cutting force (Axelsson et al., 1993) while simultaneously increasing work piece density (mass) and the power needed for chip formation. Due to the complexity of modelling the sawing process and the anisotropic effects of wood (Sjöström, 1993), power consumption is best determined through direct experiment.

Power consumption with circular sawblades depends on the position angle between the sawblade teeth and the work piece (Cristovao et al., 2013) as well as the number of teeth engaged, i.e., in contact with the kerf (Orlowski et al., 2013). The question arises, is power consumption in MBSM milling analogous to sawing wood with a singular circular saw blade? The answer has practical implications for improving mill design and the potential benefits of the technology.

This study aimed to deepen the understanding of multi-blade shaft milling technology from earlier work (with cylindrical logs) by applying it to rectangular shaped boards. The main objective was to see how work piece shape affects the energy requirements of size reduction.

2. Materials and methods

Experimental work was performed at the Biomass Technology Centre at the Swedish University of Agricultural Sciences in Umeå, Sweden.

2.1. Multi-blade shaft mill

A multi-blade shaft mill (Klingmill AB, Torshälla, Sweden) that has been described in an earlier study (Das et al., 2021) was used here. The machinery mills the work piece using two shafts of packed circular sawblades driven by two separate electric motors (55 kW, 1480 rpm) (Fig. 1). The first shaft is the primary milling shaft and consists of 110 parallel-mounted 352 mm diameter and 3 mm thickness blades having eight teeth per blade. The clearance angle, rake angle and kerf of the blade teeth are 18°, 5° and 4.2 mm, respectively. Every second blade on the shaft is rotated by 360/16° so that around the circumference of the packed blades there are 16 rows of teeth. The second shaft has 137 parallel-mounted blades having 24 teeth per blade and rake angle and kerf of each tooth are 15° and 3 mm, respectively. The feeding level was tangent to the lower side of the blades. Wood powder was collected in a plastic bag through a filtered vacuum system. The mill can accept log diameters and board widths up to approximately 280 and 300 mm, respectively.

2.2. Experimental design

MSBM milling was performed according to a full factorial (two-level) experimental screening design with one centre point varying three factors in their corresponding ranges: board moisture content (13–33%, wet basis), board feeding speed (1.3–2.3 m min^{-1}) and blade speed (52–72 m s^{-1}). The analysed response was the specific milling energy (kW h t^{-1} [DM]). Experiments from each of the experimental design points were replicated three times, bring the total number of MBSM experiments for the response to 27. The experimental range of the feeding speed and blade speed was defined previously (Das et al., 2021).

2.3. Material preparation

Ten boards were collected from a saw mill (Sävar såg, Norra Timber, Umeå, Sweden) and cut to obtain 27 boards having equal length. Board samples had dimensions of approximately 1100 × 150 × 50 mm. The boards came from trees having a minimum average age of 60 (SD = 18) years, as determined by counting growth rings. Three moisture content ranges, approximately at and below the fibre saturation point, were used: 13 to 16, 20 to 24 and 21–33% wet basis (w.b.). To achieve the three ranges, the boards were dried at 25 °C in a drying cabinet (Elvärmedetaljer, Skurup, Sweden) to minimise wood properties changes. The boards were kept separate from each other and wrapped in plastic to prevent changes in moisture content prior to experiments. An overview of the experimental procedure is presented in Fig. 2.

2.4. Milling procedure

All boards were weighed, and within each moisture content range, ordered randomly with relation to the experimental design. During milling, the electric power (kW) was monitored and data gathered (1 Hz) with an acquisition system (INTAB PC-logger 3100). The MBSM was cleaned thoroughly between each experiment.

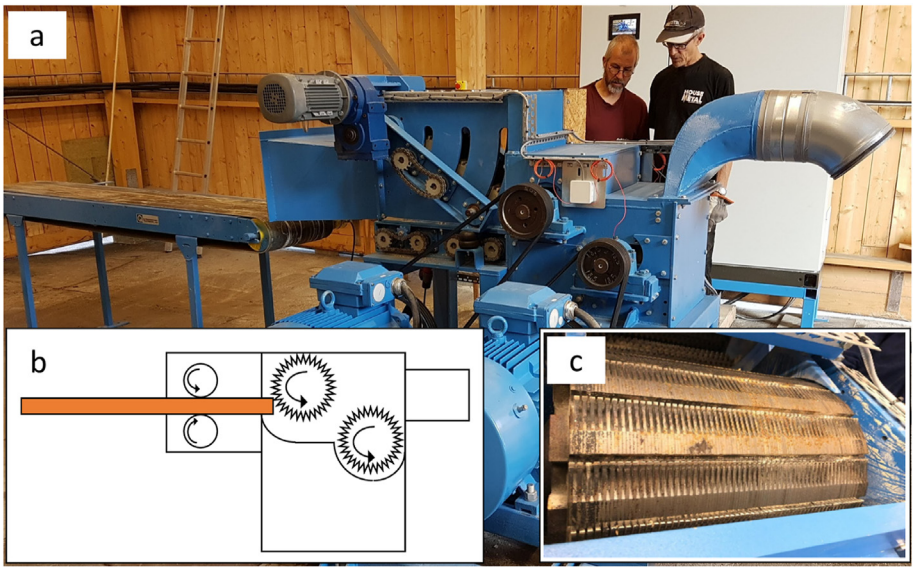

Fig. 1 – (a) The prototype multi-blade shaft mill (MBSM) without its housing enclosure. The roller table, feeder and the two shafts connected to the motors are visible. The sample collector is not fitted to the outlet in the photograph. (b) The principle of operation of the MBSM and (c) the multi-blade shaft (Das et al., 2021).

2.5. *Milling energy analysis*

The specific milling energy e_M (kWh t^{-1} [DM]) of MBSM milling was calculated using the following equation:

$$e_M = m_M^{-1} \sum_{t_M} (P_f + P_m)\, t_M$$

in which m_M (kg [DM]) is the dry mass of the milled board, t_M (s) = board milling time, P_f (kW) = board feeding power and P_m (kW) = board milling power.

Multilinear regression (MLR) analysis was utilised to build predictive models for the measured responses from input parameters. The modelling was performed with MODDE Pro-12 software (Umetrics Sartorius, Umeå, Sweden).

3. Results and discussion

The MLR modelled effects and observed versus predicted plots are shown in Fig. 3. The feeding speed (FS) has significant ($p < 0.05$) negative effects on milling energy, whereas, the board moisture content (MC) and blade speed (BS) have significant positive effects. Specific milling energy decreased by 48 kWh t^{-1} [DM] over the full range of FS variation. Full range increases of MC and BS produced higher specific energy by 48 and 18 kWh t^{-1} [DM], respectively. No significant interaction terms were observed between effects. The model's R^2 and Q^2 values are 0.79 and 0.72 which represent good model validity and predictability (Eriksson et al., 2008).

The influence of the three design factors on the milling energy response is presented as contour plots (Fig. 4), a representation of the obtained specific milling energy equation: Y_E (kWh t^{-1} [DM]) = − 48.13FS + 2.38MC + 0.91BS + 93.58 in which FS, MC and BS have units of m min^{-1}, % and m s^{-1}, respectively. Y_E decreases with increasing FS and increases with MC and BS. The lowest specific milling energy (60 kW h t^{-1} [DM]) occurs for a FS of 2.3 m min^{-1}, a MC less than 17% and a BS less than 64 m s^{-1}.

Rectangular pine board milling had an observed specific milling energy range of 60–172 kWh t^{-1} [DM] (Table 1), almost half of that observed using cylindrical pine logs (99–232 kWh t^{-1} [DM]) (Das et al., 2021). The only significant differences between the boards and logs were the shape, average age of wood (60 versus 29 years) and range of moisture content (13–33% versus 11–51%).

The rectangular (cross-sectional) shape of the boards (50 × 150 mm) differed from that of the cylindrical logs (100–140 mm diameter). With singular circular saw blades, the thickness of the work piece, determines the angle of teeth engagement and consequently the path length travelled by the teeth through the kerf (Orlowski et al., 2013). As power consumption depends on the path length, because greater frictional forces act over a longer path (Chuchala et al., 2014), the involvement of more teeth for a thicker work piece (Fig. 5)

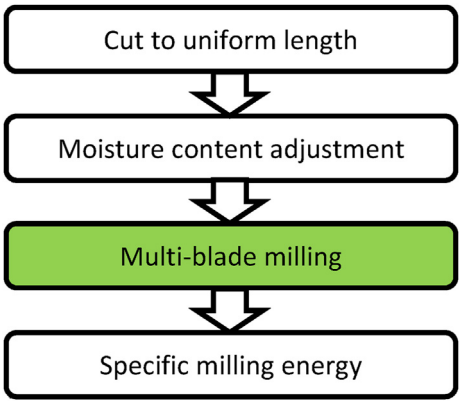

Fig. 2 – An overview of the experimental procedure used in the study.

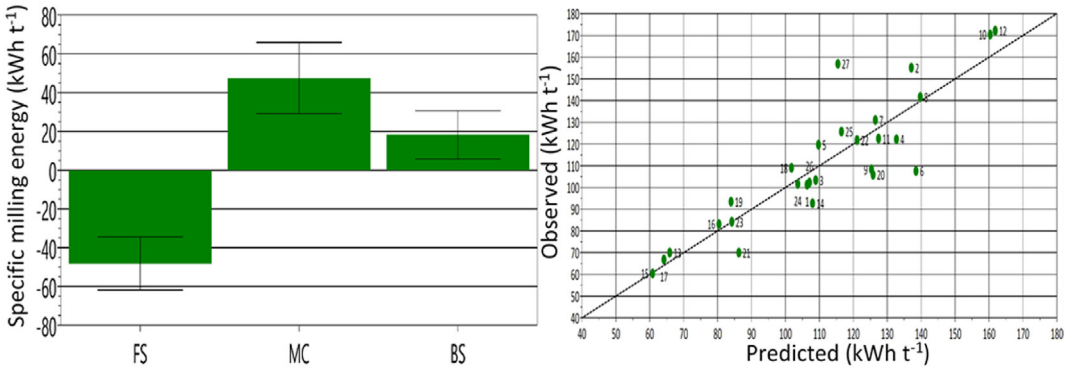

Fig. 3 – Effects of scaled and centred factors in the response models for the specific milling energy, when each individual factor is varied from its lowest to its highest value, keeping all other factors at their average values in the design. The error bars indicate 95% level of confidence. Symbols refer to FS = feeding speed, MC = moisture content and BS = blade speed.

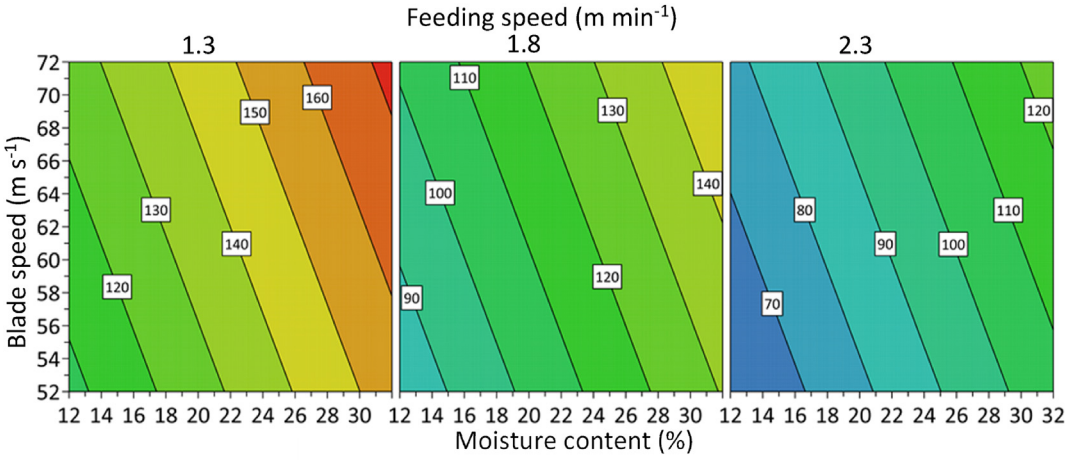

Fig. 4 – Contour plots showing the influence of the three experimental design factors (feeding speed, moisture content and blade speed) on the specific milling energy.

increases the specific milling energy. These relationships have been confirmed during sawing of *Pinus sylvestris* L. by a singular working blade (Cristovao et al., 2013). In board milling, there were comparatively fewer teeth engaged in the vertical plane and a shorter path length due to the thinner work piece.

Because the MBSM has parallel blades along the shaft, there is also teeth engagement in the horizontal plane, which depends on the work piece width (Fig. 5). The boards, which were wider than the logs, engaged more teeth from parallel blades in the horizontal plane. The number of teeth and engaged angle of teeth have influence on the specific milling energy during size reduction of wood (Orlowski et al., 2013). The cutting time also influences the energy consumption; the longer the cutting time the higher the energy consumption (Morita et al., 1999). Thus, more teeth involvement along the shorter path may reduce the specific milling energy. In this case, the wider and thinner work piece may be easier to mill compared to the thicker work piece.

Therefore, the combination of thickness and width differences of the boards is suggested to be responsible factor for the differences in observed milling energy with the MBSM. This suggests that the MBSM milling action is a two-dimension extension of singular circular blade milling.

However, the modelled effect of MC on milling energy was opposite to log milling (+48 versus −18 kWh t^{-1}[DM]) (Das et al., 2021). Why does moisture play an opposite role in the models? The work piece shape appears to affect the influence of MC on the observed and modelled energy use but the precise reason is unclear. The presence of heartwood in the material may have contributed to the observed differences in the specific milling energy as the proportion of heartwood (where extractive content is high) increases with tree age. In order to optimise the configuration of the mill, it is important to clarify the effect of work piece shape and MC on the specific milling energy. Future work will investigate the influence of extractive content and tree species on specific milling energy

Table 1 – Full factorial design (2 Levels) for MBSM board experiments and specific milling energy.

Experiment name	Run order	Feeding speed (m min^{-1})	Moisture content (%)	Blade speed (m s^{-1})	Specific milling energy (kW h t^{-1} [DM])
N1	18	1.4	13.7	52	101.2
N2	9	1.4	26.6	52	155.3
N3	8	1.4	14.8	52	103.4
N4	1	1.4	24.8	52	122.2
N5	20	1.4	15.1	52	119.6
N6	6	1.3	25.2	52	107.7
N7	22	1.4	14.5	72	130.9
N8	23	1.5	22.1	72	141.6
N9	4	1.4	14.0	72	108.2
N10	2	1.4	28.7	72	170.5
N11	17	1.4	14.9	72	122.6
N12	27	1.3	27.3	72	172.2
N13	11	2.3	14.9	52	69.90
N14	16	2.3	32.6	52	92.80
N15	7	2.3	12.8	52	60.40
N16	15	2.3	21.0	52	83.10
N17	21	2.3	14.2	52	66.80
N18	10	2.3	30.0	52	109.0
N19	25	2.3	14.8	72	93.30
N20	5	2.3	32.4	72	106.0
N21	24	2.3	15.8	72	69.90
N22	14	2.3	30.4	72	122.0
N23	19	2.3	14.9	72	84.10
N24	26	2.3	23.1	72	101.7
N25	3	1.8	22.2	62	125.8
N26	13	1.9	20.3	62	102.2
N27	12	1.9	23.8	62	157.1

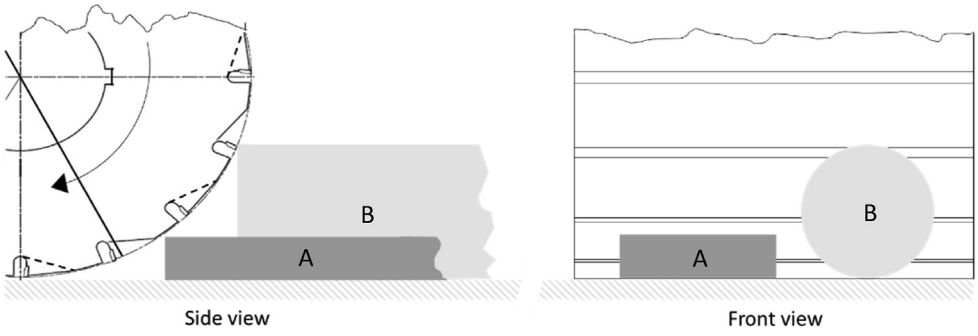

Fig. 5 – Side and front views of the main shaft of the multi-blade shaft mill. The thickness and width of the boards (A) and logs (B) influence the engagement angle and the number of teeth engaged, both in the vertical (left) and horizontal (right) planes.

and particle size distribution so that MBSM technology can be fully characterised.

4. Conclusions

Pine boards at moisture contents up to the fibre saturation point, were milled using a novel multi-blade shaft mill (MBSM). According to the generated MLR model, the milling energy was proportional to the moisture content of the wood. The effects of blade speed (BS), feeding speed (FS), engagement of number of teeth and shape of the work piece indicate that MBSM milling energy is analogous to the sawing of wood and opposite to impact-based milling. The effect of work piece geometry may explain the observed differences in specific milling energy from previous work in two ways: 1) differences in height and width determine the number of blade teeth engaged in milling and 2) height differences alter the angle of engagement with blade teeth.

Declaration of competing interest

The authors declare that they have no known competing financial interests or personal relationships that could have appeared to influence the work reported in this paper.

Acknowledgements

Funding from the Swedish Energy Agency, Sweden, Swedish Bio4Energy Strategic Research Environment, Sweden, and the Department of Forest Biomaterials and Technology, Swedish University of Agricultural Sciences, Sweden is acknowledged. The authors thank Gunnar Kalén, Markus Segerström, Borislav Vujadinovic and KlingMill AB for their assistance and technical support.

REFERENCES

Axelsson, B. O. M., Lundberg, Å. S., & Grönlund, J. A. (1993). Studies of the main cutting force at and near a cutting edge. *Holz als Roh- und Werkstoff: European Journal of Wood and Wood Industries, 51*(1), 43–48. https://doi.org/10.1007/BF02615376

Chuchala, D., Orlowski, K. A., Sandak, A., Sandak, J., Pauliny, D., & Baranski, J. (2014). The effect of wood provenance and density on cutting forces while sawing Scots pine (*Pinus sylvestris* L.). *Bioresources, 9*(3), 5349–5361.

Cristovao, L., Ekevad, M., & Gronlund, A. (2013). Industrial sawing of Pinus sylvestris L.: Power consumption. *Bioresources, 8*(4), 6044–6053.

Das, A. K., Agar, D. A., Larsson, S. H., Holdo, T., Fernando, D., & Rudolfsson, M. (2021). Multi-blade milling from log to powder in one step – experimental design and results. *Powder Technology, 378*, 593–601.

Eriksson, L., Johansson, E., Kettaneh-Wold, N., Wikström, C., & Wold, S. (2008). *Design of experiments: Principles and applications*. Stockholm: Umeå Learnways AB.

Karinkanta, P., Ammala, A., Illikainen, M., & Niinimaki, J. (2018). Fine grinding of wood - overview from wood breakage to applications. *Biomass and Bioenergy, 113*, 31–44. https://doi.org/10.1016/j.biombioe.2018.03.007

Moradpour, P., Doosthoseini, K., Scholz, F., & Tarmian, A. (2013). Cutting forces in bandsaw processing of oak and beech wood as affected by wood moisture content and cutting directions. *European Journal of Wood and Wood Products, 71*(6), 747–754. https://doi.org/10.1007/s00107-013-0734-z

Morita, T., Banshoya, K., Tsutsumoto, T., & Murase, Y. (1999). Corrosive-wear characteristics of diamond-coated cemented carbide tools. *Journal of Wood Science, 45*(6), 463–469. https://doi.org/10.1007/bf00538954

Nordstrom, J., & Bergstrom, J. (2001). Wear testing of saw teeth in timber cutting. *Wear, 250*, 19–27. https://doi.org/10.1016/s0043-1648(01)00625-1

Orlowski, K. A., Ochrymiuk, T., Atkins, A., & Chuchala, D. (2013). Application of fracture mechanics for energetic effects predictions while wood sawing. *Wood Science and Technology, 47*(5), 949–963. https://doi.org/10.1007/s00226-013-0551-x

Sjöström, E. (1993). Chapter 5 - Extractives. In E. Sjöström (Ed.), *Wood chemistry* (2nd ed., pp. 90–108). San Diego: Academic Press.

III

Powder Technology 407 (2022) 117664

Contents lists available at ScienceDirect

Powder Technology

journal homepage: www.journals.elsevier.com/powder-technology

Wood powder characteristics of green milling with the multi-blade shaft mill

Atanu Kumar Das *, David A. Agar, Mikael Thyrel, Magnus Rudolfsson

Swedish University of Agricultural Sciences, Department of Forest Biomaterials and Technology, SE-901 83 Umeå, Sweden

HIGHLIGHTS

- Investigation of wood powders made from green wood via a new one-step technology.
- Produced powders had much finer particle sizes than from attritional milling techniques.
- Particle properties include large surface area, more spherical shape and high porosity.
- Finer particles with spherical shapes had an influence on bulk density.
- The technology enables tailor-made particle size distributions for downstream processes.

GRAPHICAL ABSTRACT

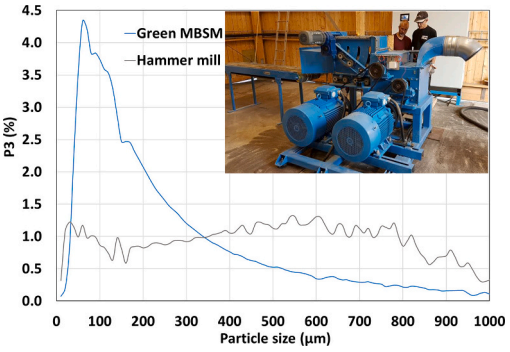

ARTICLE INFO

Keywords:
Powder technology
Pinus sylvestris L.
Aspect ratio
Sphericity
Image analysis
Particle morphology

ABSTRACT

The quality of wood powders depends on the size reduction technology used to produce them. The pre-drying, chipping, and conventional (impact and attritional) size reduction steps, commonly employed in industry, act to degrade wood and diminish its full potential as a renewable feedstock. In this study, the effect of using a new green (i.e. freshly harvested) milling technology, the multi-blade shaft mill (MBSM), on wood powder properties was investigated. Particle size distribution (PSD) and shape properties were measured by two-dimensional image analysis and surface area analysis was performed. The results showed that the MBSM can produce much finer powders compared to hammer milling, with particles demonstrating unique morphology and high specific surface area. Green wood milling yielded particles with the highest sphericity (0.64), aspect ratio (0.58), and micropore diameter (4.5 nm). Finer particles with spherical shapes enhanced the bulk density. Moreover, mill settings permit tailor-made powders according to the desired PSD.

1. Introduction

The transition from the fossil-based economy to a circular and sustainable bioeconomy relies on greater utilisation of renewable biomaterials and the phasing out of fossil-based feedstock [1]. Wood powders are used in many different industrial applications such as refinement of bio-based platform chemicals [2,3], additive manufacturing (3D printing) [4], paperboard production [5], paper

* Corresponding author.
E-mail address: atanu.kumar.das@slu.se (A.K. Das).

https://doi.org/10.1016/j.powtec.2022.117664
Received 31 March 2022; Received in revised form 15 June 2022; Accepted 19 June 2022
Available online 22 June 2022

making [6], water treatment [7,8], fuel pellet production [9] and the manufacture of wood-based composites, wood plastic composites (WPC) and particleboard [10–12]. In these applications, their physical structure and chemical composition are often important considerations.

Wood powders consist of particles of different shapes and sizes; the application sets the requirements for the desired particle specifications. The size reduction method leaves its signature on particle morphology, including the surface distribution of wood's macromolecular components, an influential factor in applications [13]. A large specific surface area and high porosity enhance reaction chemistry by facilitating penetration of chemicals and enzymes [14]. As particle size decreases, so does cellulose crystallinity [15] and this increases specific surface area [14] and has benefits, for example, when converting cellulose to glucose via hydrolysis. Improved conversion of glucose has also been observed from finely milled oak [16] and loblolly pine [3] compared to courser powders. Improved isolation of macromolecular components is correlated to the fineness of wood particulates [17] and are important for the extraction of lignin [18,19].

Particle size is also important for thermal conversion processes using wood as it affects heat transfer and the rate of devolatilisation. Effective (pulverised-fuel) boiler performance in co-firing wood, requires that particles should be <1 mm in diameter for optimal combustion efficiency [20]. During pyrolysis, particle size influences reaction and heating rates [21] and directly affects carbon yield in the char product [22]. Smaller particle diameters lead to enhanced bio-oil [23] and tar yields [21] due to a reduction in vapour-phase residence time and the suppression of char-forming reactions [24].

Wood powders can be produced from a range of mill types that usually operate with pre-dried feedstock. The resulting particle size distribution (PSD) of a powder depends on the comminution technology employed [25]. For example, the particle size can be controlled to some extent using different rotation speeds and actuators in hammer mills (e.g. the number of hammers [26]). The common two-stage hammer mill can generally produce a wood powder with PSD below 1 mm (sieving, mass basis) from pre-dried wood chips [20]. Knife mills can also reduce pre-dried chips to a powder with PSD below 1.5 mm [27].

Hammer mill powders have narrow elongated particles with angular profiles; this shape could be classified as a regular shape for wood powders. Knife mills, on the other hand, yield particles with rectangular shapes [28]. The bulk densities of powders are affected by their particle morphologies. Thin and long or hook-shaped particles increase the tendency of the powder to bridge [28]. This and large interparticle voids can lead to low packing efficiency. Although optimal packing is a complex problem, smaller particles diameters, tending towards spherical shapes, increase packing because of their ability to more freely move and fill gaps [29]. Therefore, in addition to the particle density and porosity, shape also plays a role in the bulk density of wood powders.

Due to the large data sets that come with studying PSDs of powders, statistical tools have been used to develop models on powder quality. MODDE Pro-12 software has been employed for investigating wood powder properties, i.e., PSD and bulk density using multi-linear regression (MLR) models [30]. The authors have used MLR models to investigate the effect of moisture content, feeding speed, and sawblade speed on energy requirements, PSD, and bulk density. Tukey's model with SAS 9.0 software has been used by Jiang et al. [31] to study the effect of moisture content in the feedstock material on powder PSD. Others have used Levenberg-Marquardt's non-linear regression model to investigate the correlation and model fitness for energy consumption, Hausner ratio, and Carr-compressibility index in relation to particle size [32]. Artificial neural network (ANN) models using back propagation (Levenberg-Marquardt) algorithms have been described to understand the relationship between energy consumption, powder moisture content, and powder size [29].

In this study, the impact of a new type of green milling technology on wood powder properties was investigated. The influence of shape properties on the bulk density of powders was studied. The effect of wood moisture content, at the time of milling, on wood powder properties and the relationship between shape properties and bulk density of wood powder were analysed using a statistical tool. The shape, size, surface area, and porosity of powders were characterised. The effect of green versus dry milling of wood on particle properties and the bulk density of powders was also examined.

2. Materials and methods

Pine (*Pinus sylvestris* L.) wood powders used in this study were obtained from a series of designed experiments using a prototype multi-blade shaft mill (MBSM) [30]. There were nine types of powders corresponding to nine different mill settings. The ranges of experimental used parameters for wood moisture contents, feeding speeds and blade speeds were 10–50% (wet basis), 1.3–2.6 m min^{-1} and 52–72 m s^{-1}, respectively. Hammer mill powders were produced from a single setting for the purpose of comparison.

2.1. Representative material sampling

The wood powder samples were sieved by a sieve shaker (Analysette 3, Fritsch, Germany) set at 1.5 mm amplitude for 10 min to obtain ≤1.0 mm particles prior to sampling by rotary sample divider for image, surface area and porosity analyses.

2.2. Two dimensional image analysis

Particle size distributions and shapes of powders were characterised with a 2D image analyser (CAMSIZER XT Particle Analyser, Microtrac RETSCH GMBH, Germany) with a designed size detection range of 0.001 to 3.0 mm at the Department of Engineering Sciences and Mathematics, Luleå University of Science and Technology, Luleå, Sweden. The image analyser used CAMSIZER XT 6.3.10 software (Microtrac RETSCH GMBH, Germany).

Three replicate samples were used for each powder type, resulting in 81 experiments with the image analyser, each producing a spectrum of data on power particle size distribution (PSD) and particle shape factors. In the analysis, the three replicates data sets were averaged. The sample sizes used in this study were 2.8–6.1 g. The software calculated the PSD and shape factors using the following relations [33].

The frequency distribution over $X_{c\ min}$ was used to analyse the results of particle size defined by Eq. (2):

$$Q_3(X_{c\ min}) = \frac{dQ_3(X_{c\ min})}{X(X_{c\ min})} \tag{1}$$

In which $X_{c\ min}$ is the shortest chord among several chords of a particle (Fig. 1a), Q_3 is the cumulative size distribution based on volume.

$$P_3(X_{c\ min}) = dQ_3(X_{c\ min}) \tag{2}$$

Where, P_3 is particle size distribution based on volume.

The aspect ratio and sphericity were used to characterise the shape of particles. The aspect ratio is the ratio of particle width (X_b) to particle

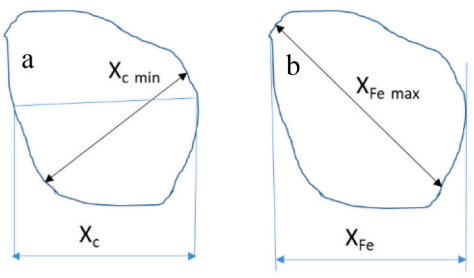

Fig. 1. Shape quantification parameters a) chord of the particle and b) Feret diameter.

length (X_l) defined by Eq. (3).

$$Aspect\ ratio = \frac{X_b}{X_l} \tag{3}$$

Where, X_b is the $X_{c\ min}$ and X_l is the $X_{Fe\ max}$. $X_{c\ min}$ is used to represent the width or breadth of a particle [33] whereas $X_{Fe\ max}$ is considered as the length of the particle [33,34]. Feret maximal diameter ($X_{Fe\ max}$) is the longest Feret diameter (The distance of two tangents placed perpendicularly in the measuring direction) (Fig. 1b) [33].

The sphericity ψ (dimensionless) of a particle expresses the deviation in shape from a sphere and depends on the area of a particle projection (X_A) and the measured circumference (X_P). The closer the value is to one, the more spherical the particle. It was calculated by the following Eq. (4):

$$\psi = \frac{4\Pi X_A}{{X_P}^2} \tag{4}$$

2.3. Geometric surface area

For a spherical particle, the simple geometric surface area A (m^2) and particle volume V (m^3) are calculated using (5) and (6) in which r (m) is the particle radius.

$$A = 4\pi r^2 \tag{5}$$

$$V = \frac{4}{3}\pi r^3 \tag{6}$$

The ratio of surface area to volume of a particle, with common terms eliminated, is (7)

$$\frac{A}{V} = \frac{4\pi r^2}{\frac{4}{3}\pi r^3} = \frac{3}{r} \tag{7}$$

As the radius of the particle approaches zero, the ratio approaches infinity. It follows that for a finite volume of material, the greater the reduction in particle size, the greater the generated surface area. The surface area of a powder A_p (m^2) consisting of n (particles) with a diameter d (m) is calculated with (8), in which A_d (m^2) is the surface area of a single particle with diameter d.

$$A_p = A_{d1}n_{d1} + A_{d2}n_{d2} + A_{d3}n_{d3}\ldots = \sum_d A_d n_d \tag{8}$$

The number of particles of diameter d can be estimated from a particle size distribution determined through sieve analysis of a representative powder sample (9) where M_d (kg) is the mass fraction of sieved particles at diameter d (from a unit mass sample) and m_d (kg) is the mass of a single particle.

$$n_d = \frac{M_d}{m_d} \tag{9}$$

The particle mass m_d is found from the relationship between volume (6) and material density (10) ρ (kg m^{-3}) with the substitution $r = d/2$, resulting in (11).

$$m_d = \rho\, V \tag{10}$$

$$n_d = \frac{M_d\, 6}{\rho\pi d^3} \tag{11}$$

With elimination of common terms, the surface area of the powder (8) can then be rewritten as (12).

$$A_p = \sum_d A_d n_d = \sum_d \left[4\pi(d/2)^2\right]\left[\frac{M_d 6}{\rho\pi d^3}\right] = \frac{6}{\rho}\sum_d \frac{M_d}{d} \tag{12}$$

The surface area generation $\mathring{A}$ ($m^2\ kWh^{-1}$) of size reduction can be calculated from the specific milling energy e_M (kWh t^{-1}) on a dry mass basis (13).

$$\mathring{A} = e_M \bullet A_p^{-1} \tag{13}$$

2.4. Measured surface area and porosity

Specific surface area (i.e. BET) of powders and porosity were determined for three powder types; i) the MBSM powder from wet wood with lowest bulk density, ii) the MBSM powder from dry wood with highest bulk density and iii) the hammer mill powder. Sample sizes ranged from 1.1 to 1.3 g. Analysis was carried out by Celignis Analytical, Ireland, using a NOVA 2200e series surface area and pore size analyser (Quantachrome Instruments, Boynton Beach, USA).

2.5. Statistical analysis

Wood powder properties, i.e., aspect ratio and bulk density were evaluated by orthogonal partial least squares projections to latent structures (OPLS) [35] and orthogonal partial least squares discriminant analysis (OPLS-DA) [36] using SIMCA 16 software (Umetrics, Umeå, Sweden). Prior to model construction of shape factors, the PSD was limited to 50 to 500 μm because of having poor statistics beyond the range (suggestion from expert of Microtrac RETSCH GMBH). All data were subsequently mean centred and scaled to equal variance (denoted UV-scaling in SIMCA). In the following modeling, the image analysis data (aspect ratio) was put in a matrix (X), and the measured responses, i.e., powder bulk density, were arranged in a matrix (Y). Moreover, the observations were divided into two groups (denoted class 1 & 2) based on initial wood moisture content. An initial principal component analysis (PCA) was conducted on each specific dataset (X) to evaluate general trends and patterns in the data and outlier detection. Cross-validation (venetian blinds) was used for evaluating the calibration (OPLS) and discriminant models (OPLS-DA) by the following diagnostics; R^2 (coefficient of determination, describing the amount of explained variation in X), Q^2 (coefficient of multiple determination, describing the amount of variation in the cross-validated subsets predicted by the model) and RMSECV (root mean square error using cross-validation, using seven cross validation groups and same number of iterations).

3. Results and discussion

3.1. Particle size distribution

The particle size distribution of MBSM powders and hammer mill powder is presented in Fig. 2. The peaks of the MBSM distributions occur in the range of 30 to 300 μm. The magnitudes of the peaks for MBSM powders are much greater and substantially narrower than that of the hammer mill powder, indicating substantially finer powders. The cumulative volume percent (insert graph) of particles <0.5 mm in MBSM powders was therefore much higher; 68.4 to 87.5% for MBSM versus 48.2% for hammer mill. In other words, there were almost twice the amount of finer particles in MBSM powders. The >1.0 mm particles for MBSM powders were 5 to 18% only depending on the mill settings and wood moisture content.

The two narrowest PSDs (C and H) were observed from both low and high moisture content wood with high blade speed and low feeding speed. The broadest PSD was observed for the MBSM settings of low moisture content with low blade speed and high feeding speed (B). BS and FS affect the PSD (peak width) and gradual transition from I to E are results of their different settings.

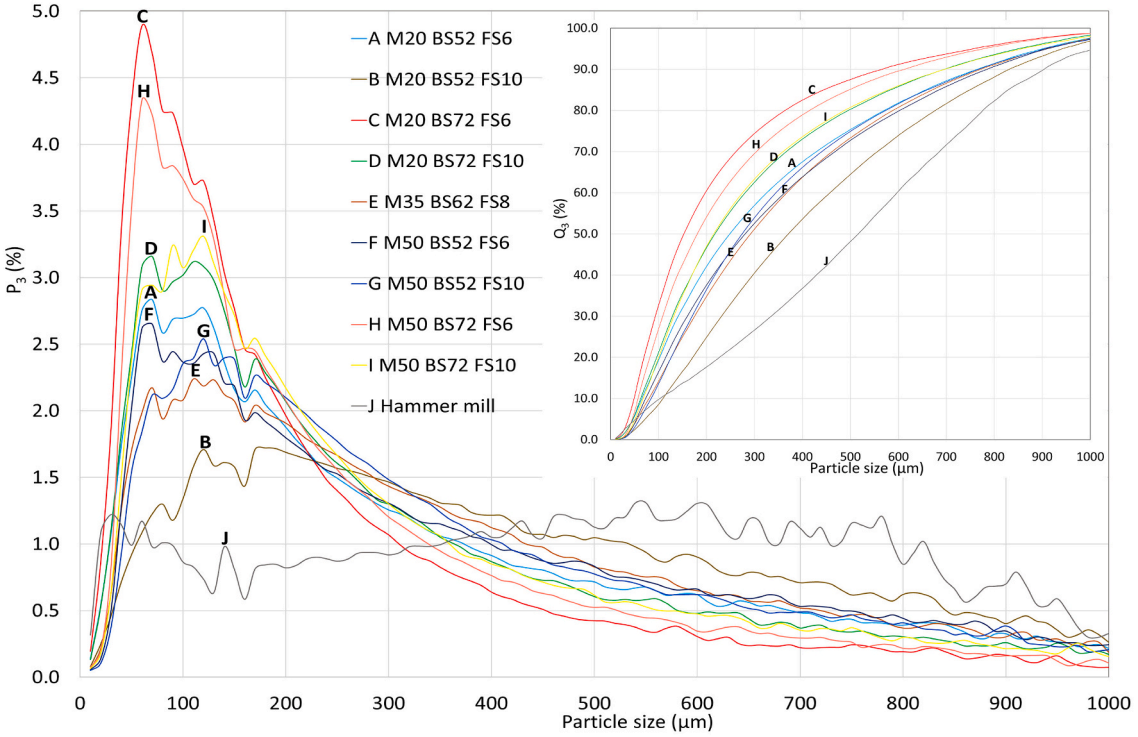

Fig. 2. Particle size distribution (P_3) of powders obtained from the multi-blade shaft mill and hammer mill. The inserted graph is the cumulative particle size distribution (Q_3). Symbols refer to M = moisture content (% wet basis). BS = blade speed (m s^{-1}) and FS = log feeding speed (m min^{-1}).

These results (volume basis) generally agree with those from mechanical sieving analysis (mass basis) of MBSM powders [30]. They show that the wood moisture content and the MBSM blade speed produce similar effects on produced powders and that these differences are small compared to the differences between MBSM and hammer mill powders.

3.2. Particle shape analysis

The aspect ratio and sphericity of powders are presenting in Fig. 3, in which MBSM data is coloured according to the moisture content of the wood used in milling (i.e. green and brown representing above and below fibre saturation point, respectively). MBSM powders obtained using different milling parameters did not show significant shape differences. The values of aspect ratio and sphericity of MBSM powders were higher than hammer-milled powders. The range of aspect ratio and sphericity were 0.54–0.61 (0.57) and 0.51 to 0.75 (0.63), respectively for MBSM powders across MBSM parameter settings. The mean aspect ratio and sphericity of hammer-milled powders were 0.41 and 0.54, respectively.

The moisture content during milling is the primary factor that determines particle shape factors of MBSM powders. This is evident by observing how high (green) and low (brown) moisture content data is differentiated from each other in two discrete bundles of curves (Fig. 3). For both shape factors, there is a clear crossover point in the data at approximately 200 μm (crossover region 150–250 um). Above this point, high moisture content yields powders with greater aspect ratio and sphericity. Below the crossover, low moisture yielded greater aspect ratio and sphericity. The shape factors for the experimental mid-point (dotted line) in the experiments were approximately intermediate between the bundles. Both shape factors of hammer-milled powders display similar behaviour and slope at different particle sizes.

The method of drying of wood powders may be a factor in this behaviour. Uneven moisture distribution in wood during drying causes internal stress due to moisture gradient leading to wood deformation [37]. This is analogous to the warping of pine boards due to internal stress while drying [38]. Trubetskaya et al. [39] observed that pine wood particles became both more spherical during rapid devolatilisation and more porous with more inner cavities. Despite the lower temperature used in drying herein, this explanation may aid the understanding of how particle shape is affected by moisture removal. Further studies are needed to investigate the morphological change of the smaller particles below the size of crossover region.

The obtained MBSM powders had higher aspect ratio and sphericity compared to those in previous studies. Aspect ratios and sphericity in hammer mill pine powders were found to be 0.21–0.22 and 0.44–0.45 for a particle size distribution of 3.2–25.4 mm [32]. Kobayashi et al. [40] found aspect ratio 0.20–0.33 for 0.02–0.5 mm pine powder milled in a vibration mill (rod and ball mill).

3.3. Surface area, porosity and powder bulk density

The measured results of surface area and porosity by BET analysis for the MBSM powders with the lowest (green wood) and highest (dry wood) bulk density and that of the hammer mill powder are presented in Table 1. The MBSM powder (green wood) showed 3.2 times higher specific surface area compared to hammer mill powders (1.378 vs. 0.4291) and 2.5 times higher surface area than MBSM powder (dry wood) (1.378 vs. 0.5573).

MBSM powders from green wood demonstrated 2.7 times (0.002759

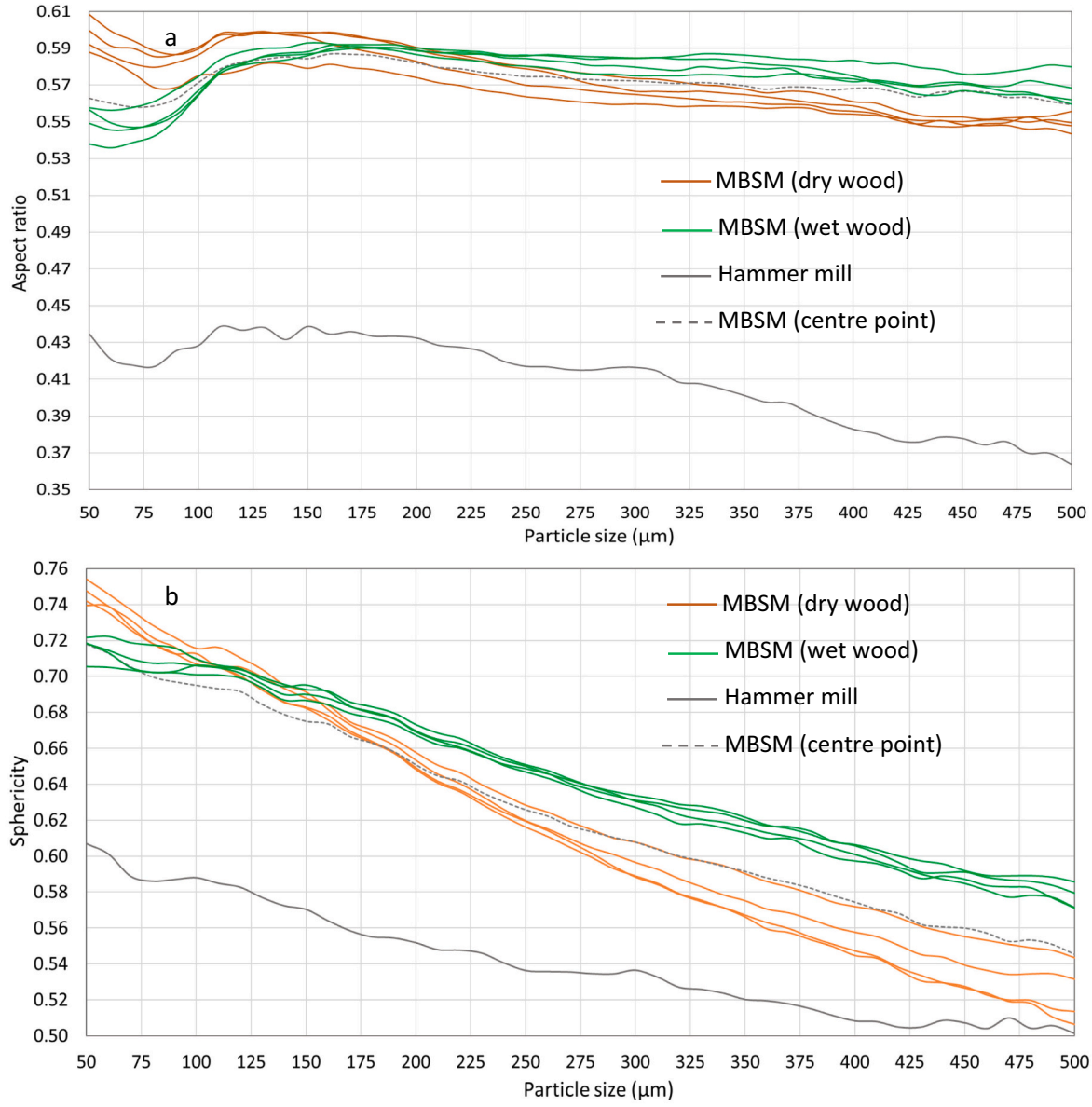

Fig. 3. Aspect ratio (a) and sphericity (b) of multi-blade shaft mill (MBSM) and hammer mill powder.

Table 1
Results from surface area and porosity analysis.

Sample description	Sample mass (g)	BET specific surface area ($m^2\ g^{-1}$)	Pore volume ($cm^3\ g^{-1}$)	Average pore dia. (nm)	BJH method dia. (nm)	QSDFT micropore dia. (nm)	Specific milling energy, dry mass ($kWh\ t^{-1}$) [30]	BET surface area generation ($m^2\ kWh^{-1}$)	Geometric surface area generation ($m^2\ kWh^{-1}$)
MBSM, N17L31 (green wood, lowest bulk density)	1.13	1.378	0.002759	8.012	3.542	4.52	197.4	6981	354
MBSM, N27L13 (dry wood, highest bulk density)	1.32	0.5573	0.001035	7.428	3.536	1.611	197.2	2826	374
Hammer mill	1.06	0.4291	0.001037	9.666	3.539	1.478	86.0	4990	588

vs 0.001037) greater pore volume and 3.1 times larger micropore diameter than hammer-milled powders (4.52 vs. 1.478). The porosity of MBSM green wood powders was 2.8 times higher than MBSM dry wood powders and 3.1 times higher than hammer mill powder. This indicates high porosity, which directly influences the bulk density of a material; the higher the porosity, the greater the volume occupied by the particles and the lower the bulk density of the material.

According to BET analysis, the milling of green wood in the MBSM yielded the greatest surface area per input of milling energy (Eq. 13), 40% more than hammer milling; the surface area generation was found to be 6981, 2826 and 4990 $m^2\ kWh^{-1}$ for green wood, dry wood MBSM powders and hammer mill powders, respectively (Table 1). Based on the sieve results, this can be compared to the calculated geometric surface area generation which were found to be an order of magnitude lower (354, 374 and 588, respectively). This is only to be expected of smooth (pore-free) spheres, on which this simple calculation is based. However, it demonstrates the importance of porosity and particle morphology in the generation of surface area in powders.

Nopens et al. [41] have measured the specific surface area of Scots pine (*Pinus sylvestris*) wood. The authors used an original wood sample with a thickness of 1.5 mm. The obtained result showed a BET surface area of 1.533 $m^2\ g^{-1}$. This value is similar to MBSM powders obtained from the green wood, although the instrument is different. It indicates that green milling can preserve the native structure of wood. This may contribute to a higher yield of value-added products, i.e., biochemical in the downstream process.

Earlier results showed that the bulk density of dry MBSM powders was only dependent on the wood moisture content at the time of milling (Table S). OPLS analysis of the bulk density mirrored this finding and showed that data form two distinct groups of green (above fibre saturation point) and dry wood (below fibre saturation point) (Fig. 4a,b). OPLS-DA analysis showed that the aspect ratio of powder obtained from dry wood was clearly separated from wet (Fig. 4a). The aspect ratio was higher for smaller particles from dry wood, while it was higher for bigger particles from green wood. This trend can also be observed in Fig. 3, where powder from dried wood had a higher aspect ratio for smaller particles. The produced models show that aspect ratio and bulk density (R^2 = 0.87, Q2 = 0.80, and RMSEcv = 17.31) (Fig. 4b) and particle number and bulk density (R^2 = 0.86, Q2 = 0.84, and RMSEcv = 15.58) are well correlated (Fig. S). The bulk density increased with the increase of aspect ratio and powder sourced from dry wood showed higher aspect ratio and bulk density (Fig. 4b).

The large differences in bulk density are attributed to the differences in aspect ratio between powders. It could also be influenced by packing efficiency, being a function of differences in particle shapes, but the evidence for this is absent in this study. For example, others have found that smaller particles can move easily and have the ability to fill up the spaces between the bigger particles [29]. In this study, the number of smaller size particles were higher for powder obtained from dry wood. Although the aspect ratio was higher and lower for dry and green wood (Figs. 3 and 4a), the higher number of smaller particles with higher aspect ratio was comparatively more for powders obtained from dry wood (for the size range 20–150 μm, there were approximately 67,000 particles g^{-1} from the driest wood compared to 38,000 particles g^{-1} from green). Therefore, the finer particles with more spherical shape (and less porosity) in powders from dry wood enhance the homogenous distribution by filling the gaps between the bigger particles and increase the compactness of powder leading to a higher density.

Nevertheless, the inherent chemical composition, for example due to varying amounts of extractives present with moisture in the wood, due to using dry and green materials may have an impact on the findings in this study. Future microscopic studies combined with chemical analysis methods may shed more light on these possible factors.

4. Conclusions

This study showed that multi-blade milling enabled unique powder production from a single-step size reduction operation. Produced wood powders were much finer with unique particle morphology compared to a reference hammer mill powder. They exhibited a higher aspect ratio, sphericity, specific surface area, pore volume, and micropore diameter. Moreover, the higher aspect ratio and sphericity of MBSM powders were observed, for the majority of the studied particle size distribution, when milling green wood. Finer particles with spherical shapes had influential factors enhancing the packing effectiveness leading to the bulk densities values. Furthermore, the multi-blade mill operational parameters did not affect, to any great extent, the shape factors of powders – leading to the conclusion that the observed particle morphology is a characteristic of this size reduction technology. Future research is needed to fully characterise the microstructure of MBSM powders but the evidence

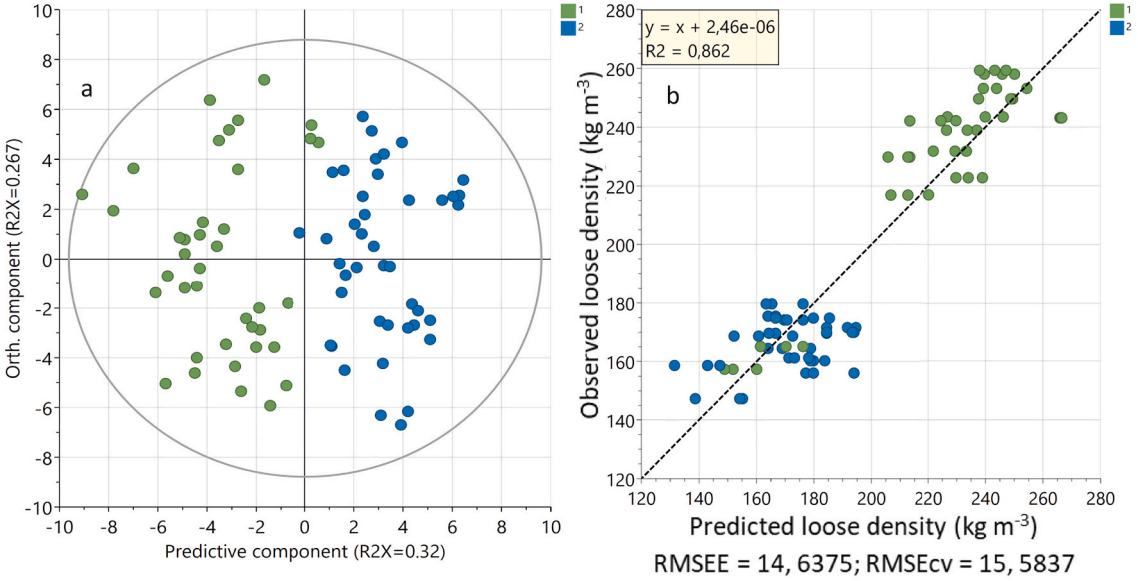

Fig. 4. (a) Score plot derived from class discriminant analysis (OPLS-DA) of AR dependence on moisture content (dry (class 1, green) and wet (class 2, blue), and (b) OPLS calibration model for aspect ratio (X) and bulk density (Y) displaying measured bulk density (kg m^{-3}) versus model predicted bulk density (kg m^{-3}). (For interpretation of the references to colour in this figure legend, the reader is referred to the web version of this article.)

suggests that their observed low bulk density from green milling can be attributed to significant differences in particle morphology and porosity.

Nomenclature

A	geometric surface area (m^2)
A_d	geometric surface area of single particle of diameter d (m^2)
A_p	geometric surface area of a powder (m^2)
$\mathring{A}$	surface area generation of size reduction (m^2 kWh^{-1})
ANN	artificial neural network
BS	blade speed (m s^{-1})
d	particle diameter (m)
e_M	specific milling energy, dry mass (kWh t^{-1})
FS	log feeding speed (m min^{-1})
M	moisture content of wood (%)
MBSM	multi-blade shaft mill
MLR	multi-linear regression
M_d	mass fraction of sieved particles at diameter d (kg)
m_d	mass of a single particle (kg)
n_d	number of particles of diameter d (particles)
OPLS	calibration model
OPLS-DA	discriminant model
PSD	particle size distribution
P_3	volume based particle size distribution
Q^2	coefficient of multiple determination
Q_3	volume based cumulative distribution (% passing)
dQ_3	difference of two consecutive values of Q_3
R^2	coefficient of determination
r	particle radius (m)
RMSECV	root mean square error using cross-validation
V	particle volume (m^3)
X_A	area of a particle projection (mm^2)
X_b	particle width (mm)
$X_{c\ min}$	width (mm)
$X_{Fe\ max}$	particle length (mm) (Feret maximal diameter)
X_l	particle length (mm)
X_P	measured circumference
ψ	sphericity (dimensionless)
ρ	material density (kg m^{-3})
WPC	wood plastic composites

Funding

This study was funded in part by the Swedish Energy Agency (Project number- 46904-1) and the Swedish Bio4Energy Strategic Research Environment. Funding from the Department of Forest Biomaterials and Technology at the Swedish University of Agricultural Sciences is also acknowledged.

CRediT authorship contribution statement

Atanu Kumar Das: Conceptualization, Methodology, Software, Formal analysis, Investigation, Data curation, Writing – original draft, Writing – review & editing, Visualization. **David A. Agar:** Conceptualization, Methodology, Validation, Formal analysis, Writing – original draft, Writing – review & editing, Visualization, Supervision, Funding acquisition. **Mikael Thyrel:** Formal analysis, Writing – review & editing. **Magnus Rudolfsson:** Conceptualization, Methodology, Validation, Formal analysis, Writing – review & editing, Visualization, Supervision, Project administration, Funding acquisition.

Declaration of Competing Interest

The authors declare that they have no known competing financial interests or personal relationships that could have appeared to influence the work reported in this paper.

Acknowledgments

The authors thank Gunnar Kalén and Markus Segerström of the Biomass Technology Centre and Professor Kentaro Umeki of Luleå University of Technology. Sven Bremenfeld and Ted Rönnevall of Microtrac Retsch GmbH are warmly acknowledged for technical consultation.

Appendix A. Supplementary data

Supplementary data to this article can be found online at https://doi.org/10.1016/j.powtec.2022.117664.

References

[1] U. Fritsche, G. Brunori, D. Chiaramonti, C. Galanakis, S. Hellweg, R. Matthews, C. Panoutsou, Future Transitions for the Bioeconomy towards Sustainable Development and a Climate-Neutral Economy, Luxembourg, 2020.
[2] M. Zhang, X. Song, T.W. Deines, Z.J. Pei, D. Wang, Biofuel manufacturing from woody biomass: effects of sieve size used in biomass size reduction, J. Biomed. Biotechnol. 2012 (2012).
[3] U.P. Agarwal, J.Y. Zhu, S.A. Ralph, Enzymatic hydrolysis of loblolly pine: effects of cellulose crystallinity and delignification, Holzforschung 67 (2013) 371–377.
[4] A.K. Das, D.A. Agar, M. Rudolfsson, S.H. Larsson, A review on wood powders in 3D printing: processes, properties and potential applications, J. Mater. Res. Technol. 15 (2021) 241–255.
[5] S.Y. Kim, J.Y. Lee, C.H. Kim, G.B. Lim, J.H. Park, E.H. Kim, Surface modifications of organic fillers to improve the strength of paperboard, Bioresources 10 (2015) 1174–1185.
[6] C.H. Kim, J.Y. Lee, Y.R. Lee, H.K. Chung, K.K. Back, H.J. Lee, H.J. Gwak, H. R. Gang, S.H. Kim, Fundamental study on developing lignocellulosic fillers for papermaking(II) - effect of lignocellulosic fillers on paper properties, Palpu Chongi Gisul/J. Korea Tech. Assoc. Pulp Paper Indus. 41 (2009) 1–6.
[7] H. Sillerova, M. Komarek, V. Chrastny, M. Novak, A. Vanek, O. Drabek, Brewers draff as a new low-cost sorbent for chromium (VI): comparison with other biosorbents, J. Colloid Interface Sci. 396 (2013) 227–233.
[8] A. Keranen, T. Leiviska, B.Y. Gao, O. Hormi, J. Tanskanen, Preparation of novel anion exchangers from pine sawdust and bark, spruce bark, birch bark and peat for the removal of nitrate, Chem. Eng. Sci. 98 (2013) 59–68.
[9] D.A. Agar, M. Rudolfsson, G. Kalen, M. Campargue, D.D. Perez, S.H. Larsson, A systematic study of ring-die pellet production from forest and agricultural biomass, Fuel Process. Technol. 180 (2018) 47–55.
[10] E.D.B. Ferreira, C.B.B. Luna, E.M. Araujo, D.D. Siqueira, R.M.R. Wellen, Polypropylene/wood powder/ethylene propylene diene monomer rubber-maleic anhydride composites: effect of PP melt flow index on the thermal, mechanical, thermomechanical, water absorption, and morphological parameters, Polym. Compos. 42 (2021) 484–497.
[11] K. Renner, C. Kenyo, J. Moczo, B. Pukanszky, Micromechanical deformation processes in PP/wood composites: particle characteristics, adhesion, mechanisms, Compos. Part A-Appl. Sci. Manuf. 41 (2010) 1653–1661.
[12] S.H. Tian, Y.F. Luo, J.Z. Chen, H. He, Y. Chen, Z. Ling, A comprehensive study on the accelerated weathering properties of polypropylene-wood composites with non-metallic materials of waste-printed circuit board powders, Materials 12 (2019).
[13] P. Karinkanta, A. Ammala, M. Illikainen, J. Niinimaki, Fine grinding of wood - overview from wood breakage to applications, Biomass Bioenergy 113 (2018) 31–44.
[14] S.D. Mansfield, C. Mooney, J.N. Saddler, Substrate and enzyme characteristics that limit cellulose hydrolysis, Biotechnol. Prog. 15 (1999) 804–816.
[15] L. Zhu, J.P. O'Dwyer, V.S. Chang, C.B. Granda, M.T. Holtzapple, Structural features affecting biomass enzymatic digestibility, Bioresour. Technol. 99 (2008) 3817–3828.
[16] R.K. Dasari, R.E. Berson, The effect of particle size on hydrolysis reaction rates and rheological properties in cellulosic slurries, Appl. Biochem. Biotechnol. 137 (2007) 289–299.
[17] K. Sarkanen, C.H. Ludwig, Lignins : Occurrence, Formation, Structure and Reactions, 1971.
[18] M. Funaoka, S. Fukatsu, Characteristics of lignin structural conversion in a phase-separative reaction system composed of cresol and sulfuric acid, Holzforschung 50 (1996) 245–252.
[19] M. Funaoka, M. Matsubara, N. Seki, S. Fukatsu, Conversion of native lignin to a highly phenolic functional polymer and its separation from lignocellulosics, Biotechnol. Bioeng. 46 (1995) 545–552.
[20] L.S. Esteban, J.E. Carrasco, Evaluation of different strategies for pulverization of forest biomasses, Powder Technol. 166 (2006) 139–151.
[21] H. Lu, E. Ip, J. Scott, P. Foster, M. Vickers, L.L. Baxter, Effects of particle shape and size on devolatilization of biomass particle, Fuel 89 (2010) 1156–1168.
[22] L. Wang, M. Trninic, Ø. Skreiberg, M. Gronli, R. Considine, M.J. Antal, Is elevated pressure required to achieve a high fixed-carbon yield of charcoal from biomass? Part 1: round-Robin results for three different corncob materials, Energy Fuel 25 (2011) 3251–3265.

[23] A.V. Bridgwater, Review of fast pyrolysis of biomass and product upgrading, Biomass Bioenergy 38 (2012) 68–94.
[24] D. Agar, N. DeMartini, M. Hupa, Influence of elevated pressure on the torrefaction of wood, Energy Fuel 30 (2016) 2127–2136.
[25] C. Mayer-Laigle, R.K. Rajaonarivony, N. Blanc, X. Rouau, Comminution of dry lignocellulosic biomass: part II. Technologies, improvement of milling performances, and security issues, Bioengineering 5 (2018) 50.
[26] D.J. Schell, C. Harwood, Milling of lignocellulosic biomass - results of pilot-scale testing, Appl. Biochem. Biotechnol. 45-6 (1994) 159–168.
[27] M. Phanphanich, S. Mani, Impact of torrefaction on the grindability and fuel characteristics of forest biomass, Bioresour. Technol. 102 (2011) 1246–1253.
[28] S. Paulrud, J.E. Mattsson, C. Nilsson, Particle and handling characteristics of wood fuel powder: effects of different mills, Fuel Process. Technol. 76 (2002) 23–39.
[29] M. Gil, I. Arauzo, E. Teruel, Influence of input biomass conditions and operational parameters on comminution of short-rotation forestry poplar and corn stover using neural networks, Energy Fuel 27 (2013) 2649–2659.
[30] A.K. Das, D.A. Agar, S.H. Larsson, T. Holdo, D. Fernando, M. Rudolfsson, Multi-blade milling from log to powder in one step - experimental design and results, Powder Technol. 378 (2021) 593–601.
[31] J.X. Jiang, J.W. Wang, X. Zhang, M. Wolcott, Microstructure change in wood cell wall fracture from mechanical pretreatment and its influence on enzymatic hydrolysis, Ind. Crop. Prod. 97 (2017) 498–508.
[32] H. Rezaei, C.J. Lim, A. Lau, S. Sokhansanj, Size, shape and flow characterization of ground wood chip and ground wood pellet particles, Powder Technol. 301 (2016) 737–746.
[33] R. Technology, CAMSIZERâ Characteristics, DIN 66141Rheinische Strasse 43 42781 Haan Germany, 2009.
[34] H.G. Merkus, Fundamentals, Practice, Quality, Particle Size Measurements, Springer, Netherlands, 2009 (pp. XII, 534).
[35] J. Trygg, S. Wold, Orthogonal projections to latent structures (O-PLS), J. Chemom. 16 (2002) 119–128.
[36] M. Bylesjo, M. Rantalainen, O. Cloarec, J.K. Nicholson, E. Holmes, J. Trygg, OPLS discriminant analysis: combining the strengths of PLS-DA and SIMCA classification, J. Chemom. 20 (2006) 341–351.
[37] H.J. Chai, C. Xu, J. Li, F.X. Kong, Y.C. Cai, Effects of pretreatment with saturated wet air and steaming on the high-frequency vacuum drying characteristics of wood, Bioresources 14 (2019) 9601–9610.
[38] J. Couceiro, L. Hansson, M. Sehlstedt-Persson, T. Vikberg, D. Sandberg, The conditioning regime in industrial drying of scots pine sawn timber studied by X-ray computed tomography: a case-study, Eur. J. Wood Wood Prod. 78 (2020) 673–682.
[39] A. Trubetskaya, P.A. Jensen, A.D. Jensen, A.D.G. Llamas, K. Umeki, P. Glarborg, Effect of fast pyrolysis conditions on biomass solid residues at high temperatures, Fuel Process. Technol. 143 (2016) 118–129.
[40] N. Kobayashi, T. Sato, N. Okada, J. Kobayashi, S. Hatano, Y. Itaya, S. Mori, Evaluation of wood powder property pulverized by a vibration mill, Nihon Enerugi Gakkaishi/J. Jpn. Inst. Energy 86 (2007) 730–735.
[41] M. Nopens, U. Sazama, S. Konig, S. Kaschuro, A. Krause, M. Froba, Determination of mesopores in the wood cell wall at dry and wet state, Sci. Rep. 10 (2020).

Acta Universitatis Agriculturae Sueciae

Doctoral Thesis No. 2023:49

This thesis investigated a new technology for obtaining wood powders from green wood. The performance of a multi-blade shaft mill (MBSM) was evaluated using a designed series of experiments and morphological characterisation of powders. Narrow particle size distributions, high aspect ratios and improved porosity were among the observed features of MBSM powders. MBSM technology enables a new approach for the greater utilisation of wood resources in the bioeconomy.

Atanu Kumar Das obtained his doctoral education at the Department of Forest Biomaterials and Technology, an MSc in Pulp and Paper Technology, Asian Institute of Technology, and an MSc in Forestry at Khulna University, Bangladesh.

Acta Universitatis Agriculturae Sueciae presents doctoral theses from the Swedish University of Agricultural Sciences (SLU).

SLU generates knowledge for the sustainable use of biological natural resources. Research, education, extension, as well as environmental monitoring and assessment are used to achieve this goal.

ISSN 1652-6880
ISBN (print version) 978-91-8046-150-4
ISBN (electronic version) 978-91-8046-151-1